University of South-Eastern Norway

www.usn.no

FMH606 Master's Thesis 2021

Process Technology

Sensitivity analysis of oil production models to reservoir rock and fluid properties

Bikash Sharma

Faculty of Technology, Natural sciences and Maritime Sciences

Campus Porsgrunn

Course: FMH606 Master's Thesis, 2021

Title: Sensitivity analysis of oil production models to reservoir rock and fluid properties

Number of pages: 98

Keywords: Sensitivity analysis, Norne, OLGA/Rocx, ICD

Student: Bikash Sharma

Supervisor: Britt M. E. Moldestad

Ali Moradi

External partner: -

Summary:

In this fast-growing world, the demands for energy supply are growing rapidly as well. The oil has become one of the basic needs of human beings in this era. Hence, to meet the supply of the growing world, the available oil cannot be extraced with primitive methods. This can be achieved by increasing the reservoir contact for which long horizontal wells can be used. Despite having many advantages of a long horizontal well, there are still some drawbacks in this type of well which is early water coning and water breakthrough. These issues can be fixed by using ICDs, which can balance the drawdown pressure in horizontal well thus delaying the water breakthrough time. With sensitivity analysis on different input parameters, not only these problems can be tackled but also can be distinguish which of the parameter affect the most to production.

Norne oil field was discovered in 1992 in Norwegian sea and the production started from 1997. Since, the main objective of this thesis is to analyze the oil production model, Norne oil field was chosen as the real case. All the simulations were done considering the characteristics of well 6608/10-D-2H of Norne oil field assuming the reservoir to be homogenous. OLGA in combination with Rocx is being used for modelling and simulations.

The base case model of well 6608/10-D-2H was first completed using the simulation tool on which differential analysis method for sensitivity analysis was implemented. The principle of this method is changing the value of one parameter and keeping all other parameter constant. So, changing the values of the parameters by $\pm$ 20% from its original value, and keeping all other parameter constant, simulations in OLGA were done for 200 days. The results shows that the most affected input parameter in case of oil production was oil density, with a value of sensitivity coefficient 1.6097, which was followed by initial water saturation, viscosity, absolute and relative permeability. Similarly, in case of water produced, the most affected input parameter was found to be initial water saturation with a sensitivity coefficient 4.515, followed by water density, viscosity, absolute and relative permeability. Moreover, it was observed that rock compressibility had no effect in either oil or water production.

Preface

This master's thesis shows the research work carried out in spring 2021 at University of South-Eastern Norway (USN), Porsgrunn. The research work and the thesis are done to fulfill graduation requirement of Master of Science degree at USN.

The major goal of this thesis was to analyze the input parameters of oil production model and check its sensitivity. In this study, the sensitivity analysis was performed on one of the well in Norne oil field.

This thesis was supervised by Prof. Britt Margrethe Emilie Moldestad and Phd scholar Ali Moradi with whom I have learned and broaden my knowledge and skills immensely during this thesis.

First and foremost, I would like to express my sincere gratitude and appreciation to Prof. Britt Margrethe Emilia Moldestad, my thesis supervisor who guided me throughout the thesis. I must specially thank her for spending her valuable time and reading my draft and providing me with important advice. I would like to thank Ali Moradi, my thesis co-supervisor, who was always there for me when I needed him. His keen observations and guidance towards work always motivated me to work harder on my thesis.

I would also like to thank IT department of USN, especially Mr. Aleksander Svanberg who helped me fix all the technical problem with the software even in the pandemic situation.

Finally, I would like to thank my family, who constantly encouraged and supported me to do my best in completing the thesis.

Porsgrunn, 02/06/2021

Bikash Sharma

Contents

Nomenclature

Symbols and expression		Units
a	Width of near-well reservoir	m
A	Area	m^2
A_{VC}	Area of Vena Contracta	m^2
b	Length of near-well reservoir	m
c	Rock Compressibility	psi^{-1}
C_D	Discharge coefficient	-
C_H	Babu and Odeh model parameter	-
d	Orifice diameter	m
D	Production tubing diameter	m
f	Mody friction factor	-
h	Thickness of near-well reservoir	m
I_{AH}	Amott-Harvey wettability index	-
J	Productivity index	bbl/psi/day
k	Permeability	D
k_H	Permeability in horizontal direction	-
k_V	Permeability in vertical direction	-
k_e	Effective Permeability	D
k_r	Relative Permeability	-
k_{rocw}	Relative permeability of oil at irreducible water saturation	-
k_{rwro}	Relative permeability of oil at residual oil saturation	-
K	Hydraulic Conductivity	m/s
L	Length	m
P_b	Bubble point pressure	Pa
P_c	Capillary pressure	Pa
Q, $\dot{Q}$	Volumetric flow through the core plug	m^3/s
Re	Reynold's number	-
R_{sb}	Solution gas oil ratio	-
R_w	Radius of wellbore	m
S_{orw}	Residual oil saturation	-
S_{wc}	Connate water saturation	-

S_g	Gas Saturation	-
S_o	Oil Saturation	-
S_w	Water Saturation	-
T	Temperature	K
v	velocity of fluid	m/s
V_{sh}	Shale volume fraction	-
ϕ_i	Sensitivity Coefficient	-
Φ	Porosity	-
ϕ_e	Effective porosoty	-
γ_o	Oil specific gravity	-
γ_g	Gas specific gravity	-
μ	Viscosity	cP
ρ	Density of fluid	kg/m^3
ΔP_f	Frictional pressure drop	Pa
ε	Pipe roughness	m
θ	Angle of contact	-

Abbreviations

AICV	Autonomous Inflow Control Valve
API	American Petroleum Institute
D	Darcy
EOR	Enhanced Oil Recovery
GOR	Gas Oil Ratio
ICD	Inflow Control Device
ICV	Inflow Control Valve
IOR	Improved Oil Recovery
MD	Measured Depth
NCS	Norwegian Continental Shelf
NPD	Norwegian Petroleum Directorate
PVT	Pressure Volume Temperature
PDO	Plan for Development and Operation
TVD	Total Vertical Depth
WC	Water Cut

List of figures

List of Tables

1 Introduction

In this chapter, the history of discovery of oil and its early production methods are described. Similarly, need of oil in current world situation is also briefed along with the problem description and objectives of the thesis.

1.1 Background of the study

The earliest discovery of the oil is said to have around 4000 years ago by Greeks, but it was just a thick liquid found by the river that they used to build their walls and not as a fuel [1]. It was not until 2000 years later the Chinese who discovered, extracted and used it as fuel [2]. The earliest oil wells were then later drilled by Chinese and even Japanese to evaporate the brine and produce salt from it [3]. In the coming year, these oils were found and used by people in middle east, in America and in Russia [1].

The industrialization of oil began when it was discovered in Pennsylvania and more modern methods and research began to start on it since oil was more flexible than coals [1]. As shown in Figure 1.1, shows the trend of world crude oil consumption.

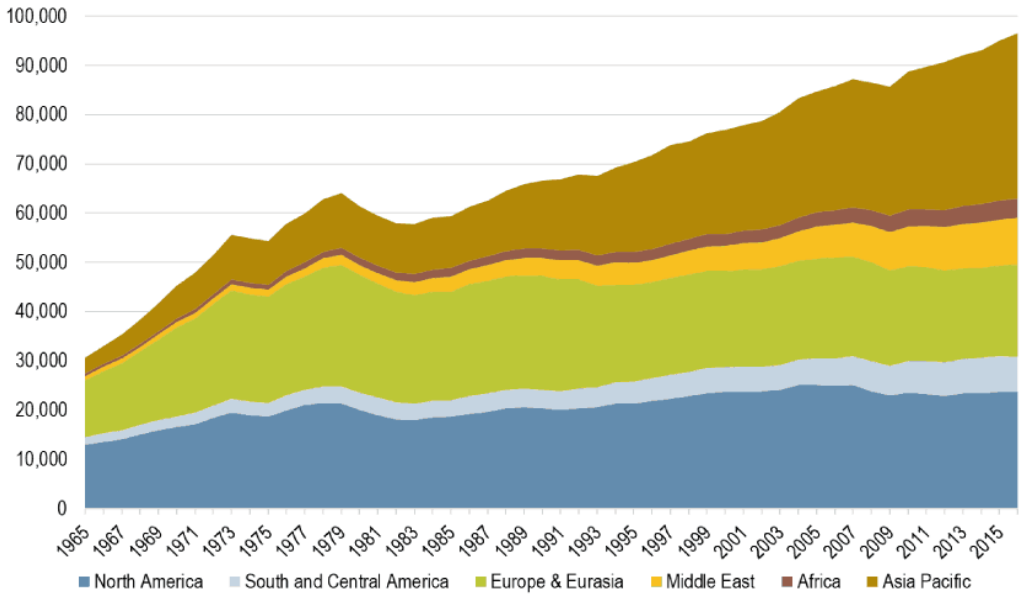

Figure 1.1 : World Crude Oil Consumption [4]

Because the oil was much easier to produce, use and transport, the demand started increasing highly throughout the world and so did the consumption. In the figure, the consumption seems to rise by three times in Asia in the recent years compared to the initial years however North Americans and Europeans have relatively constant use of oil throughout the period of time [4].

From here we can understand the growing demand of oil and to meet the growing needs research and studies in this field must be done which is one of the major objectives of this thesis. As per the demands given in Figure 1.2, Norway contributes about 2% of the oil demand of world [5].

1 Introduction

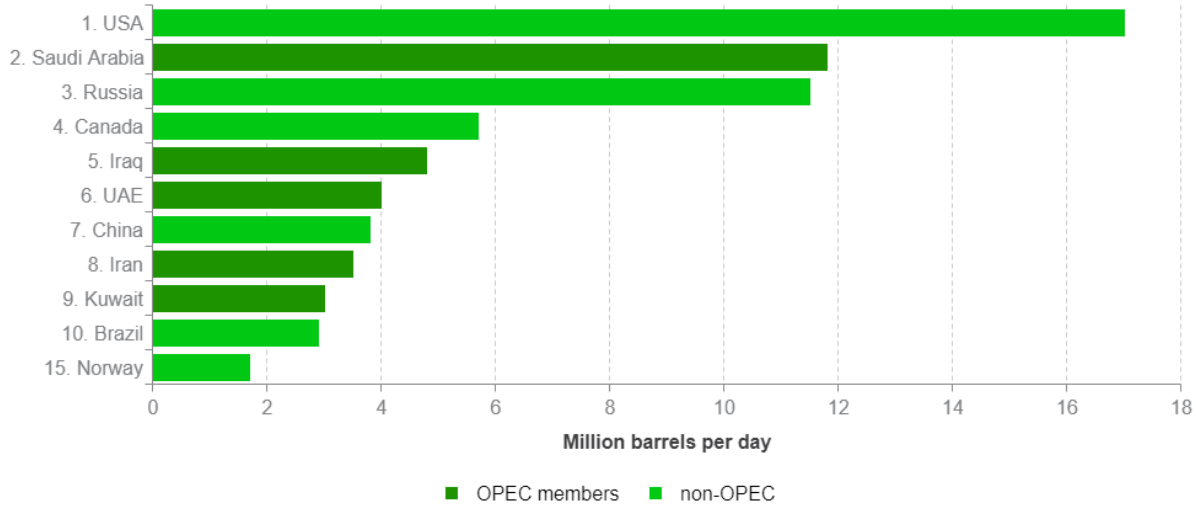

Figure 1.2: Norway and other largest oil producing countries [5]

Norwegian Continental Shelf (NCS) is a continent shelf over which Norway exercises sovereign rights to produce oil and gas. The area of the shelf is four times the mainland and is very rich in petroleum and gas and that is why it is the base of petroleum economy in Norway [6]. The conventional methods of oil production are not so efficient and only 15% to 20% is recovered, hence the Ministry of Petroleum and Energy has appointed OG21 board to improve the oil recovery in a clean way. For instance, in Figure 1.3, the graph of oil production of Gullfaks field by conventional and by Improved Oil Recovery (IOR) is shown and it can be clear distinguished that the efficiency can be highly increased by the IOR methods [7].

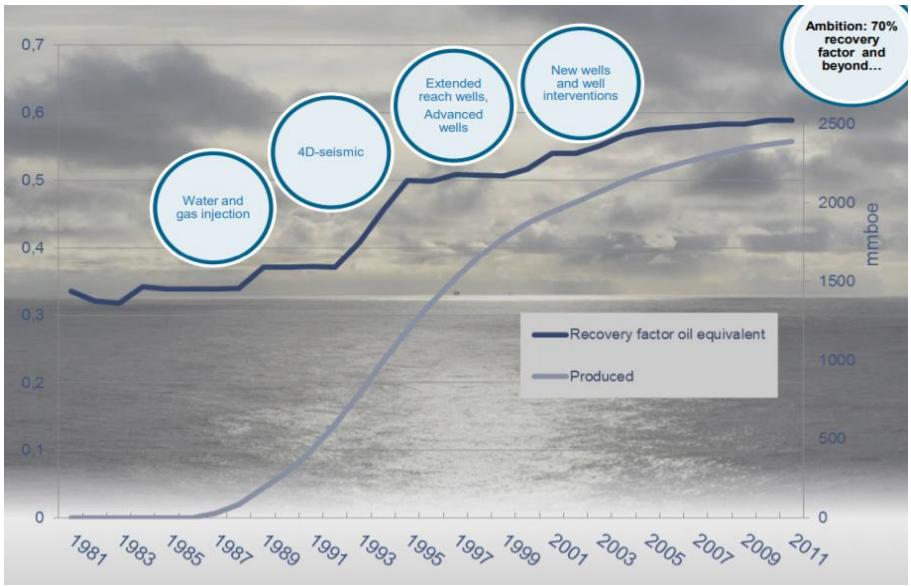

Figure 1.3: Enhanced Oil Recovery (EOR) data of Gullfaks Field [7]

Over the period Norway has successfully been able to improve the recovery process in a very high extent. The chart in Figure 1.4 informs that production in Norway was highest in the year

2005 and was almost 250 mil Sm^3 oil equivalent that is about five times of what was produced around 1980s.

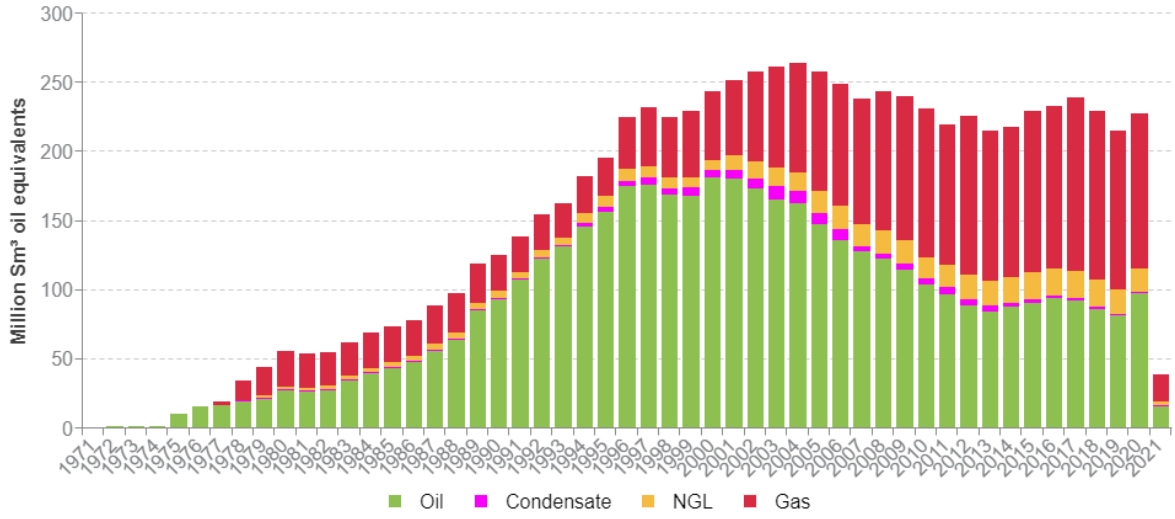

Figure 1.4: Annual production of Norway from 1971 to 2021 [8]

1.2 Problem description

The most commonly occurring problems during the oil production are water coning towards heel due to heel-toe effect and early water breakthrough where water starts to enter the well that leads to heterogeneity in fluids throughout the well. These problems arises due to higher frictional pressure drop in the well or higher permeability areas or even due to ruptures in reservoir [9] [10].

The change in the technique from vertical oil drilling to horizontal oil drilling has impacted highly in the production output despite its own disadvantages. The use of Inflow Control Valves (ICVs) in the wells to control the flow from separate reservoirs or zones has increased in past decades. These valves can reduce and delay the time of early water breakthrough hence understanding the problem of water coning is necessary because it allows us to evenly distribute the drawdown along the well [11].

In order to understand the problems, characteristics, behavior and design of the oil field that is to be studied will be required where it is possible to analyze the multiphase flow behavior of fluids through Inflow Control Devices (ICDs) from reservoir pores to wellbore and then to production tubing. To achieve this, a complete investigation of reservoir properties, both rock and fluid, is needed. After these are done, using a multiphase flow and dynamic modeling simulator, an extensive model is made. By simulating this model, it can be found out which of the properties are most sensitive input parameter affecting oil production.

Norne field is a field located in Norwegian Sea which was discovered in 1992 and the production started in 1997. Since the field is very old, a lot of production has already been done but there has been new field established in recent years where new innovative ideas have been implemented which would give rise to more oil production in coming future [12]. Out of many

oil wells, 6608/10-D-2H is being modelled and studied in this thesis for near well simulation and oil production of Norne Field.

Similarly, a powerful software tool that is used in this thesis is OLGA in combination with Rocx. OLGA is a dynamic multiphase fluid flow simulator whereas Rocx is reservoir simulator that is plugged in with OLGA and together they prove to be very effective and accurate in producing the results. By investigating the characteristics of 6608/10-D-2H well of Norne field, it is very important that the model that is prepared must be as realistic as possible and for that finding the values of various feed parameters required in OLGA/Rocx is a difficult task. Moreover, the Norne field is an old field so gathering proper information and modelling the well with available data is also challenging.

1.3 Objectives

Sensitivity Analysis of oil production to reservoir rock and fluid properties is the significant objective of this thesis so in order to achieve the aim the following tasks must be done.

- Literature study of uncertainty quantification and sensitivity analysis.
- Detailed study of reservoir rock and fluid properties.
- Studying and understanding the oil production techniques in horizontal wells using ICDs.
- Investigating characteristics and gathering the data and information of 6608/10-D-2H well of Norne field.
- Calculating the values of the parameters required for Rocx a to prepare a mathematical model describing the well 6608/10-D-2H.
- Estimation of valve orifice diameter and pressure drawdown values.
- Preparing a dynamic model of oil production from the well 6608/10-D-2H in OLGA.
- Near well simulation of oil production with ICDs for homogenous reservoir.
- Evaluating the effects of production of oil by changing the values of sensitive parameters.
- Analyzing the results obtained from simulation to find out which parameter is most sensitive to production output.

1.4 Thesis outline

The thesis consists of 8 chapters. The first chapter describes about the background of the study, problem description and objectives of the thesis. Literature review on sensitivity analysis, its method and enhanced oil recovery, horizontal well and ICD are given in chapter two. Likewise in chapter three, the background on the reservoir rock and fluid properties are described. Fluid and rock properties of well 6608/10-D-2H of Norne oil field is investigated in chapter four. Similarly, methods and calculations required for the parameters are shown in chapter five. In chapter six, development of model in OLGA and in Rocx are detailly written. The results and discussion are described in chapter 7 and lastly in chapter eight is the conclusion and future works.

2 Literature review

This chapter is focused on describing relevant techniques and methods that are being used in the thesis along with the description of wells and its component.

2.1 Sensitivity analysis

It has been in the trend since old days that before putting some engineering equipment to work, it must be designed and tested first. There are several methods and approaches to achieve that. One of the methods is to develop a model using several logical steps and one of the steps is to determine the parameters which influence the results the most. This is known as 'Sensitivity Analysis' and it is not only important for validation of model but also guides to future research [13].

Sensitivity Analysis is done because of number of reasons which includes [14]:

- For strengthening our knowledge base, which parameters needs additional research, hence reducing the output uncertainty.
- Parameters that are not insignificant can be eliminated.
- Analyzing which input affects the most to output variability.
- The most highly correlated output parameters can be known.

2.2 Methods of sensitivity analysis

Usually to perform a sensitivity analysis, a model must be well defined along with its dependent and independent variables and a probability density function must be assigned to the input parameters. Models are sensitive to input parameters in two different ways: the variability linked to input sensitive parameter which is propagated through the model that results in large contribution to overall output variability and model results can highly be correlated to input parameters that small change in input value result can have significant change in output value [13] [15].

There are two types of analysis that are being done to the parameters, namely important analysis also unknow as the uncertainty analysis and the other one is sensitive analysis the major distinction between these parameters is that an important parameter is always sensitive because parameter variability will not appear in the output if the model is sensitive to input whereas sensitive may not be important because it may be known accurately thus could have a little variability to add to the output [16]. The one that is applied in this thesis is the later one because it is not know which parameter affects the result the most and it is also the major objective of the thesis.

Depending upon the complexity of the model and the type of parameters being used there are many methods of sensitivity analysis. These different methods are differential analysis, one-at-a-time sensitivity measures, factorial design, sensitivity index, importance factors, subjective sensitive analysis and many more [16]. All of these methods are unique and can be used for the models that are suitable according to the type of results that needs to be obtained. In this thesis, differential analysis method is applied which is the simplest and the generalized method of the analysis. Because of its simplicity and generalization, this method is also considered to the backbone of all other analysis techniques [13].

2.2.1 Differential sensitivity analysis

Differential analysis also sometimes known as the direct method, is a technique structured on the basis of the model with a set of specific parameter values. Assuming this case as a base case scenario, where all other parameters are held constant, they are set to their mean value. A sensitivity coefficient is termed to the value that describes the parameter's change. Basically, sensitivity coefficient is the ratio of change in output to change in input by keeping all other parameters constant [17].

The differential analysis of parameter sensitivity is based on partial differentiation of the model in comprehensive from. A Taylor series approximation is used for dependent variable, y, as a function of independent variable X so the variance of Y is calculated as given in Equation 2.1 [13]:

$$V(Y) = \sum_{i=1}^{n} \left(\frac{\partial Y}{\partial X_i}\right)^2 V(X_i) \qquad 2.1$$

Here in Equation 2.1, Y is used to measure the uncertainity in model prediction whereas X_i , being first order partial derivative of Y with respect to X_i is used to measure the model sensitivity in X_i . Using this method is computationally efficient but it is a linearized theory and is valid for only small parameter uncertainities [18]. The sensitivity analysis is easier to perform when an explicit algebraic equation describes the relation between dependent and independent variables. The assumptions made for this equation are the higher order partials are neglected and there is no correlation between the input parameters [19]. So, neglecting non-linearities, the partial derivatives for large sets of equations can be approximated as a finite difference and output values for small change in input parameters that is simplified to the given Equation 2.2 [13]:

$$\phi_i = \frac{\%\Delta Y}{\%\Delta X_i} \qquad 2.2$$

where ϕ_i is sensitivity coefficient which is dimensionless quantity.

2.3 Horizontal wells

To extract oil from under the earth, a well with proper casing must first be dug, then it must meet the point where the wellbore comes into contact with oil. Since the contact surface is one of the key factors for the production, it is logical that higher the contact surface with oil, higher is the production. There are basically two ways to create this contact surface, by creating either vertical wells or horizontal wells. As shown in Figure 2.1, vertical wells have less contact with the oil as compared to horizontal wells. The horizontal wells differ from vertical wells by an angle of inclination greater than 80° [20]. Vertically drilled wells can only access oil that is directly surrounding the well's end however horizontal wells can access the oil that surrounds the entire horizontally drilled segment. Additionally, they intersect several fractures which helps them drain more effectively. Hence, the oil production rate is approximately two to five times higher than unstimulated vertical wells due to the large contact surface area in horizontal

wells [21]. Even though the drilling process and the initial capital cost of horizontal wells are very high, there are many benefits that surpasses the disadvantages of using these wells.

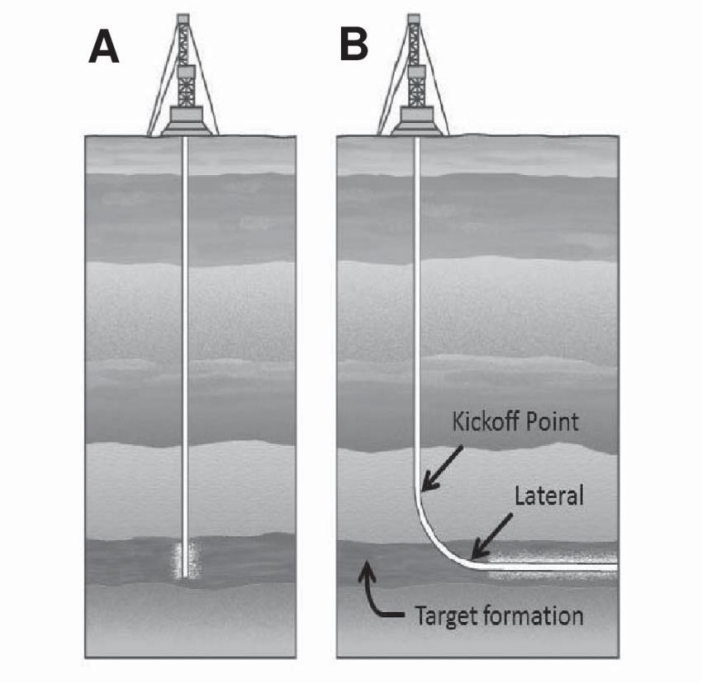

Figure 2.1: Vertical Well (A) and Horizontal Well (B) [21]

2.3.1 Benefits of horizontal wells [22] [23]

- Horizontal wells can be constructed where there are subsurface obstructions such as infrastructure and homes, railroad lines and so on. Directional drilling allows wells to be drilled in places that vertical drill rigs are unable to reach.
- Due to the larger contact area fewer wells are required, resulting in fewer pumps, less piping and lower operation and maintenance costs.
- Reduced water and gas coning as a result of reduced reservoir drawdown for a given production rate, minimizing potential remedial activity.
- Increased production rate as a result of the longer wellbore exposed to the reservoir.
- Reduced pressure drop and lower fluid velocities around the wellbore that leads to lower sand production.

2.3.2 Types of horizontal wells

Buildup rate in horizontal well is the positive change in the inclination over a normalized length and based on it horizontal wells are characterized into three different types namely, short radius, medium radius, long radius which is shown in Figure 2.2. As previously shown in Figure 2.1 in horizontal wells, the kickoff point is the depth in vertical hole at which the deviation for the horizontal drilling starts and depending on the requirement of the oil field different types of horizontal wells are installed [9].

As described in Figure 2.2, short radius has a range of 20 to 40 feet of build up section that is almost 1.5° to 3° per feet and a horizontal section of less than 1000 feet, usually 800 feet radius. On the other hand, a medium radius consists of range 140 to 700 feet which is around 8° to

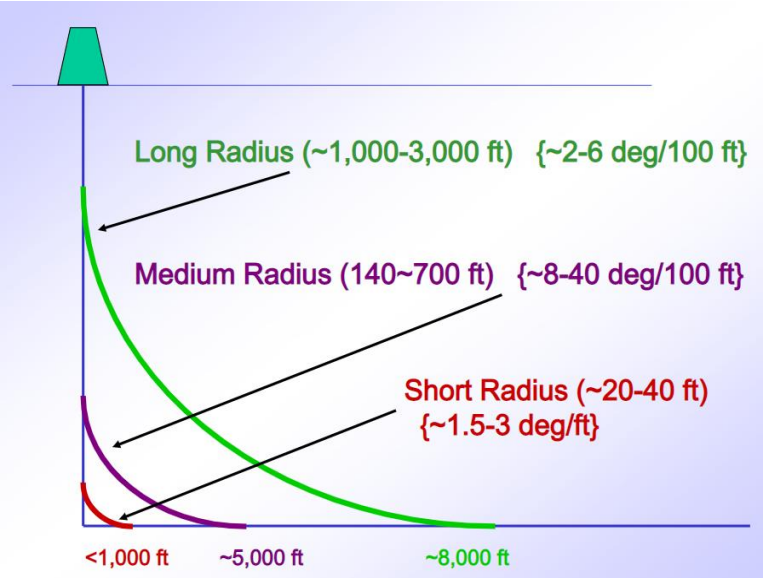

Figure 2.2: Types of horizontal wells [24]

40° per 100 feet of buildup section and a radius length of approximately 5000 feet. And lastly, long radius has horizontal section radius of around 8000 feet and buildup section 1000 to 3000 feet (2°- 6°/100 feet) [25].

2.3.3 Gas and water coning

Water and/or gas coning is a major issue in many reservoirs of wells producing from an oil zone under a gas cap, over an aquifer or both. Coning happens in an oil producing well as the water or gas zone rises up into the wellbore in the shape of a cone as shown in Figure 2.3 [26].

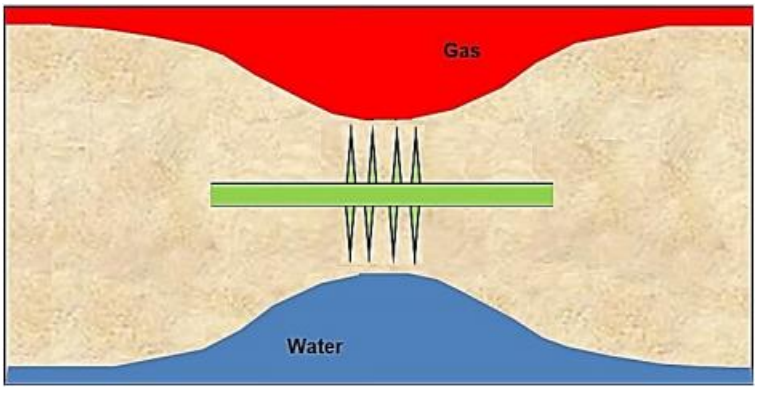

Figure 2.3: Gas and water coning in horizontal well [9]

Water or gas enters the well and water from the aquifer and gas from the gas cap are released alongside the crude oil. Water or gas production increases gradually after the breakthrough period and may dramatically decrease crude oil production [26].

Three primary factors influence the fluid flow distribution around the well: capillary forces, gravitational forces, and viscous forces and the distribution of fluid movement across the well is determined by the equilibrium of these forces. Pressure gradients generated by the well's production will appear to lower the gas-oil contact and raise the water-oil contact in the immediate vicinity of the well. The ability of gas to stay above the oil zone due to its lower density and of water to remain below the oil zone due to its higher density counterbalances these flow gradients. Eventually, this water-oil and gas-oil contacts therefore appear to bend into a cone like shape as shown in Figure 2.3 which is due to the result of counterbalancing these forces [9] [27].

2.3.4 Heel-toe effect

The heel-toe effect is defined by the difference in specific inflow/outflow rates between different sections of the wellbore, which is especially noticeable when comparing the shoe segment (the heel) and the near target depth section (the toe) as shown in Figure 2.4 [28].

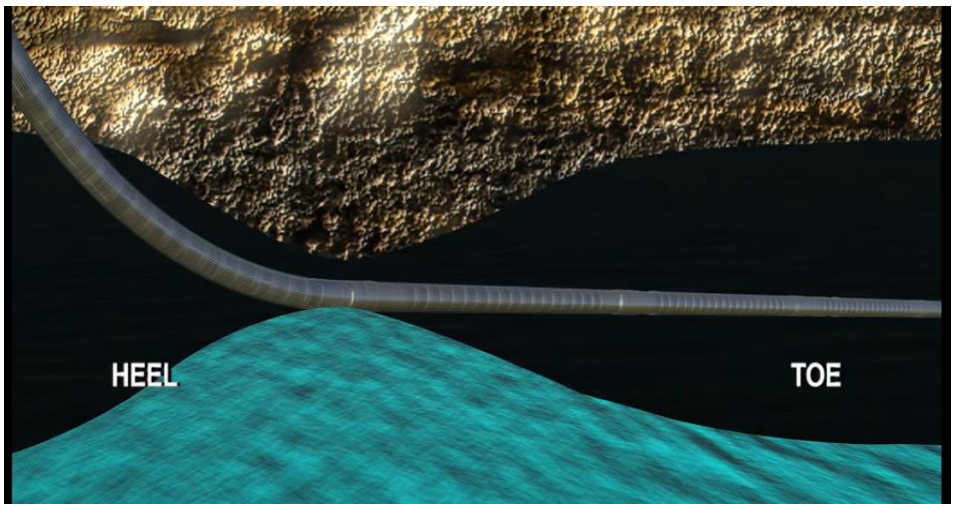

Figure 2.4: Heel – toe effect [29]

This effect occurs as a result of the frictional pressure decrease along the wellbore, which becomes increasingly important as its value exceeds the threshold drawdown pressure. The heel-toe phenomenon is most noticeable in high permeability reservoirs that produce at high fluid rates, resulting in increase in frictional coefficient along the wellbore. Therefore, the higher value of pressure drawdown towards the heel of the reservoir will absorb the water faster compared to the toe [28].

2.3.5 Heterogeneity along the well [9] [30]

The reservoir heterogeneity is the effect in reservoir where water enters the well in spatial locations due to variability in permeability of rocks along the well. Figure 2.5 represents the heterogeneity of reservoir. According to Darcy Law, the fluid flow resistance is lower in high permeability zones therefore, the inflow is higher in that zone compared to other.

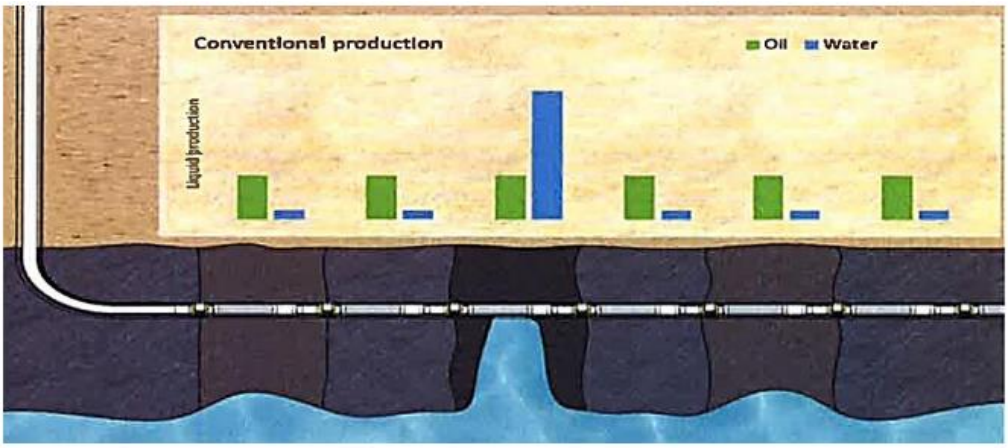

Figure 2.5: Heterogeneity in reservoir

2.4 Inflow control technology

As discussed in subchapters 2.3.4 and 2.3.5, heel toe effect and heterogeneity in reservoir are very common and major issue occurring in horizontal well. Because of these problems the production efficiency decreases with decrease in the quality of oil produced and sometimes even the oil site is shut down. Hence, to remedy this problem Inflow Control Devices (ICD) were introduced. These devices are installed along the well to even out the pressure drop where required hence eliminating the chances of heel toe effect as well as heterogeneity in well. In the Figure 2.6, the graph has been shown where there is comparison of flow rates of oil and water in the reservoir and a clear distinction can be seen in the graph in the flow rates with using ICD and without using ICD.

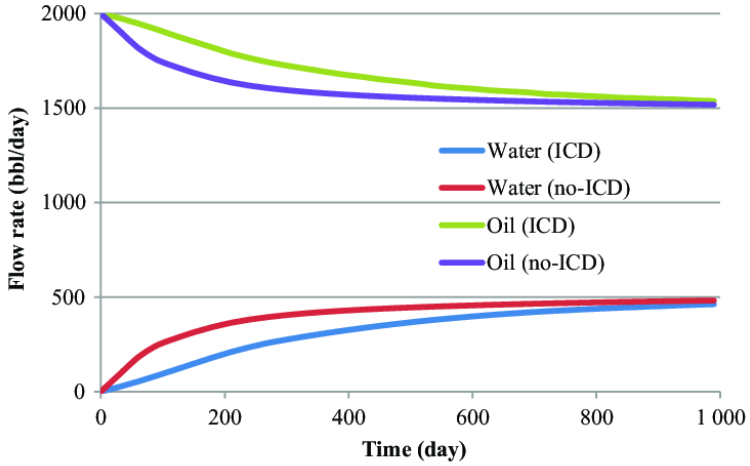

Figure 2.6: Oil and water production rates with and without ICD [31]

Inflow control devices were introduced in the early 1990s to control the wellbore inflow profile. The basic operation of various ICDs is to restrict inflow by creating an additional pressure drop. As a result, the distribution of wellbore pressure will be adjusted, resulting in an evenly distributed inflow profile along the horizontal well [32]. ICD is a flow restrictor device with no moving parts. ICDs are used to choke the flow by introducing extra pressure drop, thereby balancing the flow influx along a horizontal well. ICDs has been developed by four main

companies including Baker Hughes, Halliburton, Schlumberger, and Weatherford and they can be classified into three different types as channel type, nozzle type and orifice type [9].

2.4.1 Channel type ICD

The ICD channel type shown in the schematic Figure 2.7 uses surface friction to generate the desired pressure drop in the well. The fluid enters the wellbore through the channels after passing through a multi-layered screen into the annulus. The fluid is forced to switch directions several times, resulting in a pressure drop across it. Because of the low fluid velocity, the chances of erosion and plugging are low [10].

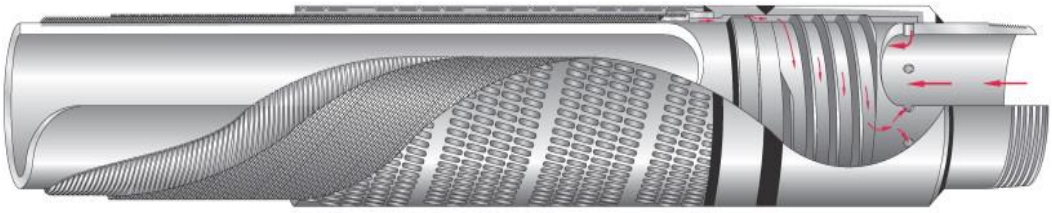

Figure 2.7: Channel type ICD [33]

Since these types of ICD are viscosity dependent, these are unable to maintain the uniform flow along the profile when water breakthrough occurs in which viscosity of oil and water are significantly different [32].

2.4.2 Nozzle/Orifice type ICD

The required pressure drop is achieved in orifice/nozzle type ICDs by forcing the fluid to pass directly through a restriction. These types of ICD are dependent on the density and velocity of the fluid and not on the viscosity of the fluid therefore the required pressure drop can be achieved by forcing the fluid to go through the restrictions [34].

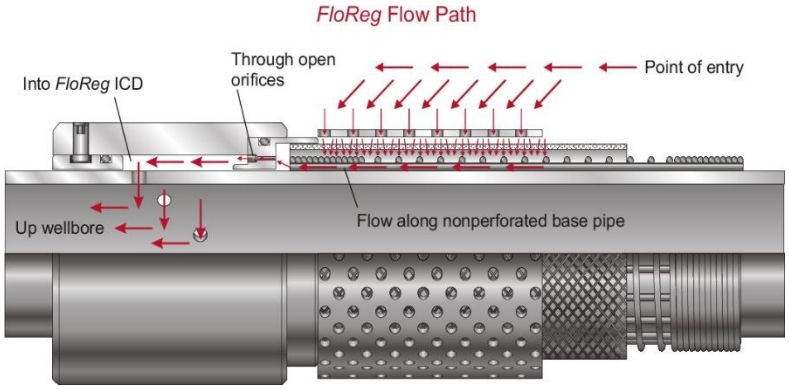

Figure 2.8: Orifice type ICD [33]

As shown in Figure 2.8 and Figure 2.9, the diagrams of orifice type ICD and nozzle type ICD, the point of entry is highly reduced to restrict the flow of fluid and because of this reason, these types of ICD are prone to sand erosion but not for plugging. Hence these ICDs are applicable where fluids are least sensitive to viscosity [32] [34].

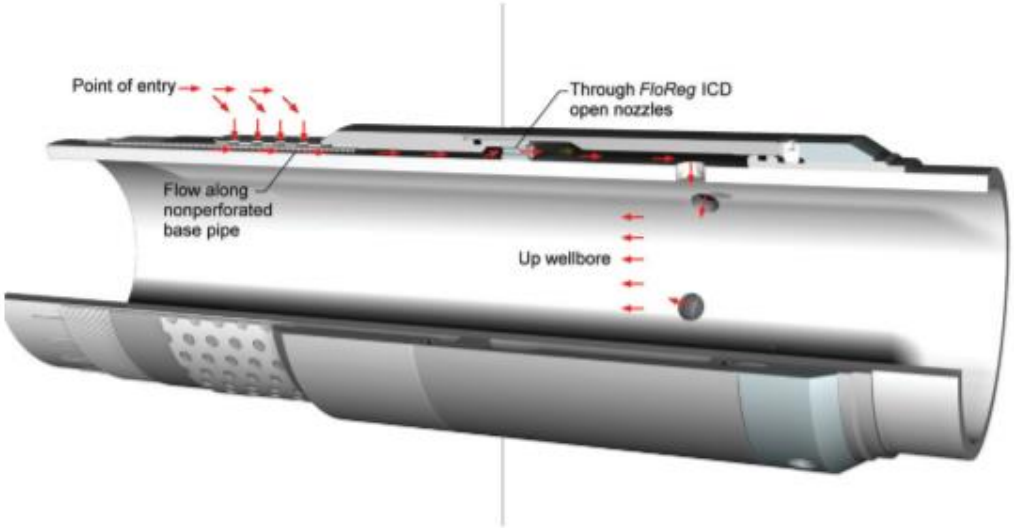

Figure 2.9: Nozzle type ICD [35]

According to [34], when the pressure drop across the pipe line is greater than the pressure difference between the well and the reservoir, only then ICD can be effective. ICD works for heterogeneity case efficiently only when permeability distributions and other important behaviors in a well is properly understood in a long period of time. Hence, these devices cannot be said to be universal solution of water breakthrough. As earlier discussed in sub chapter 2.4 that ICD are installed with no moving parts, its location and relationship between pressure drop and flow rate cannot be changed. But with a little modification in some part a new type of device can be installed called Inflow Control Valve (ICV) which contains sliding-sleeves along the pipeline. By controlling the downhole monitoring system, ICVs can be operated from the surface. Therefore, they are also known as active controllers whereas ICD are known as passive controllers [32].

Even though ICV has more flexibility and better recovery rates than ICD, they are very expensive, more complicated design and less reliable because if their moving parts. Hence, with the latest inflow control technique, autonomous parts are installed which can be controlled for low viscous fluid in comparison with oil. These devices are called Autonomous Inflow Control Devices (AICVs) [32].

2.5 Modelling tool

For this thesis, all modelling and simulation work were done in an advanced tool OLGA + Rocx. There are many other tools that are freely as well as commercially available in markets such as OLGA+Rocx/ECLIPSE or LedaFlow+ECLIPSE or some special application tool such as NETool that are used for designing and modelling for advanced well completion, but because of the simple and effictiveness of OLGA+Rocx is used.

The combination of OLGA and Rocx results in one of the most advanced and dependable tools for modeling and simulation of multiphase flow behavior from the reservoir pore to the production pipe and process facilities. OLGA is a dynamic multiphase flow simulator and Rocx is a reservoir simulator that can be coupled to OLGA as a plug-in. The coupling is done via an implicit scheme based on same PVT file. The wellbore pressure information is calculated and sent to Rocx by the OLGA for the simulation of multiphase flow near the wellbore in three

dimensions then flow rate for each phase of the reservoir fluids is calculated and returned to OLGA by Rocx [9].

The combination OLGA and Rocx has been used for various studies for many years and have proven to be dynamic for many types of studies. For example, studies for comparision of ICD and AICV has been done in [9] whereas in [32], same tool is being used to evaluate the performance of AICV in different reservoir. Similarly, the use of AICV in homogenous reservoir is less significant compared to ICD was also done in [10].

3 Theoretical background

In order to use the modelling tool effectively, it is very important to understand the parameters that are being used. Governing laws, properties of parameters and their behavior when changed are the backbone of the study with which it is possible to evaluate our objectives. All these contents are described in this chapter.

3.1 Reservoir rock properties

At first, the description of various rock properties is discussed. The reservoir rocks are composed of rocks that vary from loose sand to very hard rock. The knowledge of the physical properties of rock are very important in order to evaluate the performance of that reservoir. The effects of changes of these properties are done in lab and may range from negligible to substantial [36].

3.1.1 Porosity

Even though the stones and rocks in the reservoir are very hard and looks solid to naked eyes, there are existence of tiny openings in those rocks if observed in microscopic level. These tiny opening are referred to as pores or void spaces. These pores in the rocks have tendency to store reservoir fluids inside them and this property of the rock is said to be porosity. The more porous a rock is, greater the amount of open space is inside the rock and higher is the storage capacity of the fluids in them [37]. In Figure 3.1 is the schematic diagram of porous rock where the pores or open spaces are seen in the rock.

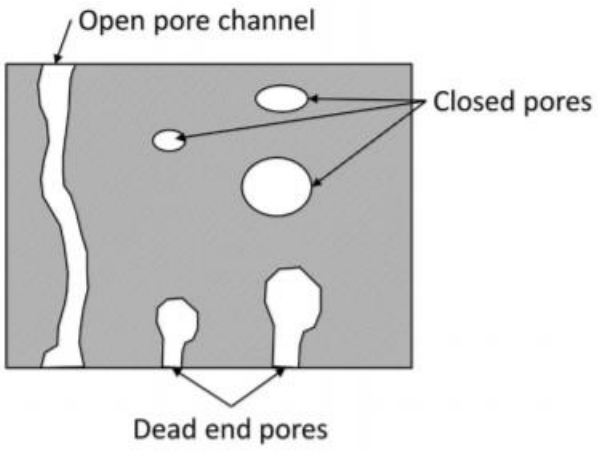

Figure 3.1: Schematic of pore types

Mathematically, the porosity can be defined as the ratio of pore volume or total or bulk volume of the rock. It has no units since it is division of volume, but it is expressed in fraction or in percentage and is denoted by the symbol ϕ and Equation 3.1 represents the porosity as [27]:

$$\phi = \frac{total\ pore\ volume}{total\ or\ \ bulk\ volume} \qquad 3.1$$

As it is seen in Figure 3.1, despite of many pores in between the rocks there are many types which are closed pores and dead-end pores. These pores could store fluid in them, but they cannot mobilize those fluids. This is because of the reason that these rocks formation over a

long period of time gets isolated from other spaces due to high cementation due to which it is not possible to recover fluids through them. Hence, while putting it correctly mathematically, it is not efficient if we consider all the pores and therefore only those pores must be considered which can flow fluid through them. This parameter is called effective porosity ϕ_e and is defined in Equation 3.2 [27]:

$$\phi_e = \frac{interconnected\ pore\ volume}{total\ or\ bulk\ volume} \qquad 3.2$$

3.1.2 Fluid saturation

As discussed in subchapter 3.1 in porosity that it is the capacity to store fluid but in those reservoir rocks there are more than one fluid stored. So, to calculate the quantity of each fluid present in the rock, fluid saturation is needed. The amount of hydrocarbons and water that can be mobilized from the rock are quantified using this parameter. Hence saturation is defined as the fraction or percent of effective pore volume occupied by a particular fluid. Mathematically, fluid saturation can be defined as the ratio of total volume of fluid to effective pore volume [38].

$$\text{Fluid saturation} = \frac{\text{total volume of fluid}}{\text{effective pore volume}} \qquad 3.3$$

Since there are three reservoir fluids which are oil, water and gas the saturations can be defined for each of them accordingly as:

$$S_w = \frac{\text{volume of water}}{\text{effective pore volume}} \qquad 3.4$$

$$S_o = \frac{\text{volume of oil}}{\text{effective pore volume}} \qquad 3.5$$

$$S_g = \frac{\text{volume of gas}}{\text{effective pore volume}} \qquad 3.6$$

By definition, each type of saturation ranges from zero to 100% and the sums of all the saturations must be 100%. So,

$$S_w + S_o + S_g = 100\% \qquad 3.7$$

3.1.3 Rock compressibility

The concept of rock compressibility is same as that of squeezing a sponge. In reservoir rocks, there are porous rocks that are subjected to overburden pressure that decreases the pore volume. In Figure 3.2, a schematic figure is shown where firstly the rock which is in grey color is shown has large space between them so higher porosity is there which indicated high fluid storage. But due to the stresses from overlying rocks from outside and stresses due to internal fluids from inside, the depletion of fluid occurs, and the result is compaction of rock structure. Therefore, rock compressibility is the fractional change in effective pore volume per unit bulk volume per unit change in pressure [38] [39].

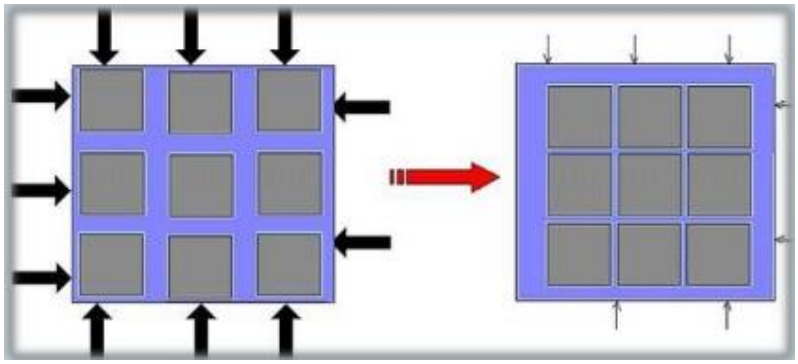

Figure 3.2: Conceptualization of rock compressibility [39]

Rock compressibility has a unit of psi^{-1}, denoted by c and are given as in Equation 3.8:

$$c = -\frac{1}{V}\left(\frac{\partial V}{\partial p}\right)_T \qquad 3.8$$

where c = rock compressibility

V =effective pore volume

$\left(\frac{\partial V}{\partial p}\right)$ = change in volume over change in pressure

the subscript T denotes that the compressibility is measured in reservoir assuming the temperature to be constant [38].

3.1.4 Absolute permeability

Permeability is a measure of ease with which fluid flows in porous medium. In the reservoir rock the permeability is a factor of paramount importance because with the properties that earlier discussed, none of them are able measure the directional mobilization of fluid. The directional movement and flow rate of fluids are necessary factors in studying about any reservoir. The permeability values are different for single fluid and for multi fluids. So, the permeability of rock measured when it is completely saturated with single phase fluid is often referred to as single phase permeability or absolute permeability. It is denoted by k and the unit of absolute permeability is Darcy (D).

3.1.4.1 Darcy's law

The measurement of absolute permeability of the rock is governed by Darcy's law which was first introduced by Henry Darcy. He performed an experiment on cylindrical sand filtrate as shown in Figure 3.3 and from that experiment Equation 3.9 was introduced [38].

3 Theoretical background

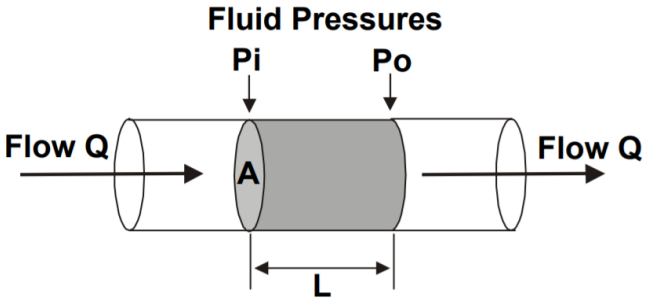

Figure 3.3: Representation of Darcy's law [40]

With this experiment setup, if Q is the volumetric flow through the core plug (m^3/s), K is the hydraulic conductivity (m/s), A is the area of cross section of the cylindrical core plug (m^2) and dP is the pressure difference across the core (Pa) and dL is the length of the core plug (m), then Darcy introduced a formula as such [38]:

$$Q = -KA\frac{dP}{dL} \qquad 3.9$$

Darcy conducted this experiment that was valid for only water but it was only later when it was established that this law can be generalized by changing the parameter K to k/μ where k is the absolute permeability (D or mD) whereas μ is the viscosity of the fluid (N·s / m^2). So the formula changes to [9]:

$$Q = -\frac{k}{\mu}A\frac{dP}{dL} \qquad 3.10$$

Equation 3.10 represents the Darcy's Law but for linear flow only however for a reservoir, radial flow represents more accurately. Figure 3.4 shows the schematic presentation of Darcy law for radial flow of fluid in reservoir.

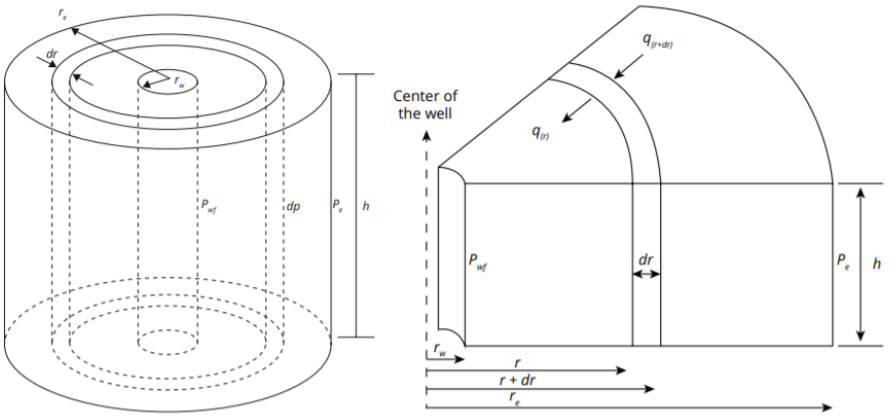

Figure 3.4: Schematics of radial flow of fluid from outer boundary to wellbore region (left) and the zoomed section of the part of the reservoir (right)

There are two change done in this case where firstly the area perpendicular to the flow is circumference multiplied to the thickness that results to A = 2πrh and secondly, the flow will vary in r-coordinate rather than x-coordinate so $\frac{dP}{dL}$ will change to $\frac{dP}{dr}$ [38].

$$Q = {}^{k}/_{\mu} A \frac{\mathrm{d}P}{\mathrm{d}r} \qquad 3.11$$

One important notable thing here is that the actual SI unit of permeability is m^2 but practically the unit is too large for the measurement therefore a suitable unit Darcy (D) and millidarcy (mD) were introduced. When a single-phase fluid with a viscosity of one centipoise (cP) completely saturates a porous medium and flows through it at a rate of 1 cm^3/s under a viscous flow regime and a pressure gradient of 1 atm/s through a cross-sectional area of 1 cm^2, it is said to have a permeability of one Darcy [9].

$$1 \text{ Darcy} = 1000\text{mD} = \frac{(1\text{cm}^3/\text{s})(1\text{cP})}{(1\text{cm}^2)(1\text{atm/cm})} = 9.869\times10^{-13}\ \text{m}^2$$

3.1.4.2 Permeability anisotropy

In most of the cases, generally the permeability in z-direction is close to that of the permeability in y-direction. This gives rise to different permeabilities in different direction because the formation of reservoir rocks are sedimentary process so, the permeability parallel to these rocks will be higher compared to the permeability perpendicular to the rocks. This property is known as the permeability anisotropy which is defined as the ratio of vertical permeability (k_v) to horizontal permeability (k_H). Figure 3.5 shows the mechanism of permeability anisotropy which is elliptical in shape because of directional dependency of horizontal and vertical permeabilities [9].

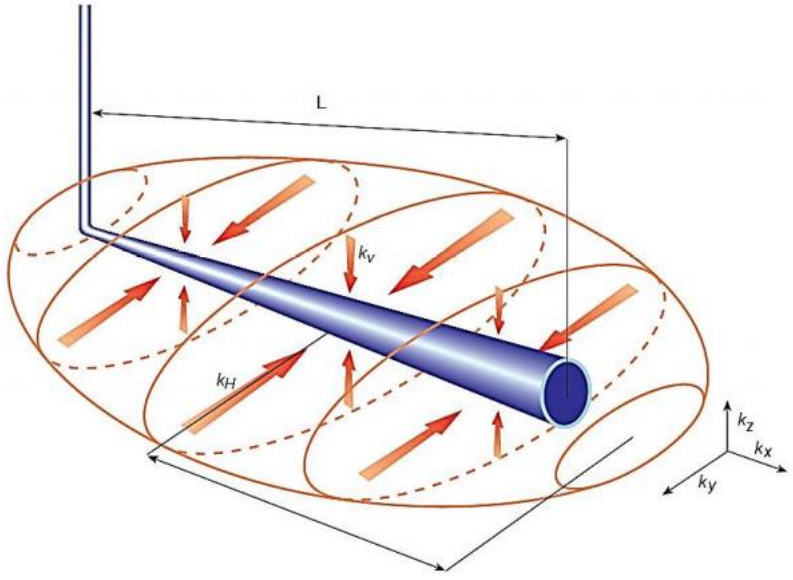

Figure 3.5: Drainage pattern formed around horizontal well [9]

In order to determine the value of permeability anisotropy, it is necessary to know the values of permeabilities in all three directions (k_x ,ky ,kz). These can be calculated as [41] [42] [9]:

$$k_H = \sqrt{k_x k_y} \qquad 3.12$$

$$k = \sqrt[3]{k_x k_y k_z} \qquad 3.13$$

To find out the value of permeability in z-direction (k_z or k_v) many correlations can be found for different types of reservoir, one of which was proposed by [43] shown in Equation 3.14 which has a correlation coefficient 0.953. If V_{sh} is the shale volume in reservoir then:

$$k_v = k_z = 0.0718 \times \sqrt{\left[\frac{k_H(1-V_{sh})}{\phi_e}\right]^{2.0901}} \qquad 3.14$$

3.1.5 Relative permeability

It is discussed in sub chapter 3.4 in absolute permeability that it is the measure of completely saturated fluid in the reservoir rock with single phase fluid. But practically, it is very rare to find such case and most of the time there are multi fluids involved. In such cases absolute permeability is not the correct approach. The pores in the reservoir rocks shares different types of fluid with different fluid saturation and effective permeability (k_e) is the parameter that can help determine these permeabilities in different fluids in the same rock. Darcy law is still valid in this type of permeability, but it needs dome extension. Effective permeability depends upon fluid saturation, geometry of porous medium and wettability. But with using the fluid saturation property, another term can be coined known as relative permeability (k_r) that is more convenient to evaluate the multiphase flow of reservoir fluid in the rocks. Relative permeability of each phase of fluid at specific saturation is defined as the ratio of effective permeability of the phase to absolute permeability, when two or more fluids flow at the same time. It is denoted by k_r and is expressed in fraction or in percentage [40] [27]. Mathematically,

$$k_r = \frac{k_e}{k} \qquad 3.15$$

In a rock if all the three types of fluids are present at a partial saturations S_o, S_g, S_w we can measure effective permeability (k_{eo} ,k_{eg} ,k_{ew}) and relative permeability (k_{ro} ,k_{rg} ,k_{rw}) can be measured and the sum of these permeabilities are always less than their absolute values [40].

When a graph is plotted for relative permeability and fluid saturation, figure 3.6 can be expected which is a typical trend followed by relative permeability for oil we and water wet rocks. In Figure 3.6, the parameter in graph refers to:

S_{wc} = connate water saturation → water saturation lower than this is immobile

S_{orw} = residual oil saturation after water flooding → oil saturation lower that this is immobile

k_{rocw} = maximum relative permeability of oil at critical water saturation → oil becomes mobile

k_{rwro} = maximum relative permeability of water at critical oil saturation → water becomes mobile

So, by knowing the meaning of these parameters figure 3.6 becomes easy to understand where between S_{wc} and (1- S_{orw}) is the region only from which the oil can be recovered [27].

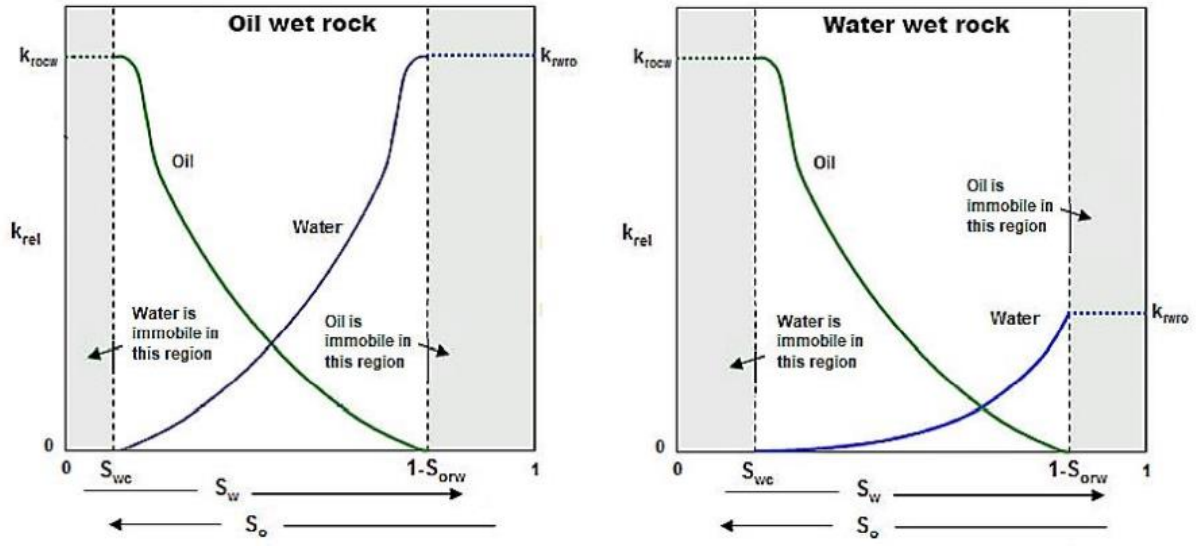

Figure 3.6: Oil wet rock permeability (left) and water wet rock permeability (right) [9]

In the numerical simulators, the equation of relative permeability is required which should define the model accurately. The most common model used is the Generalized Corey model that can estimate relative permeability of two-phase systems and is given by:

$$k_{ro} = k_{rocw}\left[\frac{1-S_w-S_{orw}}{1-S_{wc}-S_{orw}}\right]^{n_{ow}} \qquad 3.16$$

$$k_{rw} = k_{rwro}\left[\frac{S_w-S_{wc}}{1-S_{wc}-S_{orw}}\right]^{n_w} \qquad 3.17$$

where n_{ow} and n_w are the Corey exponents [9].

3.1.6 Wettability

In a system of two or more immiscible fluids, wettability refers to a solid's preference for one fluid over another. The ability of a liquid to spread across the surface of a solid indicates the liquid's wetting characteristics for the solid. The angle of contact at the liquid-solid surface can be used to more easily express this spreading tendency. The contact angle is the angle between the liquid and the solid that is always measured through the liquid. The distribution and movement of fluids within a reservoir rock are heavily influenced by the wettability of the rock [27].

In an oil-water reservoir wettability are of four types [38]:

- Water-wet: the rock surface has tendency to get coated with water.
- Oil-wet: the rock surface has tendency to get coated with oil.
- Intermediate-wet: the rock surface has equal tendency to get coated by either of the fluids (oil or water).
- Mixed-wet: part of the rock has tendency to get coated with oil and part of it with water.

Wettability, quantitively is represented by I and it can be measured by Amott-Harvey wettability index (I_{AH}) which is given in Equation 3.18 [37].

$$I_{AH} = \delta_w - \delta_o \qquad 3.18$$

Here, δ_o and δ_w are displacements by oil ratio and water ratio respectively. When the rock is strongly water-wet value of δ_w tends to 1 and when it is strongly oil-wet value of δ_o tends to 1 [37].

3.1.7 Capillary Pressure

The tendency of fluid to rise or fall through capillary tube is called capillary pressure. In oil reservoir the pore inside the rocks acts as the capillary tube. Reservoir fluid displacement can be in the direction of adhesive forces or against them. The surface forces of capillary pressure help in the displacement of one fluid by another in the pores of a porous medium. As a result, it is necessary to keep the pressure of the nonwetting fluid higher than the pressure of the wetting fluid in order to keep a porous medium partially saturated with nonwetting fluid while also exposing it to wetting fluid. Capillary pressure is denoted by P_c and it is measured in Pa. The equation to measure capillary pressure is different for water-air system and water-oil system that is shown in Equations 3.19 and 3.20 respectively [38] :

$$P_c = P_{nw} - P_w \qquad 3.19$$

$$P_c = \frac{2\sigma_{wo}cos\theta}{r} \qquad 3.20$$

Here, P_{nw} is pressure of non-wetting phase, P_w is pressure of wetting phase, σ_{wo} is the surface tension between water and oil, θ is the angle of contact and r is the capillary radius.

3.2 Reservoir fluid properties

Just as the reservoir rock, the reservoir fluids have also many contributing properties that helps broaden our knowledge about the reservoir wells. These reservoir fluids stored in the rocks are found in three types which are either water or liquid hydrocarbon or gases whose composition depends on the history, source and current thermodynamic conditions. The distribution of fluids in the reservoir rely on the thermodynamic condition and petrophysical properties or even the physical and chemical properties of the fluid [44].

Reservoir fluids are complex mixture of many hydrocarbons and non-hydrocarbon component where the hydrocarbon components are evolved from a source rock which undergoes breakdown of organic material under high temperature and pressure that migrates upward and gets trapped in the permeable rocks and displaces the water present there. In Figure 3.7, the formation and accumulation of hydrocarbon fluid is shown [45]. The properties of fluid, both hydrocarbon and non-hydrocarbon, are discussed as such.

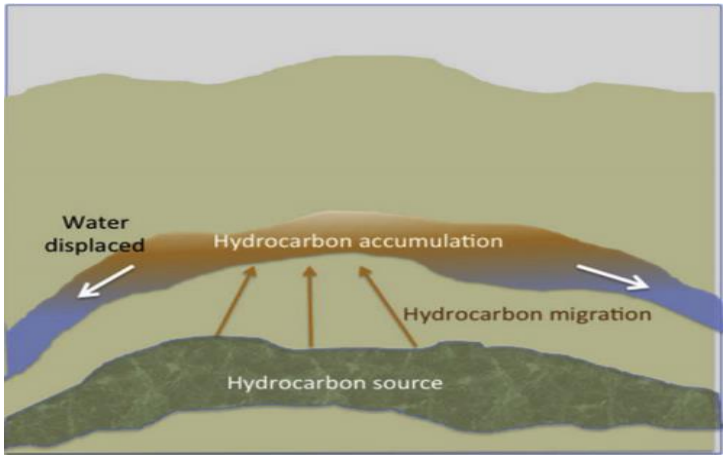

Figure 3.7: Hydrocarbon accumulation in reservoir [45]

3.2.1 Property of reservoir fluids

- Gas-Oil Ratio (GOR)

It is defined as the ratio of volume flow rate of gas produced to the volume flow rate of oil produced and its unit is Sm^3/Sm^3 [46].

$$GOR = \frac{\dot{Q}_{gas}}{\dot{Q}_{oil}} \qquad 3.21$$

- Water cut

It is defined as the ratio of volume of water produced to the volume of total liquid produced which is a dimensionless quantity and is given as [47]:

$$Water\ Cut(WC) = \frac{\dot{Q}_{water}}{\dot{Q}_{liquid}} = \frac{\dot{Q}_{water}}{\dot{Q}_{oil}+\dot{Q}_{water}} \qquad 3.22$$

- Gas specific gravity

It is defined as the ratio of density of gas to density of air at 1 atm pressure and temperature of 60°F which are the standard temperature and pressure. It is also unitless quantity [48].

$$Gas\ specific\ gravity = \frac{\rho_{gas}}{\rho_{air}} \qquad 3.23$$

- Oil specific gravity

Specific gravity is defined as the ratio of the density of liquid to the density of water at 4℃. In that case, when the liquid is oil, it is referred to as oil specific gravity and will be given as

$$\gamma_o = \frac{\rho_o}{\rho_w} \qquad 3.24$$

where, γ_o is the oil specific gravity, which is dimensionless quantity [52].

- API gravity [49]

It is the acronym for American Petroleum Institute gravity which is defined as a parameter that is used for measuring the weight of petroleum liquids in comparison to water. It is calculated on the basis of the oil specific gravity of the fluid and is given as:

$$API = \frac{141.5}{\gamma_o} - 131.5 \qquad 3.25$$

On the basis of comparison of reservoir fluid with water it is classified into four categories which is shown in Table 3.1.

Table 3.1: Oil categories on the basis of their °API

Type of Oil	Values
Light Oil	API $>$ 31.3°
Medium Oil	22.3° $<$ API $>$ 31.3°
Heavy Oil	10° $<$ API $>$ 22.3°
Extra-heavy Oil	API $<$ 10°

3.2.2 Characterization of reservoir fluids

On the basis of pressure and temperature of hydrocarbon fluids, they are divided into five types which are:

- Dry gas
- Wet gas
- Gas condensate
- Volatile oil
- Black oil

These types of different reservoir fluids are the function of temperature and pressure. From their formation to their current existence and the state they are found underneath is highly dependent on temperature. In Figure 3.8, the blue curve represents the border where the existence of liquid and gas depends on both temperature and pressure and an example has been described where water at 15 psi and 100℃ boils and if the temperature is further increased the state of water changes to gas [45].

Among the five types of reservoir fluids, dry gas, wet gas and gas condensate lies in the gaseous side of the plot whereas volatile oil and black oil remains on the other side.

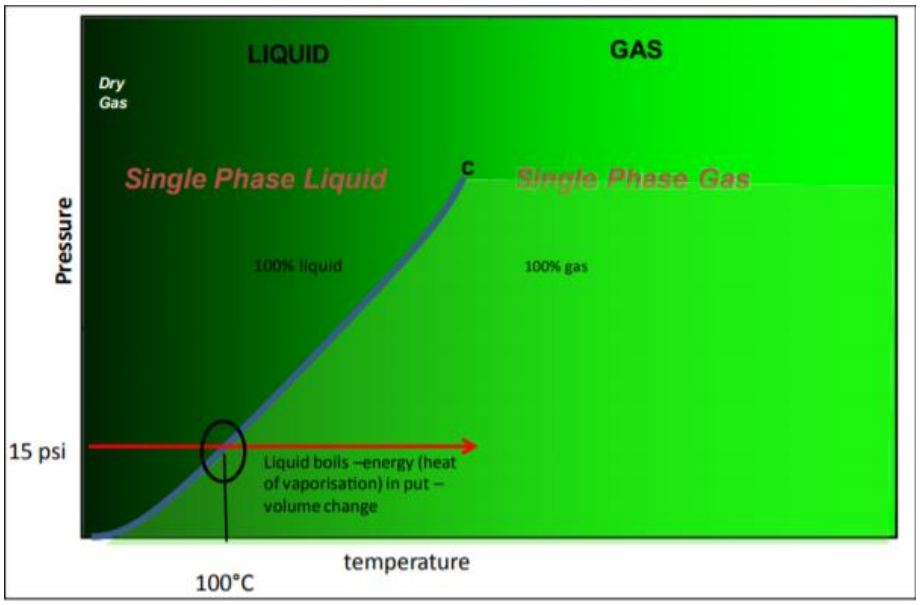

Figure 3.8: Single component pressure temperature relation [45]

Some other properties of these fluids is described in Table 3.2 where the physical appearance of the fluids along with their API value are given.

Table 3.2: Properties of reservoir hydrocarbons [50]

Reservoir fluid	Surface appearance	API gravity (degree)
Dry gas	Colorless gas	
Wet gas	Colorless gas + small amount of clear liquid	60~70
Condensate	Colorless gas with significant amounts of light-colored liquid	50~70
Volatile oil	Brown liquid with various yellow	40~50
Black oil	Dark brown to black viscous liquid	30~40

But in order to understand the properties of multi component fluid system, another phase diagram plotted between temperature and pressure will be required and such a graph is shown in Figure 3.9 in which CP is the critical point and it is the point where all the properties of liquid and gases are equal, the dashed lines represent the percentage of liquid and separator conditions of each type of fluids are shown.

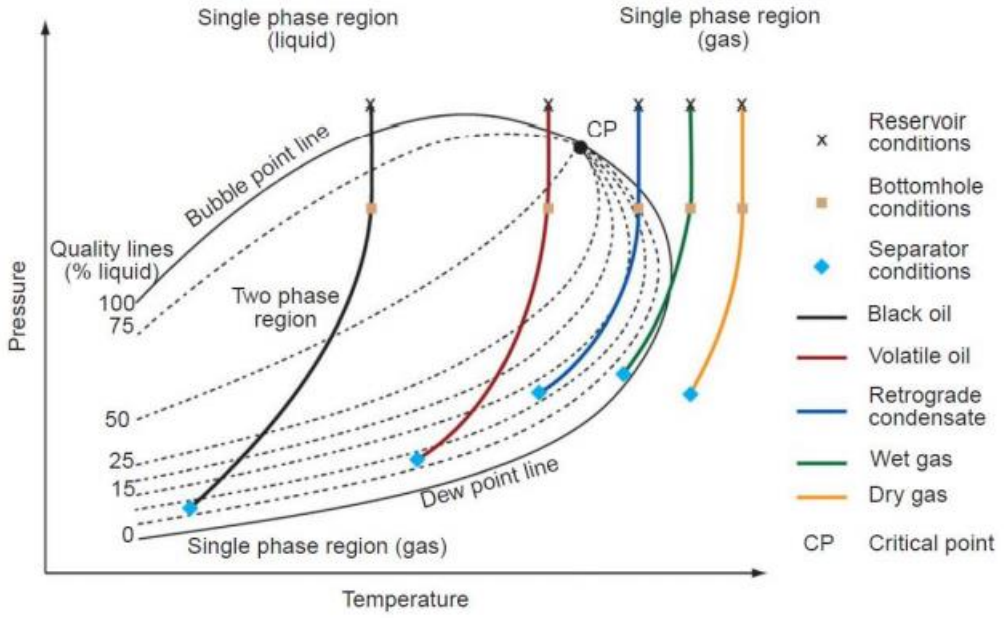

Figure 3.9: Phase equilibrium of multi-component system [9]

- Dry gas

Dry gas is the natural gas that occur without the presence of any liquid hydrocarbons. From the Figure 3.9 for dry gas, the separator conditions fall way out of the phase diagram, so no liquid is formed either in reservoir or at the surface and it is completely gas [51].

- Wet gas

Wet gas is the natural gas which is the mixture of hydrocarbon gas and liquids. Throughout the reduction in reservoir pressure, wet gas exists solely as a gas in the reservoir and no liquid is formed inside the reservoir. However, separator condition in this case lies inside the phase diagram that cause the formation of some liquid at the surface [51].

- Gas condensate

Condensate gas also referred to as retrograde gas is a part gas and part liquid phase where according to the figure the reservoir temperature of the condensate gas reservoir is more than that of the critical temperature of the fluid so at reservoir pressure and temperature, condensate gas is gas. When the pressure in a condensate gas reservoir is reduced, the fluid passes through the dew point, causing large amounts of liquid to condense in the reservoir and because the gas preferentially to oil so most of the oil is unrecoverable but if the dry gas is re-injected keeping the reservoir pressure above dew point, those liquid oil can be recovered [51].

- Volatile oil

Volatile oil is the type which contains heavy molecules and intermediate gas which tends to be very rich and similar to condensate gas. When compared to condensate gas, the phase envelope of a volatile oil tends to cover more wider temperature range and the reservoir temperature is always lower than the critical temperature for the fluid. As the reservoir temperature approaches the critical temperature, a volatile oil becomes more gas-like, to the point where a volatile oil reservoir can flash primarily to gas and have a low liquid content even with moderate depletion [51].

- Black oil

Black oil is the type which contains large, heavy and non-volatile hydrocarbons. According to Figure 3.9, the reservoir condition is above the bubble point line which indicates the fluid is unsaturated and can dissolve more gas in it. When this line intersects the bubble point line, it becomes saturated and can not dissolve any more gas however, any further reduction in pressure causes formation and release of gas inside the reservoir. Additional gas evolved from the oil flows from reservoir to surface which leads to shrinkage of oil due to which black oil are also referred to as low shrinkage crude oil or ordinary oil [51].

3.2.3 Black oil model

Now using the properties of the black oil type of fluid, simulations can be run in multiphase tools which is known as black oil model. This model can be used for any type of reservoir because it can predict compressibility and mass transfer effects between the phases that are needed to model pressure depletion and water injection [55].

3.2.4 Lasater correlation

Black oil model uses many correlations as per the requirement of the reservoir well and the most commonly used one is the Lasater correlation. According to his correlation, with effective molecular weight of the given black oil sample, different carriable can be defined to specify the PVT relation of that crude oil. Below is the Table 3.3, which shows the data used in Laster correlation [52] [56].

Table 3.3: Data used in Lasater correlation [53]

Conditions	Units
$17.9^\circ < \text{API} < 51.1^\circ$	°API
$48 < P_b < 5780$	psia
$82 < T < 272$	°F
$3 < R_{sb} < 2905$	scf/stb
$0.574 < \gamma_g < 1.223$	$\gamma_{air} = 1$

where P_b is the bubble point pressure, T is reservoir fluid temperature, R_{sb} is the solution gas-oil ratio and γ_g is the specific gravity of gas.

3.3 Productivity index

The productivity index is a method for determining the relative ability of wells to produce oil without open flow. When determining productivity index, the well is operated at low rates, eliminating gas waste, the risk of water-coning, and the need for unnecessary oversize and expensive equipment for open-flow potentials. The productivity index is calculated by measuring the pressure differential at the sand face, which only considers the resistance of the

sand or producing formation to yield oil and ignores the resistance of the flow string. It is denoted by *J* and is defined by barrels of oil per day per pound differential between static and bottom-hole pressure (bbl/psi/day) [54].

In order to calculate the productivity index, there are many models proposed in recent years for both vertical and horizontal wells. Babu and Odeh introduced one of the best models that have proven useful in practice for estimating the productivity index of open-hole horizontal wells with a nearly rectangular drainage area and eccentric in the horizontal direction. Figure 3.10 represents the diagrammatic representation of the rectangular drainage area and this figure has been used to the derive the equation 3.26 which is the generalized mathematical expression of this model [9].

$$J = \frac{7.08\times10^{-3}\times b\sqrt{k_x k_z}}{B\mu\left(ln(C_H\sqrt{ah}/r_w)\right)-0.75+S_r} \qquad 3.26$$

where *J* is the productivity index in stb/d/psi, k_x and k_z are the permeability of the reservoir in x and z direction respectively in mD, μ is the viscosity of oil in cP and B is the formation volume factor which is the ratio of gas volume at reservoir condition to gas volume at standard condition and is expressed in bbl/stb.

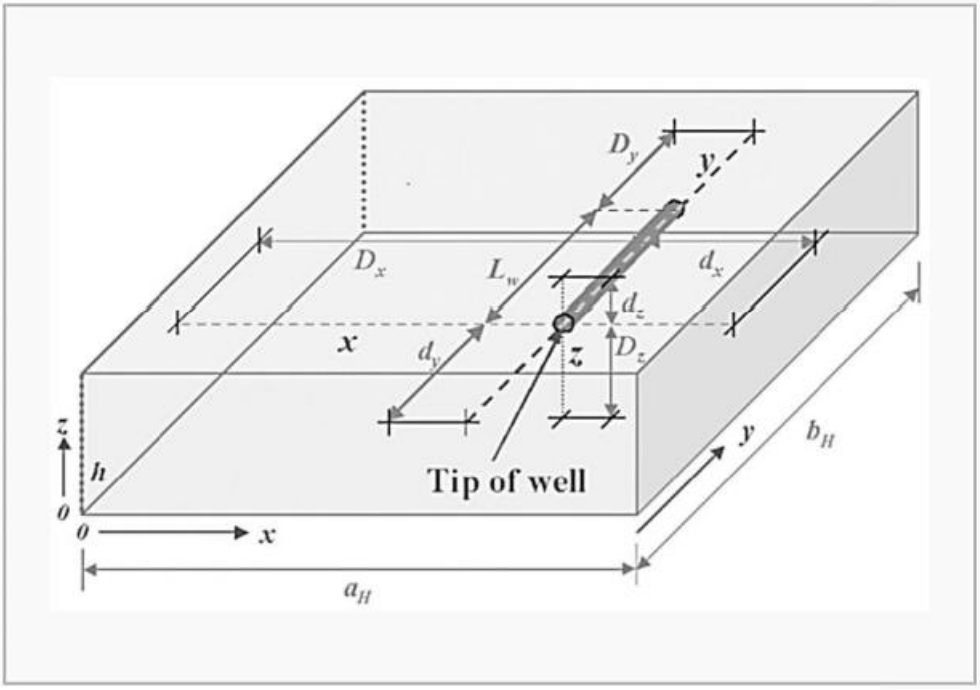

Figure 3.10: Nomenclatures used in Babu and Odeh model for reservoir and well geometry [55]

And the remaining unknow quantities in Equation 3.26 which are a, b and h are the geometric parameters in ft. Also C_H and S_r are Babu and Odeh model's parameters which are the function of geometry of drainage area related to the location of well and the permeability of reservoir in x, y, z direction. To calculate these parameters, equation 3.27 must be satisfied which is [55] [9]:

$$\frac{b}{\sqrt{k_y}} > \frac{1.33a}{\sqrt{k_x}} \gg \frac{0.75h}{\sqrt{k_z}} \qquad 3.27$$

If the parameters satisfies this condition, then the value of S_r can be calculated as:

$$S_r = P_{xyz} + P_y + P_{xy} \quad 3.28$$

where,

$$P_{xyz} = \left(\frac{b}{L_w} - 1\right)\left\{ln\left(\frac{h}{r_w}\right) + 0.25ln\left(\frac{k_x}{k_z}\right) - ln\left[sin\frac{\pi d_z}{h}\right] - 1.838\right\} \quad 3.29$$

assuming, $y_m = d_y + \frac{L_w}{2}$

and,

$$P_y = \frac{6.28b^2}{ah}\frac{\sqrt{k_x k_z}}{k_y}\left[\left(\frac{1}{3} - \frac{y_m}{b} + \frac{y_m^2}{b^2}\right) + \frac{L_w}{24b}\left(\frac{L_w}{b} - 3\right)\right] \quad 3.30$$

when $d_x \geq 0.25a$, then

$$P_{xy} = \left(\frac{b}{L_w} - 1\right)\left(\frac{6.28a}{h}\sqrt{\frac{k_z}{k_x}}\right)\left(\frac{1}{3} - \frac{dx}{a} + \frac{d_x^2}{a^2}\right) \quad 3.31$$

Also,

$$lnC_H = \frac{6.28a}{h}\sqrt{\frac{k_z}{k_x}}\left(\frac{1}{3} - \frac{dx}{a} + \frac{d_x^2}{a^2}\right) - ln\left[sin\frac{\pi d_z}{h}\right] - 0.5ln\left[\left(\frac{a}{h}\right)\sqrt{\frac{k_z}{k_x}}\right] - 1.088 \quad 3.32$$

3.4 Mathematical model of ICDs [9]

As earlier discussed in subchapter 2.4.2 about nozzle/orifice type ICDs which works by passing the fluid through restriction to achieve required pressure and a schematic of ICD is also shown in Figure 2.8. Now dive into the working principles and mathematics of it, Figure 3.11is shown which is the diagram of orifice plate in the middle of the pipe. The flow of fluid inside the pipe and into the orifice is governed by Continuity equation (Equation 3.33) and the Bernoulli's equation (Equation 3.34) that assists to derive a mathematical equation.

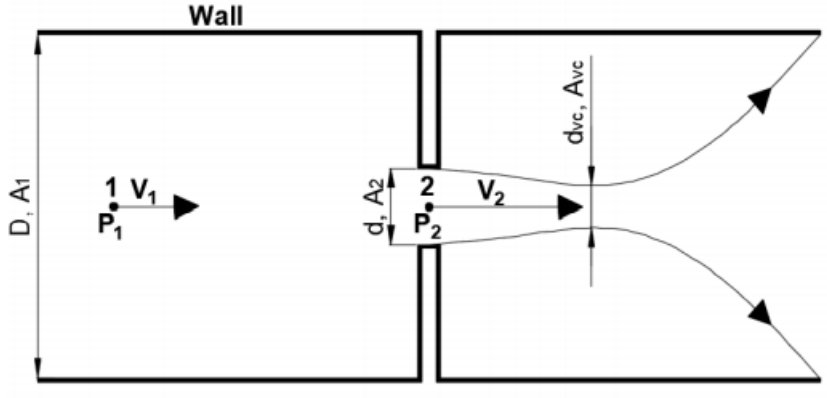

Figure 3.11: Orifice plate inside the pipe [9]

Assuming steady-state, incompressible and laminar flow with uniform velocity at points 1 and 2, the frictional losses can be neglected and also points 1 and 2 are at the same height so continuity equation can be given as:

$$\dot{Q} = A_1 v_1 = A_2 v_2 \Rightarrow v_1 = \frac{\dot{Q}}{A_1}, v_2 = \frac{\dot{Q}}{A_2} \quad 3.33$$

Similarly, Bernoulli's equation can be written as,

$$P_1 + \frac{\rho v_1^2}{2} = P_2 + \frac{\rho v_2^2}{2} \quad 3.34$$

By combining Equations 3.33 and 3.34, we can write the equation as,

$$\dot{Q} = A_2 \sqrt{\frac{2(P_1 - P_2)/\rho}{1-(A_2/A_1)^2}} \quad 3.35$$

Equation 3.35 is only derived for ideal cases and in non-ideal cases $\dot{Q}$ is lower due to the geometric conditions of the ICDs. If C_D is the discharge coefficient, then we can modify the given equation for real cases as,

$$\dot{Q} = C_D A_2 \sqrt{\frac{1}{1-\beta^4}} \sqrt{\frac{2\Delta P}{\rho}} \quad 3.36$$

Here, $\dot{Q}$ → volumetric flow rate of fluid passing through orifice [m^3/s]

ΔP → pressure drop over the orifice plate [Pa]

ρ → density of fluid [kg/m^3]

β → d / D, where d is orifice diameter and D is pipe diameter in meters [-]

C_D → A_2 / A_{vc} [-]

A_2 → Area of cross-section of orifice hole [m^2]

A_{vc} → Minimum jet area just downstream of orifice known as Vena Contracta [m^2]

In orifice type ICDs, we can assume $\beta \rightarrow d / D \approx 0$ because the orifice diameter (d) is very small in compared to the production tubing diameter (D).

If a is parameter representing valve opening and closing such that $0 \leq a \geq 1$, then Equation 3.36 can be re-written as:

$$\dot{Q} = a C_D A_2 \sqrt{\frac{2\Delta P}{\rho}} \quad 3.37$$

This Equation 3.37 is the generalized mathematical equation which describes the flow of fluids inside ICDs.

4 Norne oil field

Norne is an old oil field which was discovered in 1992. It is located 80 kilometers north of Heidrun field and approximately 200 kilometers north of Norwegian coast whose water depth is about 380m. After the discovery of the field, the Plan for Development and Operation (PDO) for this field was approved in 1995 and lastly the production started in 1997. The geographic location of the field is shown in Figure 4.1 [12].

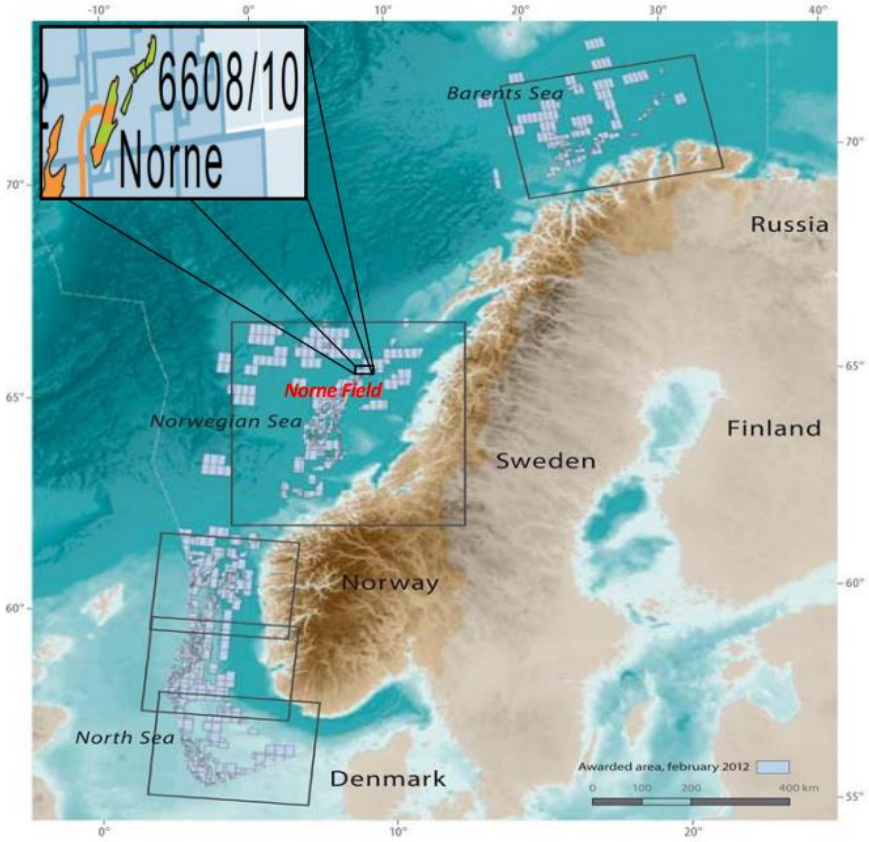

Figure 4.1: Location of Norne field on the Norwegian Continental Shelf [56]

The oil from the field is transported using tankers while the gases are transported using dedicated pipelines. Norne produces oil and gas which are of good quality from lower to middle Jurassic sandstones and the reservoir lies at the depth of about 2500 meters [12].

Norne field started its production of oil in 1997 with The Norwegian Petroleum Directorate (NPD) has estimated that the original recoverable oil quantity from Norne field is 94.68 million Sm^3 while according to the current data the remaining recoverable oil is 3.12 million Sm^3. Currently, the owner of the business arrangement area is Norne Inside and the operation is handled by Equinor Energy AS likewise, the license holding companies are Petoro AS, Equinor Energy AS and Vår Energi AS with share of 54%, 39.1% and 6.9% respectively [12].

4.1 Well 6608/10–D–2H

Since Norne had potential for yielding high amount of oil and gas, there were several wells developed for maximum and optimized extraction of oil. Well 6608/10-D-2H is one of them and for this thesis all the data needed for OLGA/Rocx were taken and calculation were made

from this well. Figure 4.2 shows the location and a small description of the well. Well 6608/10-D-2H has a water depth of 375m, the Total Vertical Depth (TVD) is 2647m and Total/Measured Depth (MD) is 4174m [57].

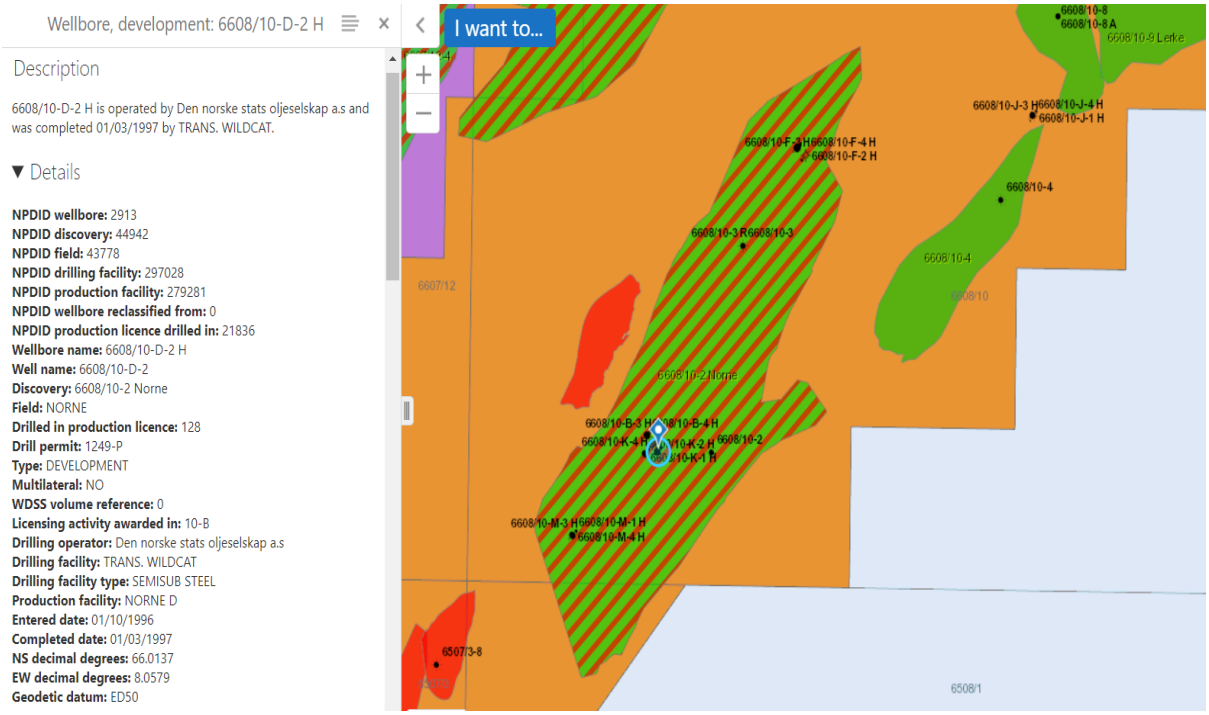

Figure 4.2: Well 6608/10-D-2H location and description [58]

Before a well is developed, an appraisal well is first set where samples of rock and fluids are taken for studies in lab and based on the research production wells around that appraisal well are where the properties of rocks and fluids are almost similar are built. So, appraisal well 6608/10-3 was the assisting well which aided in identifying the properties of well 6608/10-D-2H. Hence most of the properties of rock and fluid parameters were either found from [59] or from Appendix B. In Appendix B, some reservoir information was provided by Equinor Energy AS for study purpose.

4.2 Reservoir characteristics

In the following subchapters, the general pressure, temperature, rock properties and fluid properties of the well is extracted from the NPD page. Also, some of the information which were not available from the NPD page were accessible from others information resources where data were shared by concerning personnel.

4.2.1 Pressure and temperature

In a reservoir, pressure and temperature plays a vital role in its study where together temperature and pressure can help us control the flow and mobilization of the reservoir fluid. The bottom hole temperature of the reservoir is 115 ℃ while to find the pressure value was not straight forward given so, it was approximated from the pressure formation data available in NPD page and was averaged to 277 bar from the graph available in Appendix C [62].

4.2.2 Reservoir fluid properties

Table 4.1 shows the basic fluid properties of well 6608/10-3 which is given by Equinor Energy AS in its report available in Appendix B. In the appendix, a lot of information has been given and Table 4.1 is made to highlight the ones that is required for OLGA/Rocx.

Table 4.1: Reservoir fluid properties values at different temperatures

Parameters	Temperature (℃)	Values
Viscosity	20	13.5 cSt
Viscosity	40	6.19 cSt
Viscosity	50	4.55 cSt
Density	15	0.865 gm/cm^3
Density	Reservoir condition	0.860 gm/cm^3
API gravity	Standard condition	32.0
GOR	Sm^3/Sm^3	82

Value of GOR is not available in the appendix but it is available in [59].

4.2.3 Reservoir rock properties

The rock properties of Norne field is quite unique as compared to other field geologically and these rocks are categorized and named after their formations. All these formations has different thickness and different rock characteristics. The names of these formations are Garn formation, Ila formation and Tofte formation [60]. As studied in subchapter 3.1, it is required to obtained all the values in order to feed the values to OLGA/Rocx which is done as follows.

- Porosity

In Figure 4.3, is the seismic data where the values of porosities of different layers of Norne field's rock is shown. From figure, it is clear that the range of porosity is from 16% to 29%, depending on the type of formation it lies in. Since reservoir fluid is present in all these formations there is no precise value of the porosity hence an average of these value was taken and found to be 0.23 or 23%.

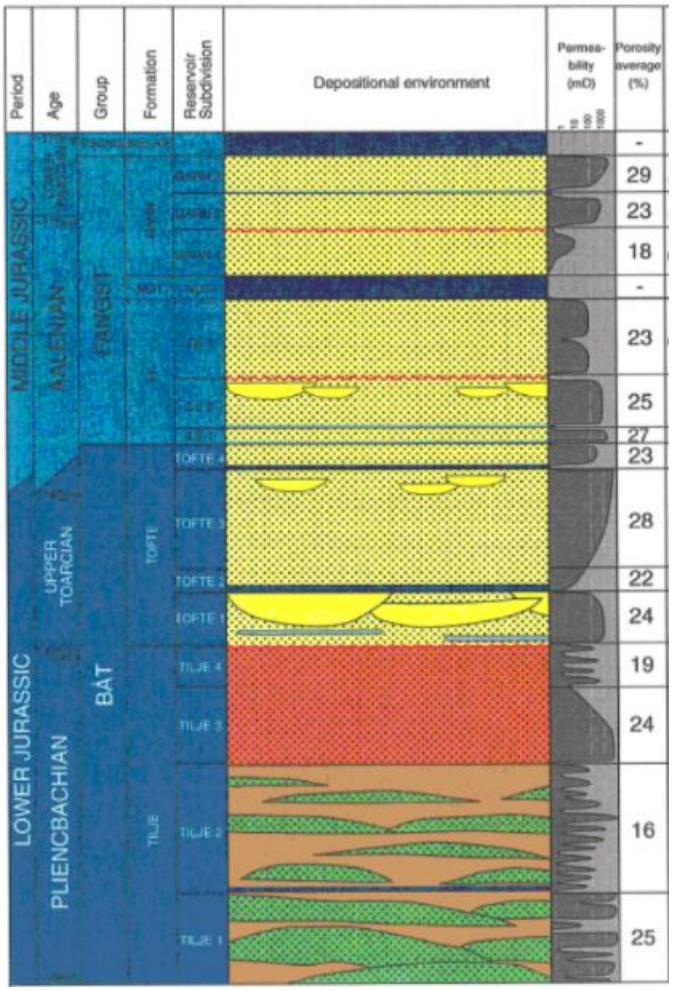

Figure 4.3: Porosity of Norne reservoir [64]

- Absolute permeability

The value of permeabilities due to the formations was also not precise and the value of absolute permeability was calculated as an average of permeabilities in different layers which is available in Appendix D. And from the available data, the value of absolute permeability, *k* was found to be 0.3D or 300 mD.

- Relative permeability and capillary pressure

The data for relative permeability and capillary pressure for different saturations is not available in the NPD factpage so just like absolute permeability, the relative permeability and capillary pressure data is given in Appendix E. The data however can be shown in the graph which is plotted with saturations, relative permeability of water and relative permeability of oil in Figure 4.4.

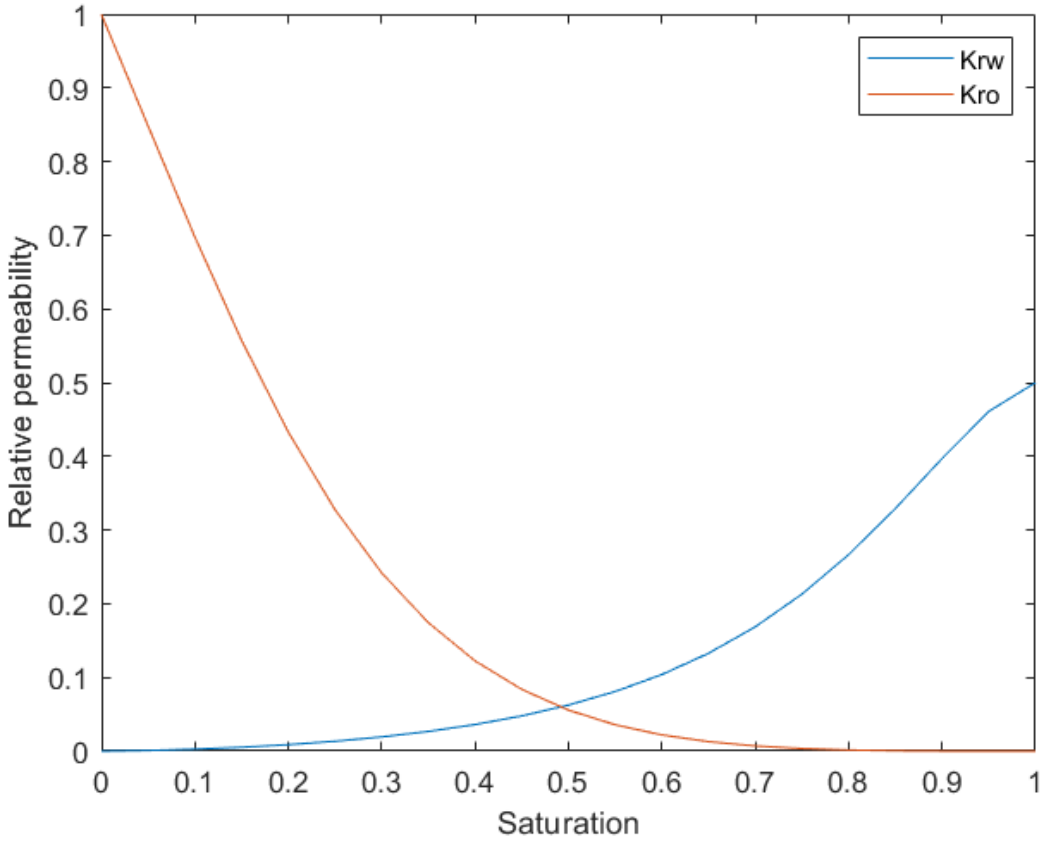

Figure 4.4: Relative permeability curve for Norne field

In Figure 4.4, k_{rw} is the relative permeability of water and k_{ro} is the relative permeability of oil.

- Reservoir length and thickness

The dimension of reservoir is also a major parameter because for the simulations in OLGA/Rocx a suitable and accurate approximation of well must be made for the results to be good. The lengths of the well is already present in [57] where the Total/Measured Depth is 4174m and Total/Final Vertical Depth (TVD) is 2647m. Similarly, for the thickness of well using the data appraisal well 6608/10-3 from [59] and [60], the thickness was found to be 135m.

- Rock compressibility

The value of rock compressibility usually ranges from 1.5×10^{-6} to 20×10^{-6} 1/psi according to [64] and the value was considered to be 0.0001 1/bar that is approximately 1.4×10^{-5} 1/psi.

5 Methods and calculations

In this chapter, the calculations that are to be done to feed the values in OLGA/Rocx are done for the parameters whose values are yet to be found.

5.1 Oil Viscosity

From Appendix B, the values of viscosities at different temperatures are already given but in the value of viscosity at reservoir condition of Norne field is still unknown. This can be achieved by a linear regression method where we can use the given values of viscosity at different temperatures. But before that a mathematical model is required to define temperature and viscosity while the effect of pressure being neglected on viscosity is assumed. So, Equation 5.1 is a commonly used empirical relation between viscosity and temperature [9] [61].

$$\mu = Ae^{B/T} \qquad 5.1$$

where μ is viscosity [cP], T is temperature[K] and A and B are unknown constant parameters which should be defined empirically. So taking logarithm in both sides, Equation 5.1 becomes,

$$ln\,\mu = ln\,A + B/T \qquad 5.2$$

Now, writing equation in matrix form,

$$ln\,\mu = [1 \quad 1/T]\begin{bmatrix} lnA \\ B \end{bmatrix} \qquad 5.3$$

which again can be written in the form of

$$y = \varphi^T(x)\theta \qquad 5.4$$

Here, by considering the value of $y = ln\,\mu$, $\varphi^T = [1 \quad 1/T]$ and $\theta = \begin{bmatrix} lnA \\ B \end{bmatrix}$, it is possible to solve the equation and find the values of A and B. The values given in Table 4.1 can be used to plug in the values of temperature and viscosity. So, to calculate the value of viscosity in reservoir condition that is at 115℃ (388K) curve fitting is done with the values obtained from linear regression and MATLAB code available from [9] is used to extrapolate the value and figure 5.1 is obtained where it can be seen at temperature 388K the viscosity was found to be 0.471cP .

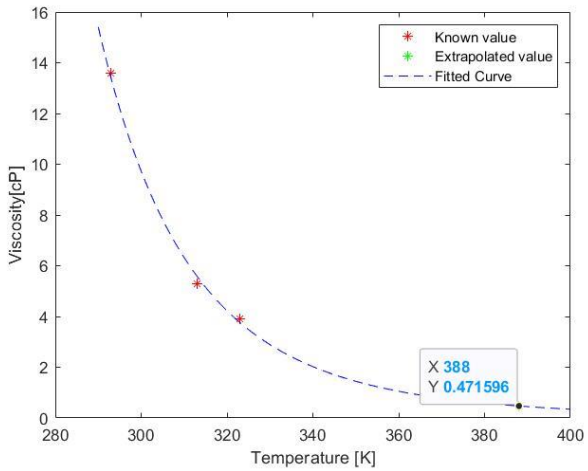

Figure 5.1: Extrapolated value of viscosity at reservoir condition

5.2 Horizontal length of well 6608/10-D-2H

For the calculation of horizontal length of well, Figure 5.2 can give the insight of Total Vertical Depth (TVD) and Measured Depth (MD). Also, for the calculation of horizontal length ($L_{horizontal}$) another parameter called kickoff length ($L_{kick\text{-}ff}$) is required. As discussed in subchapter 2.3.2 about kickoff point, which is the point from which the deviation starts for drilling the hole in horizontal direction, its length is also needed to determine.

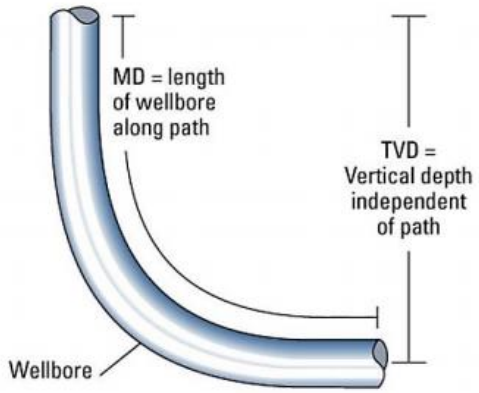

Figure 5.2: Diagram of Measured Depth and Total Vertical Depth [9]

The horizontal length can be calculated using equation 5.5 which is

$$L_{MD} = L_{TVD} + L_{horizontal} + L_{kickoff} \quad 5.5$$

The calculation of horizontal length of well 6608/10-D-2H is available in Appendix F where it is found to be 945m.

5.3 Frictional pressure drop of well 6608/10-D-2H

The flow of the fluid is highly affected by the friction in the pipe which is caused by viscosity within the liquid and the turbulence that occurs around the surface of the wall of pipe which again is caused by the roughness of the material of the pipe. This resistance is usually referred to as the pipe friction or frictional pressure drop [62]. The calculation of this pressure drop can be achieved using Darcy-Weisbach equation which is shown in equation 5.6. If L is the length of the pipe in meter, μ is the viscosity in cP , ρ is the density of fluid in kg/m^3, v is the velocity of fluid in m/s, D is the diameter of the pipe then frictional pressure drop (ΔP_f) is given by Darcy-Weisbach equation as,

$$\frac{\Delta P_f}{L} = \frac{f \rho v^2}{2D} \quad 5.6$$

where f is the Mody friction factor which depends on the type of flow inside the pipe. If the flow is laminar, Mody friction factor can simply be calculated by using Equation 5.7 which is,

$$f = \frac{64\mu}{\rho v D} \quad 5.7$$

where $\rho vD/\mu$ is the Reynold's Number (Re).

But in practical cases, most of the time the flow is turbulent and not laminar. So, when the cases are turbulent Mody frictional factor becomes the function of roughness of the pipe (ε).

Therefore, an equation which has the correlation between the friction factor and roughness of the pipe is needed which is given by Colebrook-White equation [62] [9].

$$\frac{1}{\sqrt{f}} = 1.74 - 2log\left(\frac{2\varepsilon}{D} + \frac{18.7}{Re\sqrt{f}}\right) \qquad 5.8$$

All the values required for the calculation of frictional pressure drop is calculated or given in Appendices but the diameter and roughness of the pipe is given in [63] which are 5.5 inches = 0.1397 m and 0.00015 m respectively. Lastly, using the MATLAB code available in the appendix of [9], the frictional pressure drop was calculated to be 0.182 bar.

5.4 Permeability anisotropy

Permeability anisotropy as discussed in sub chapter 3.1.4.2 is the ratio of vertical permeability (k_v) to horizontal permeability (k_H). The well 6608/10-D-2H of Norne field is divided into several layers and each layers or formations has different values of permeabilities so these layers are called as zones and each zone has the values as shown in Table 5.1.

Table 5.1: Zones thickness and the values of its rock parameters [60]

Zones	Net pay thickness[m]	Porosity	Permeability [mD]	Average V_{sh}	Average S_w
Zone 1	35	0.2	580	0.31	0.36
Zone 2	46	0.24	495	0.15	0.20
Zone 3	55	0.27	1087	0.14	0.32

After having these data, it is possible to calculate the values of relative permeability is x, y and z direction and hence the value of permeability anisotropy can be calculated. Equation 5.9 is the formula to calculate average shale volume ($V_{sh,average}$),

$$V_{sh,average} = \frac{h_{zone1}.V_{sh,zone1} + h_{zone2}.V_{sh,zone2} + h_{zone3}.V_{sh,zone3}}{h_{zone1} + h_{zone2} + h_{zone3}} \qquad 5.9$$

here, h_{zone1} , h_{zone2} , h_{zone3} are the net pay thickness of the zones and $V_{sh,zone1}$, $V_{sh,zone2}$, $V_{sh,zone2}$ are the average shale volumes of the zones. Therefore, using Equations 3.12, 3.13, 3.14 and 5.19 the value of permeability anisotropy a is found to be 0.257 for which the calculation is given in Appendix F [9]. Also the results obtained from calculations are presented in Table 5.2

Table 5.2: Values of parameters used in calculating permeability anisotropy

Parameters	$V_{sh,average}$	k_x	k_y	k_z	a
Values	0.187 m	0.469 D	0.469 D	0.121 D	0.257

5.5 Productivity index

As previously discussed in subchapter 3.3 about the productivity index, this parameter can be calculated using Babu and Odeh model. So, using equations 3.26 to equations 3.32, calculations are done shown in Appendix F and the value obtained from the calculation is , J = 928.16 stb/d/psi or 2140 m^3/d/bar .

5.6 Pressure drawdown

The differential pressure that helps in the movement of reservoir fluids from a reservoir into the wellbore is known as pressure drawdown. There is a pressure drop along a horizontal wellbore due to frictional losses in flow. If the pressure drop is significant compared to drawdown, the pressure far down hole could nearly equal the reservoir pressure, rendering a portion of the well unproductive. Therefore, frictional loss inside pipe can reduce the productivity. In Figure 5.3, the graph of drawdown pressure along the length of pipe is shown and it is clear from the graph that the horizontal well's producing end will be at a lower pressure than the other tip [64] [65] [66].

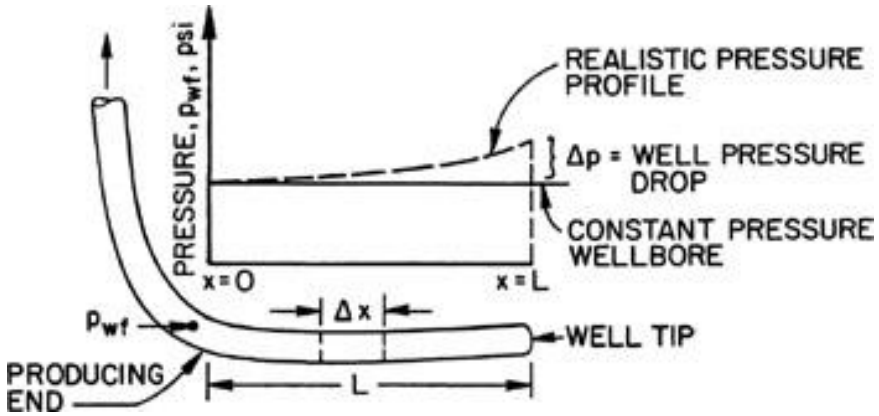

Figure 5.3: Pressure profile along the length of pipe [66]

In the figure, the horizontal well represents a long wellbore with consistent well pressure throughout but in practice maintaining fluid flow within the wellbore requires some pressure drop from the tip of the horizontal wellbore to the producing end [66]. Therefore, some pressure drive is needed to overcome this pressure to keep the reservoir fluids moving inside for smooth production.

In this thesis, the well 6608/10-D-2H of Norne field is assumed to be homogenous and only ICD valves have been used to design in OLGA, the significance of calculating pressure drawdown would increase if the reservoir was heterogenous and if AICD valves have been used but, in this case, none are used hence a suitable value was approximated for the pressure drawdown which is 12 bar.

6 Development of model

From all the chapters above, the necessary data needed to model the well 6608/10-D-2H of Norne oil field are found from various sources. Now the next step is to create a model of the well that is very similar to that of the real well 6608/10-D-2H. In this chapter, the preparation of Rox model is discussed at first then OLGA model is discussed and finally the cases that are to be simulated are briefed.

6.1 Development of Rocx model

In this subchapter, the input parameters needed to model the well are being interpreted. Those parameters include grid setting, reservoir and rock properties, relative permeability and capillary pressure, initial and boundary conditions and time step input.

6.1.1 Drainage area

To prepare a grid for reservoir model, drainage area of the near-well reservoir must be made. In actual practice the area of the drainage is ellipsoidal as shown in Figure 3.5 in subchapter 3.1.4.2. But in while modelling in Rocx, it is not possible to feed the data for ellipsoidal area hence close to ellipsoidal area is a rectangular and for drainage area of well, rectangular well is considered. So, using the dimensions previously calculated, the length of the drain in x direction is 992 m. It should be noted that originally the length of the well was found to be 945 m but it is an approximation length which could be more or less than the calculated value. Later while dividing the wellbore in sections, considering the length of the well as 992 m was easier and did not affect the output of the well. Similarly, the thickness of the near-well reservoir in z direction was 136 m.

After this, the size of width was required for the completion of drainage area, so an assumption was made for the width to be twice the thickness which is ≈ 270 m. This selection was made on the basis of [9] where after the mesh completion of the model in that paper the width was found to be twice the thickness.

Now based on the dimensions, geometry of drainage area was drawn to visualize the near-well reservoir which is shown in Figure 6.1.

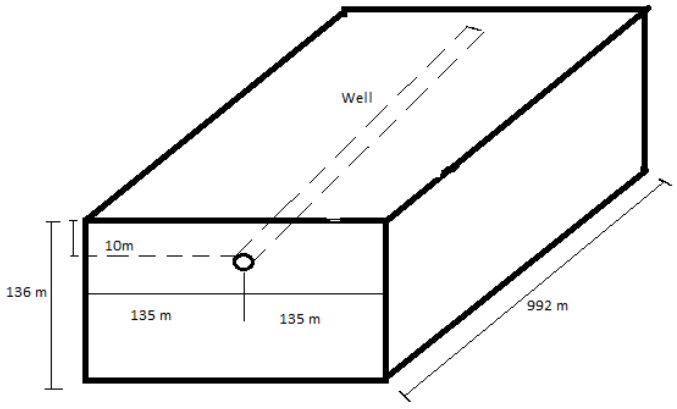

Figure 6.1: Geometry of the drainage area

In this figure, it should be noted that the near-well reservoir is placed in the middle of the width of drainage area while it is placed only 10 m below the surface because the farther the well is from the aquifer, the more is the delay in water breakthrough.

But since the width of drainage area is just an approximation, five different cases were done with length and thickness of the well keeping constant while changing the width of the well as shown in Table 6.1.

Table 6.1: Different simulation cases for the selection of width of drainage area

Cases	Width [m]	Thickness [m]	Length [m]
Case 1	230	136	992
Case 2	250	136	992
Case 3	270	136	992
Case 4	290	136	992
Case 5	310	136	992

With the widths of 20 m difference higher than the approximated value as well as lower than the approximated value, simulation was run in OLGA for 200 days and the graph shown in Figure 6.2 was obtained.

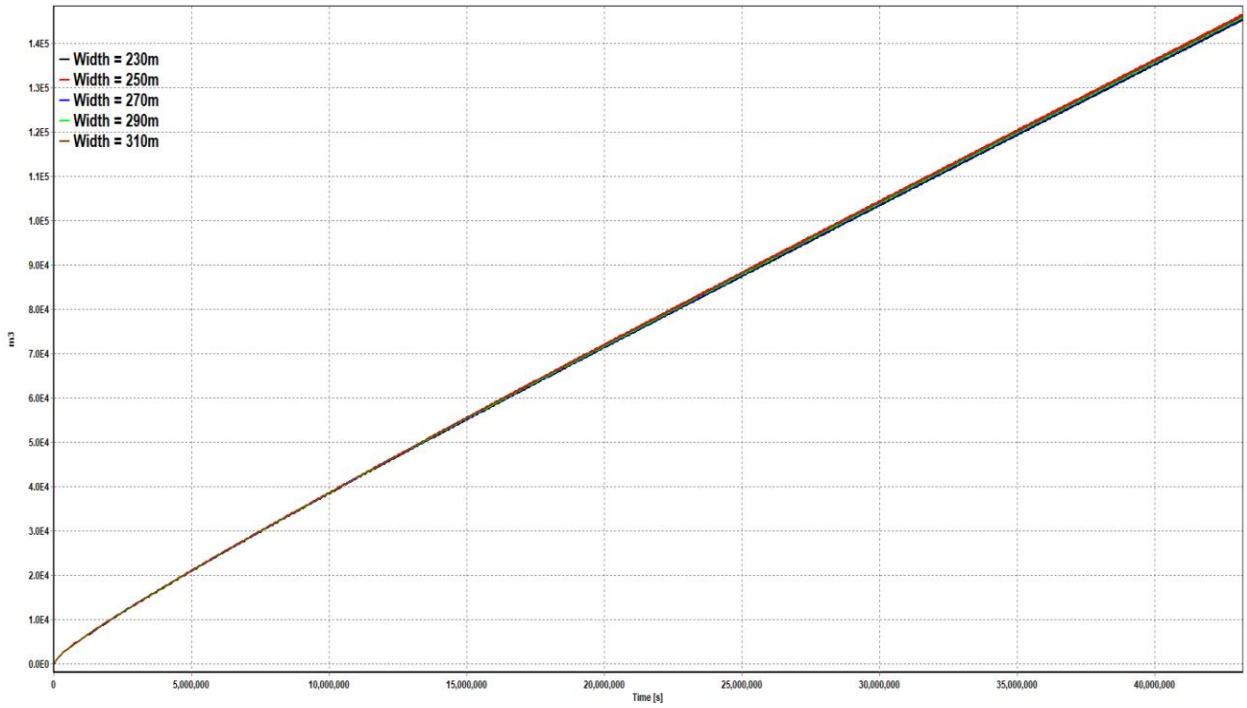

Figure 6.2: Simulated cases for different widths of drainage area

From Figure 6.2, it can be seen that all the widths have started the production with the same accumulated volume of oil in the start and at the end of 200 days, there is not much difference in the production of accumulated volume of oil. From this result, the width of drainage area was changed from 270 m to 230 m because while setting up the mesh of the drainage area, the less is the number of cells the faster is the simulation, given that the change in width does not affect the production volume.

6.1.2 Grid setting

The grid setting in Rocx is the first step of modeling the reservoir where in easy words the drainage area created in Figure 6.1 must be set up in an appropriate mesh or discretized the reservoir for the simulation in OLGA/Rocx. Firstly, number of grids must be entered for x, y and z directions which is a challenging task. Now this value must be chosen in an optimized way because if the number of cells in the grid is higher it can increase the time of simulation. This can be achieved in two ways where in the first method a grid of equal mesh size can be made but because the pressure variation in the hole is higher in the areas close to the well and least when it is away from it which can be shown in Figure 6.3. Hence, the resolution close to the well will not be good enough to show the accuracy of the well.

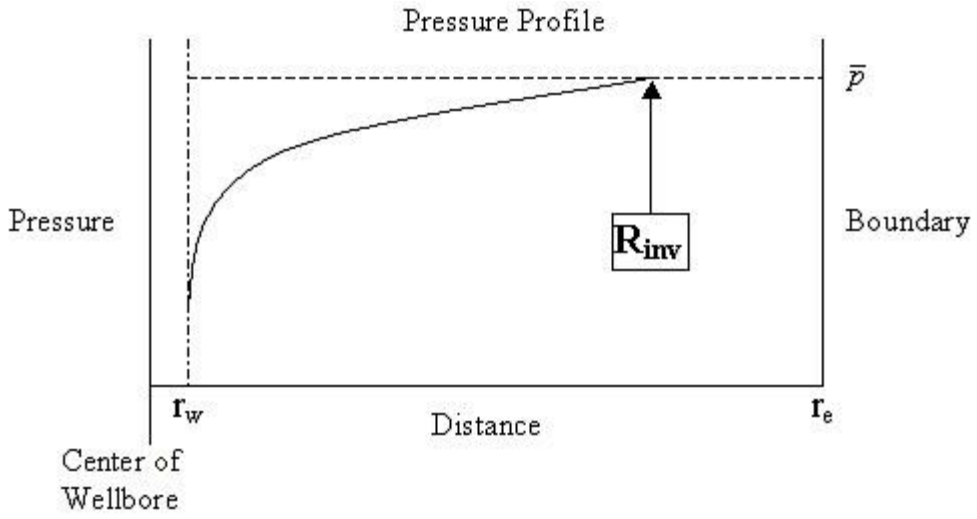

Figure 6.3: Variation of pressure

Therefore, the second method where the mesh is finer where the pressure is high and coarser where the pressure is low, can be used. In this way the resolution of the mesh is not altered, and the results obtained is much better than the previous method in the same simulation time.

The number of grids chosen for *nx, ny, nz* are 8, 19 and 12 respectively. Here, the value of *nx* was chosen 8 because the length of the well is 992 m and the standard ICD size is 12.4 m. In the production tubing of Norne reservoir ICD along with other components are used to develop the model hence in the x direction the length of reservoir was divided in 8 uniform zones or cells with the length of 124 m each that sums up to 992 m.

The fluid flow and the pressure variation inside the wellbore is only properly visible in Y-Z plane so, the mesh in these planes is not uniform as in x direction. The grid size is then defined in *ny* and *nz* direction as 19 and 12 where the grid block sizes as set coarser away from the well and finer near the well as shown in Figure 6.4. The grid block sizes can be entered for both

radial and rectangular (cylindrical and cartesian coordinates systems) and input is given in rectangular since our drainage area is rectangular. The direction vector for gravity can be denoted in (x,y,z) coordinates and since the gravity is acting in z direction it can be written as (0,0,1).

The number of grids in y and z direction will have to be changed and analyzed before the actual simulations is started because the change in the number of grids may affect the result. Therefore, mesh sensitivity analysis is done to check if the number of grids in y and z directions are suitable enough to use for the simulation in OLGA/Rocx. In order to analyze the number of grids in y direction, 3 cases will be simulated where the value of *ny* is change from 19 to 36 and 57 keeping all other parameters constant and similarly, for the number of grids in z direction, 3 cases will be simulated where the value of *nz* is changed from 12 to 24 and 48.

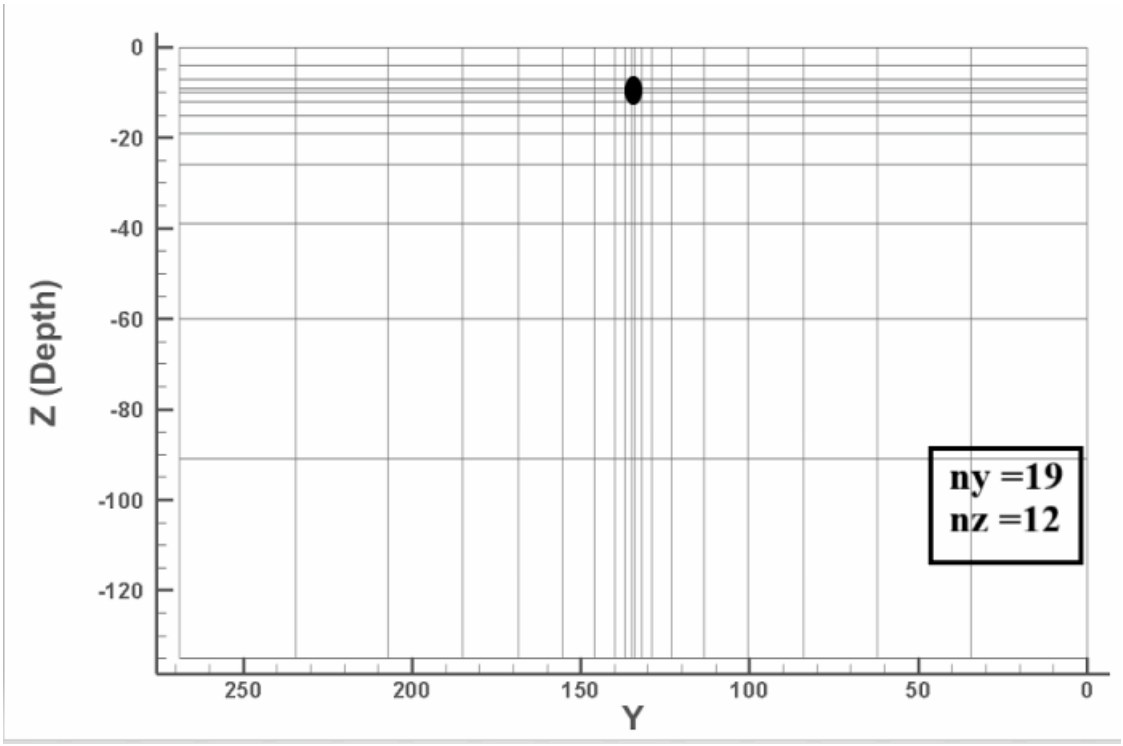

Figure 6.4: Mesh refinement in y and z direction

6.1.2.1 Mesh sensitivity analysis in y direction

For the sensitivity analysis of number of grids in y direction, the value of *ny* in Rocx is change for 19, 39 and 57 and a graph is plotted against time and accumulated volume of oil and water and volumetric flow rate of oil and water for 200 days shown in Figure 6.5. The figures shows that the accumulated oil volume as well as volumetric flow rate of oil for *ny* 19 and 57 does not have much difference while the accumulated volume of water and volumetric flow rate of water seems to have no changes which is not possible in real practice. But even when the refinement of mesh until 57 grid size does not shows the water inside the reservoir then there is a chance that change of grid size in z direction may show some good results. Hence, fo the number of grids in y direction the value of *ny* can be set to 19.

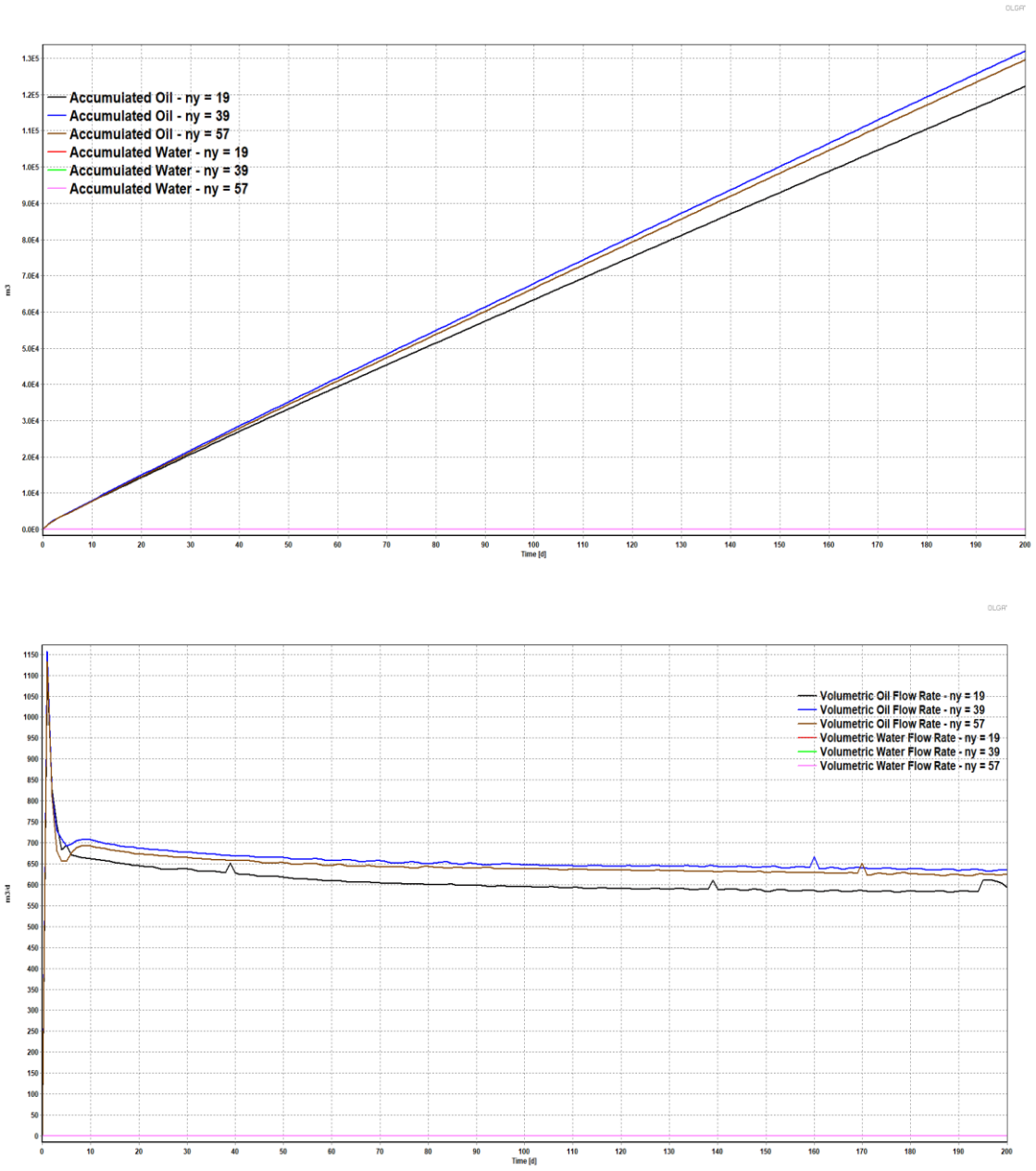

Figure 6.5: Accumulated volume (up) and volumetric flow rate (down) of oil and water for different values of number of grids in y direction

6.1.2.2 Mesh sensitivity analysis in z direction

Similarly for the sensitivity analysis of grid block size in z direction *nz* is varied to 12, 24 and 48 for accumulated volume and volumetric flow rate of oil and water keeping all other parameters same for 200 days. Figure 6.6 shows the result obtained after the simulation and observing the graph, it shows the same results for the accumulated volume and volumetric flow rate of oil as it did for the cases of *ny* but with *ny* = 12 there is still no water seen in the reservoir however water starts showing when the grid size is changed to 24 and 48. But as already mentioned that the number of cells must be optimized, *nz* = 48 yields to higher number of cells therefore for the base case *nz* is selected 24.

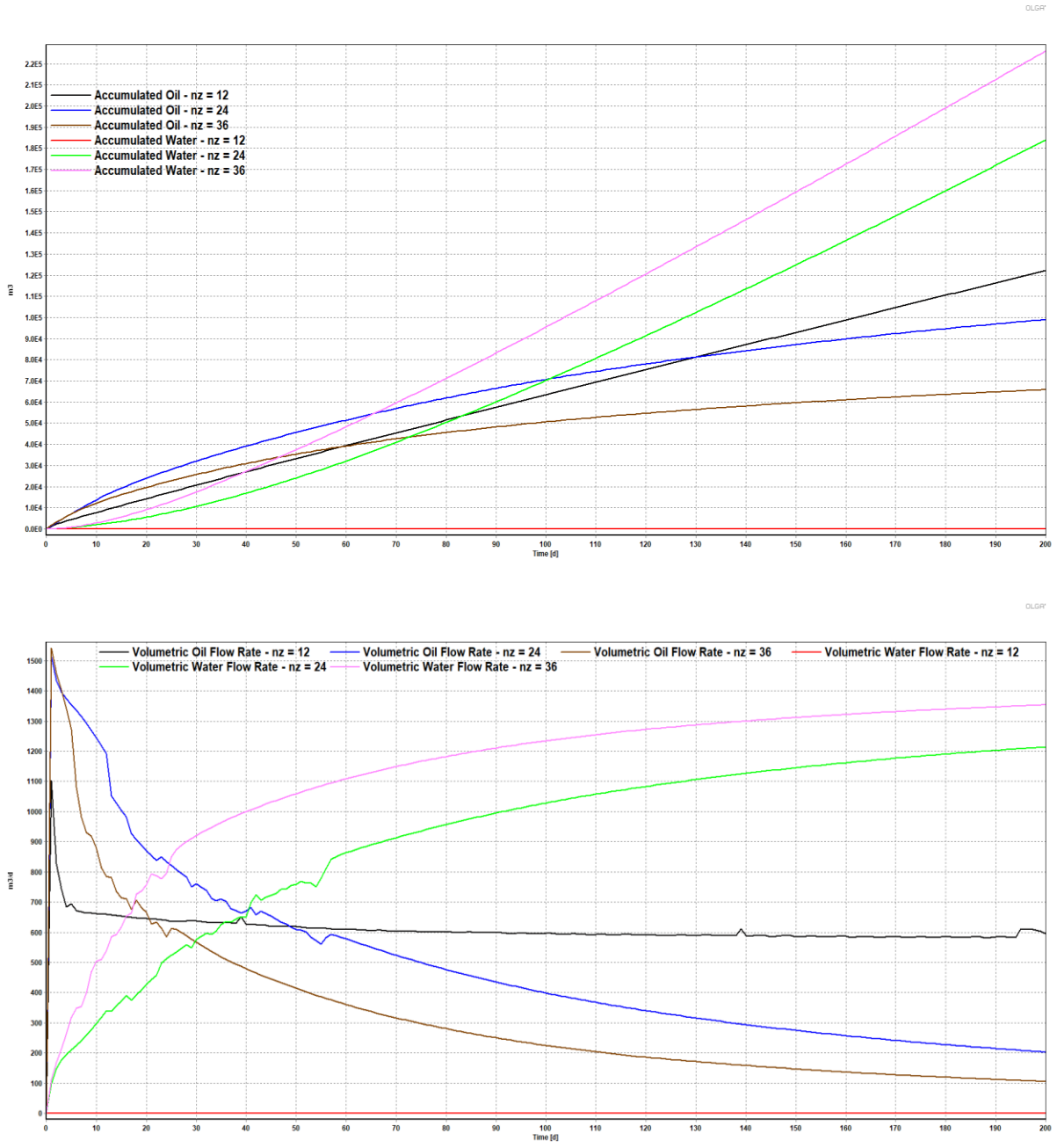

Figure 6.6: Accumulated volume (up) and volumetric flow rate (down) of oil and water for different values of number of grids in z direction

6.1.2.3 Final grid setting for base case of model

Therefore, for the base case model of the well 6608/10-D-2H of Norne oil field, by the help of sensitivity analysis, the final number of grids in y and z directions are 19 and 24 respectively. The mesh refinement after the selection of final mesh sizes are shown in Figure 6.7 and in the figure note must be taken that the grid sizes are not in the scale.

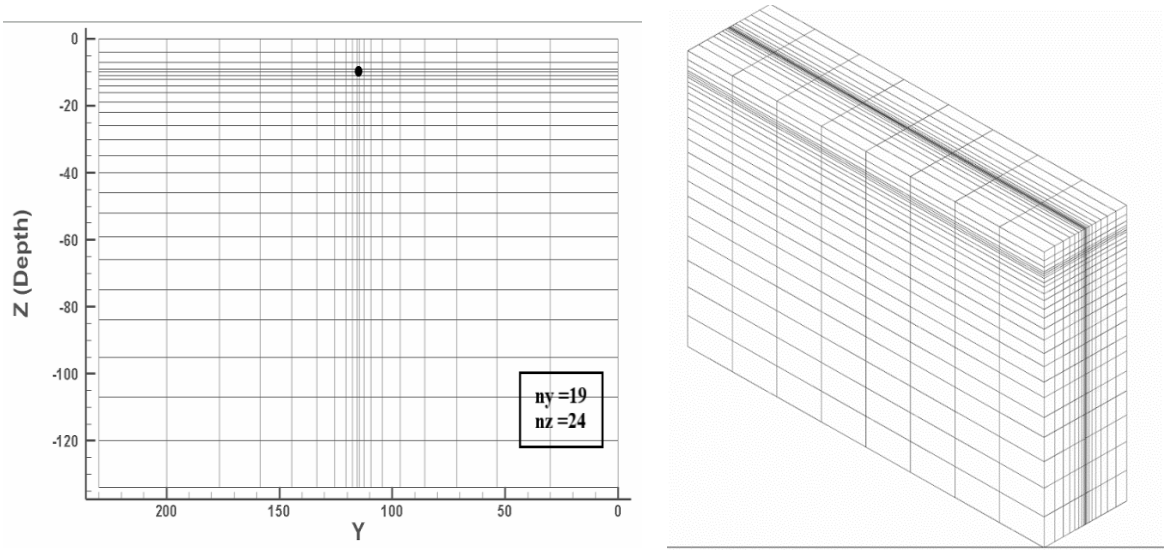

Figure 6.7: Final grid setting for base case model in YZ direction and in 3D

Likewise, the sizes of grid block sizes are shown in Table 6.2 where the values of each blocks in x direction is same while the sizes in y and z directions are as such.

Table 6.2: Number of grids and mesh block sizes for base case of well model

Directions	Number of grids	Size [m]
x	nx = 8	124
y	ny = 19	30,23.5,18,14,11,8,5,3,2,1,2,3,5,8,11,14,18,23.5,30
z	nz = 24	4,3,2,1,1,1,2,2,3,3,4,4,5,5,6,6,7,7,9,9,11,12,13,14

6.1.3 Fluid properties

The fluid properties that are discussed in subchapter 3.2 are specified here. Firstly, there is an option of PVT table and Black oil. Now, PVT module uses lookup table with one fluid however Black oil module gives us the option of feeding more parameters in which the properties of the fluid can be defined in descriptive way. Moreover, Black oil selection is also dependent on API as shown in table 3.2 which in this case is 32 so it is the most favorable choice. Previously mentioned that Black oil model can be solved by many correlations among which Lasater is the most common one so it is selected in GOR model, the fraction type used is the mass fraction. After that the fluid properties are fed with the values as shown in Table 6.3

Table 6.3: Fluid properties parameters values for Rocx

Parameters	Values
GOR	82 Sm^3/Sm^3
Gas specific gravity	0.64
Oil specific gravity	0.86

Viscosity	0.47107 cP
Temperature	115℃
Pressure	277 bar

After these inputs, there is an option for feed oil and feed water which defines the water drive properties of Norne oil field. Table 6.4 represents the values provided to the feed.

Table 6.4: Oil and water feed components

Feed	Gas fraction	Water cut
Oil component	82 (GOR)	0.0001
Water component	0.0001 (GLR)	0.99

6.1.4 Reservoir properties

In the reservoir properties, the rock properties of Norne oil field is to be provided. There are some assumptions made while entering the inputs to the parameters which are the porosity of the Norne oil field is considered to be constant everywhere and the rock thermal properties has no effect on the production hence in Rocx it is marked off. The permeabilities in x, y and z direction asked to input is in radial directions but while modeling, a rectangular drainage area is considered. The values of these permeability along with permeability anisotropy is already being calculated in Appendix F and rest of the input values are shown in Table 6.5.

Table 6.5: Reservoir properties of Norne oil field

Parameters	Values
Porosity	0.23
Rock compressibility	0.0001 1/bar
Reference pressure of rock compressibility	1 bar
Permeability in x direction	469 mD
Permeability in y direction	469 mD
Permeability in z direction	121 mD

6.1.5 Relative permeability and capillary pressure

The relative permeability data is provided to the modules by the data provided in Appendix E. Here, in the residual saturations module the values of water connate saturation (*swc*) is 0.05, residual oil saturation (*sor*) is 0.1 and residual gas saturations (*sgr*) is zero. These values were approximated from the data and graph obtained in figure 4.3. Here, residual gas saturation is

zero because it is assumed that there is no gas production in reservoir. However, it is discussed in subchapter 3.2.2 that when the black oil goes through pressure reduction below the bubble point line, there is a release of gas inside the reservoir and considering this situation the relative permeability of gas is also fed to the module of relative permeability of gas. The values of relative permeability of oil, water and gas for different values of saturation is plugged in.

Likewise, the capillary pressure data is available in same appendix for different saturations and only the capillary pressure of oil water is considered while for oil gas is kept zero.

6.1.6 Initial condition

Initially the reservoir is saturated with oil so, feed oil module is defined to be almost pure (fraction value = 1). The values of temperature and pressure are same as provided in fluid property setting which are 115℃ and 277 bar respectively. As for the values of saturations of water (s_w), oil (s_o) and gas (s_g) , they are 0.3, 0.7 and 0 respectively.

6.1.7 Boundary condition

In boundary condition, there are two tabs for well pressure and reservoir pressure. In well pressure well the length of the well that was discretized in x direction into 8 uniform zones in subchapter 6.1.2 must be defined. So, well source as P1 to P8 is defined in each zones. In each of these zones, the values of (*ix, iy, iz*) must be defined. Value *ix* defines well position in x direction in the first zone (P1) until last zone (P8), *iy* and *iz* defines the well position in y and z direction respectively where their position are set in the block sizes of grid as 10^{th} and 4^{th} position in y and z direction. The direction index of well iDr is 1 because well trajectory direction is along radial x direction. The temperature, pressure and saturations of oil, water and gas must also be fed to the feed oil component for each well sources. Finally the diameter of the wellbore is set be 0.2286 m.

Because of the presence of aquifer, the pressure reservoir has feed water option with temperature and pressure values given same as before but since there is no oil in aquifer the value of water saturation is 1.

6.1.8 Simulation

In simulation tab, the values of minimum time step was set to 0.01s and the maximum time step was 10000 s for the simulation to run.

6.1.9 Model completion

When all the above mention parameters are provided in Rocx a proper file name must be assigned and after pressing the run command on the top of the task bar, a dialogue box appears which either shows error if there is something wrong with parameters input or if every parameters are correct dialogue box shown in figure 6.8 appears which says Rocx is done.

6.2 Development of OLGA model

OLGA is the main program to run the simulations and it has many settings and addition of components to build a proper model which must appear close to well 6608/10-D-2H of Norne oil filed. These settings are explained and the model that was designed in OLGA is shown in

Figure 6.8. The upper figure illustrates the left end of the model where both in production tubing and wellbore the flow is zero. The near-well source extracts the information of reservoir from Rocx file attached to it. Then, there is valves in each section boundary from which the fluids enter into the wellbore. Similarly, leaks are the connectors of wellbore and production tubing whereas packers divide two different zones. For 8 zones the model has same component except at the end of the right end of the model is pressure node outlet. This pressure node creates the pressure difference between the production tubing and wellbore that makes the reservoir fluid to move towards the pressure node.

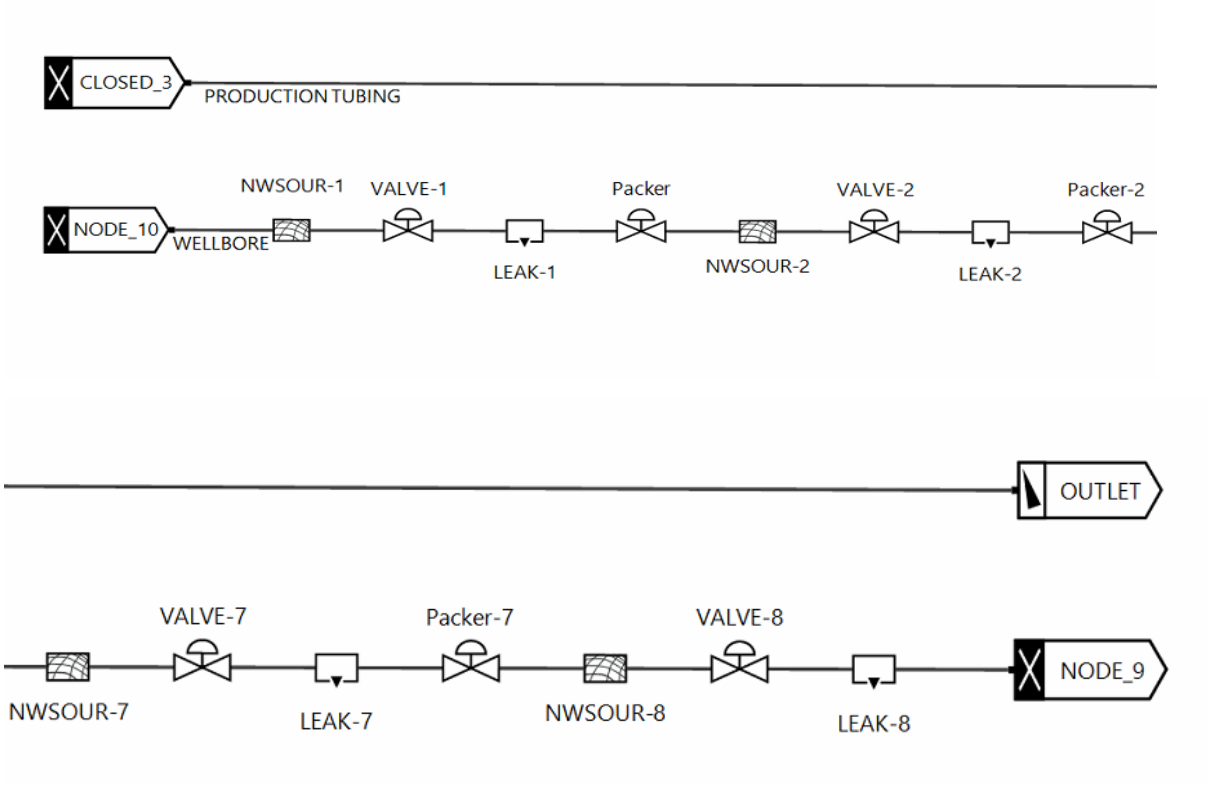

Figure 6.8: OLGA model of well 6608/10-D-2H of Norne oil field

6.2.1 Case definition

In case definition, a PVT file defining three phase system is used for developing OLGA model and an integration time is given for minimum time step of 0.01 s , maximum time step of 10000 s and the case is simulated for 200 days.

6.2.2 Composition

Three Black oil components for oil, water and gas must be defined in this setting since the simulation is being run for all three components and it should be the same values as defined in Rocx. Also, water drive and oil drive is defined same as done in Rocx.

6.2.3 Flow component

The flow component describes about the properties of components being used in production tubing and in wellbore. As shown in Figure 6.8, the OLGA model for well 6608/10-D-2H of

Norne oil field, to understand it better, a simplified diagram of how the models are designed with the components is shown in Figure 6.9.

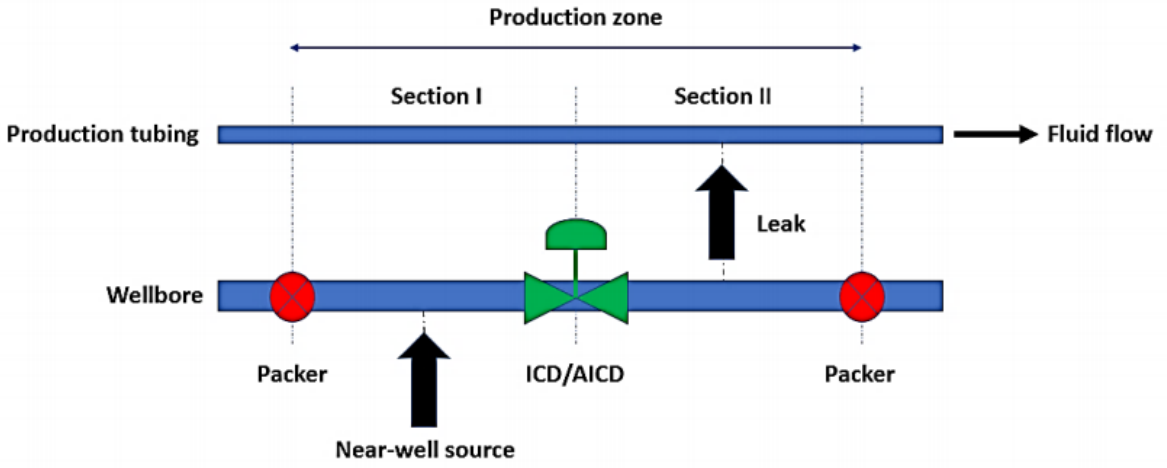

Figure 6.9: Diagrammatic representation of a simple OLGA model with its basic components [9]

From the Figures 6.8 and 6.9, it is shown that there are two pipes, one for wellbore where various components are installed, and another is the production tubing from where the reservoir fluid flows. The information of each of this tubes along with the information of its properties is required in OLGA model. So, the diameter of production tubing is 0.1397 m which is 5.5 inches, and the tube is 992 m long while the diameter of wellbore is higher than that of production tubing which is 0.2286 m or 9 inches and has same length as production tubing. The material of the pipe being used is same in both pipes therefore the value of surface roughness (ε) is same for both which is 0.00015 m.

As it is discussed earlier in subchapter 6.1.2 that length of the pipes are divided into 8 zones and these zones are the production zones shown in Figure 6.9 which are further divided to 16 sections, each zones subdivided into two hypothetical sections, making the length of each sections to be 62 m.

Each of the zones containing two sections in wellbore has four components. The first component is a packer, and it is a device that stops the fluid flow from one zone to another so, basically packer is used to separate zones. Then comes the nearwell source in first section of each zone that is plugged in with Rocx. The ICD valves are then installed in the imaginary boundary of the two sections from which reservoir fluids enters the wellbore and flows through leak in second section of each zones entering the production tubing. These fluids from all the zones collects the reservoir fluids from wellbore and moves towards the heel. The designation of each component is shown in Table 6.6.

Table 6.6: Description and specification of components of wellbore

Components	OLGA module	Description
Near-well source	Near-well	Linked with corresponding Rocx file
ICD valve	Valve	Diameter = 0.09 m, CD = 0.84, connected to wellbore from which reservoir fluids enter

Leak	Leak	Diameter = 0.12 m, CD = 1, connected to production tubing
Packer	Valve(closed)	Diameter = 0.09m, opening = 0 (fully closed), connected to wellbore

After these zones are modelled for production, the boundary conditions must also be defined for the final step. There are four boundary conditions of the flow path that are given in Table 6.7. The boundaries of wellbore, both inlet and outlet, are closed node which also acts as packer for the first and the last section of wellbore however, the inlet boundary of production tubing is closed node, but the outlet acts as the pressure node because all the fluids collected from wellbore is driven towards the heel using this pressure outlet also called as pressure node. This is the same pressure node whose drawdown pressure was estimated as 12 bar in subchapter 5.6 and the temperature is assumed to be constant.

Table 6.7: Boundary conditions for wellbore and production tubing

Flow path	Boundary name	Boundary type
Production Tubing	Inlet	Closed node
	Outlet	Pressure node, Pressure = 265 bar, Temperature =115℃
Wellbore	Inlet	Closed node
	Outlet	Closed node

6.3 Simulated cases

Once all the parameters are set and the model is completed in OLGA/Rocx, a base case model is made first on which sensitivity analysis is done for different rock and fluid properties of well 6608/10-D-2H of Norne oil field. The cases of parameters whose sensitivity analysis are done are shown in Table 6.8. In the table base values of all the parameters are given and those parameters are increased by 20% in case 1 and decreased by 20% in case 2 from its base value.

Table 6.8: Simulated cases for well 6608/10-D-2H

Parameters	Base case values	Case 1 (+20%)	Case 2 (-20%)
Porosity	0.23	0.276	0.184
Viscosity	0.471107 cp	0.5653284	0.3768856
GOR	82 Sm^3/Sm^3	98.4	65.6
Oil density *	865 kg/m^3	951.5	778.5
Initial water saturation	0.3	0.36	0.24

Absolute Permeability	0.3 mD	0.36	0.24
Rock compressibility	0.0001 1/bar	0.00012	0.00008
Permeability anisotropy	0.257	0.309	0.206

*Oil density cases are changed by only 10% of its base value because increasing the value of oil density by 20% of its base value, it becomes greater than 1 which is not possible for oil because the density of oil is always lower than that of water.

There are two more parameters, relative permeability and capillary pressure, whose sensitivity analysis are done but since their data is presented in Appendix E in the form of table which is their base case, Case 1 (+20%) and Case 2(-20%) for both relative permeability and capillary pressure are available in Appendix G.

7 Results and discussion

In this chapter, the outcome of the simulations done in OLGA/Rocx for well 6608/10-D-2H is decscribed in detail and also some discussions are made at the end for the sensitivity analysis of the parameters.

7.1 Model base case

The base case of well 6608/10-D-2H is simulated in the first case in order to check the accuracy of the near-well reservoir being modelled. In the base case of this model, all the fluid as well as rock properties of the well are plotted for accumulated volume of oil and water and volumetric flow rate of oil and water in y axis and time in x axis. These graphs give the idea of the characteristics and behavior of the well and one can judge by these graphs that for the given values of the rock and fluid parameters if the well is accurate. Figure 7.1 show the graphs obtained by simulation of OLGA/Rocx model for 200 days.

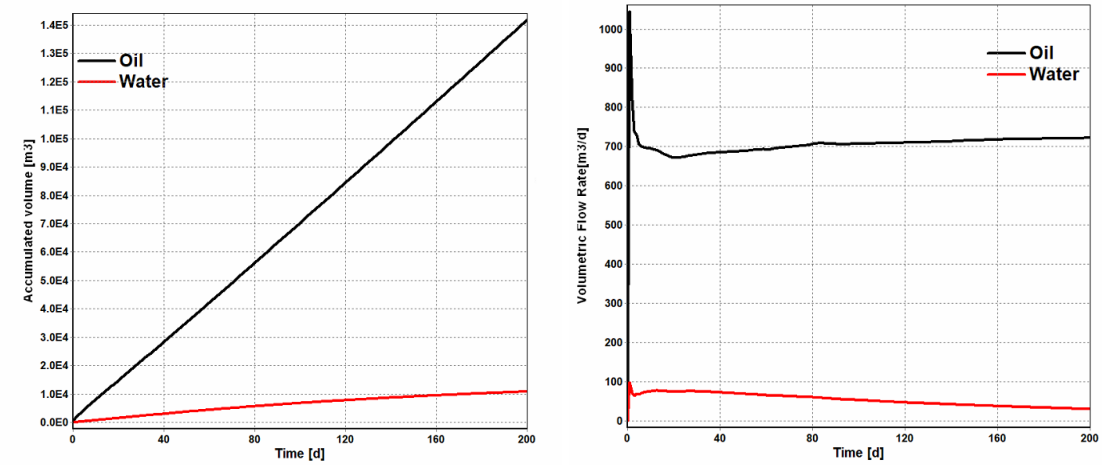

Figure 7.1: Accumulated volume and volumetric flow rate of oil and water for the base case model of Norne oil field

This model of the base case is the basis of performing the sensitivity analysis to the rock and fluid parameters so to verify the precision of graph is required. It can be done by the volumetric flow rate result obtained from the graph where the value is almost 1150 m^3/d for oil and according to NPD page data from [57] the actual volumetric flow rate of oil in the reservoir is 1250 m^3/d. Therefore, the percentage error in the model is approximately 8% which is an acceptable value. Another way of verification of model accuracy is by relative permeability curve shown in Figure 4.3 from which it can be observed that initially the saturations of oil and water are zero, but from the points where the water and oil saturations starts increasing in the curve, the ratio of that value can be noted which is approximately 0.2. Similarly, in the base model case the behavior of the graph is same with initial oil and water saturation is zero and when they start rising and reaches its peak value the ratio of flow rates of water and oil yields approximately 0.1 which is almost the same which again proves the model to be accurate. So, the nature of the curve in Figure 7.1 shows expected behavior thus it can be implied that base case model for Norne oil field is sound and can be used for sensitivity analysis.

7 Results and discussion

Further visualization of the reservoir model is being done using the Techplot software which is shown in Figure 7.2. The figure shows the discretization of the mesh that was made for smooth and gradual flow of reservoir fluids inside the reservoir.

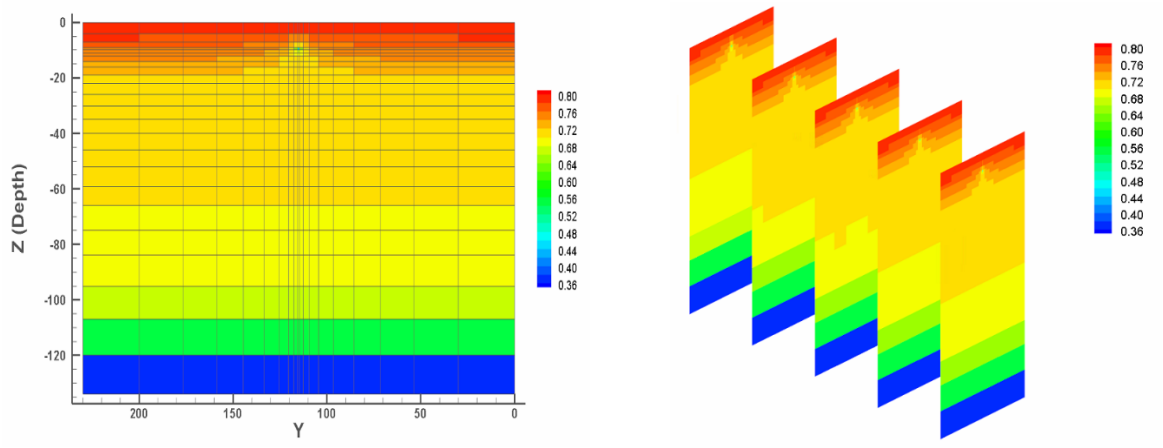

Figure 7.2: Reservoir fluid saturation distribution using techplot

The figure shows the location of wellbore from YZ plane in first figure and in 3D plane in second figure. Here, the well is in 10th position in Y axis and 4th position in Z axis and the oil saturation is gradual as the formation of cone like shape is seen in the figure. Moreover, the figure also proves that the mesh setting for the well is good enough for the simulations to run.

7.2 Sensitivity analysis of rock and fluid parameters

After the validation of base case of the model, sensitivity analysis of the parameters mention in sub chapter 6.3 is being done. This performed in the base case model where only one parameter is changed keeping other values to be constant. The values are changed by increasing and decreasing by 20% of the mean value of each parameters and the comparison is done to see the results from the graphs obtained for accumulated volume and volumetric flow rate of water.

7.2.1 Porosity

The accumulated volume and volumetric flow rate of oil and water for porosity sensitivity analysis is shown in Figure 7.3.

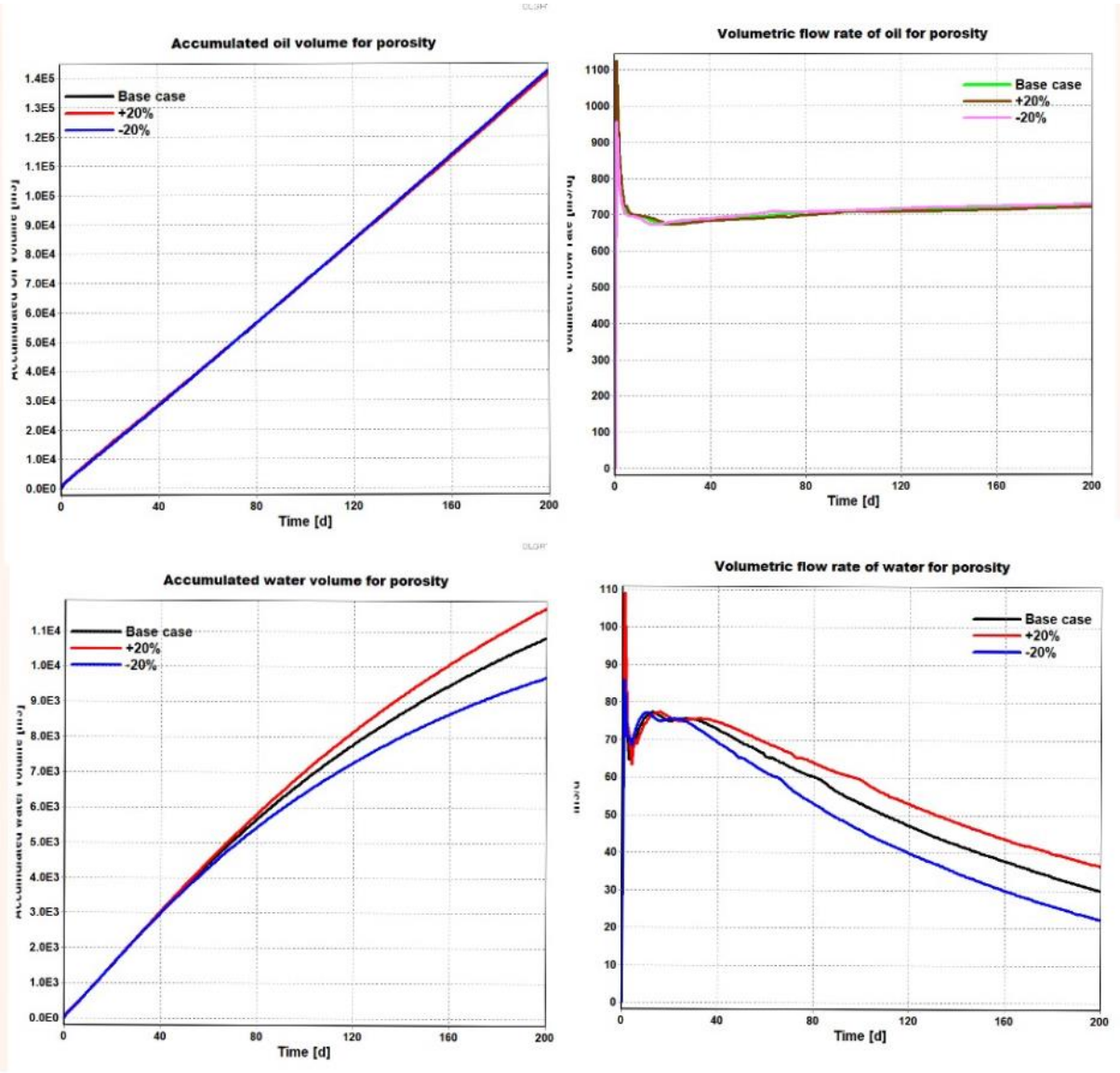

Figure 7.3: Sensitivity analysis of oil and water for porosity

In the figure, for 20% change in porosity value the effect of production after 200 days is not so different than that of the mean value however for the case of water the change is small until about 100 days and the value keeps increasing. For the increased value of porosity, oil production is decreased (by small amount) while the production of water increases and vice versa. Table 7.1 shows the values changes in the porosity for base case, 20% increased and 20% decreased porosity.

Table 7.1: Values of accumulated volume and volumetric flow rate of oil and water for porosity

Item	Accumulated oil volume [m^3]	Accumulated water volume [m^3]	Volumetric flow rate of oil [m^3/d]	Volumetric flow rate of water [m^3/d]
Base case	141853.3	10837.4	722.1	29.9

20% increase	141414.7	11681.4	719.2	36.4
20% decrease	142461.7	9707.8	727.5	22.2

7.2.2 Absolute permeability

The accumulated volume and volumetric flow rate of oil and water for absolute permeability sensitivity analysis is shown in Figure 7.4. In the graph, for the increased value of absolute permeability, the oil production increases while water production decreases. The change in values after the sensitivity analysis is given in Table 7.2.

Table 7.2: Values of accumulated volume and volumetric flow rate of oil and water for absolute permeability

Item	Accumulated oil volume [m^3]	Accumulated water volume [m^3]	Volumetric flow rate of oil [m^3/d]	Volumetric flow rate of water [m^3/d]
Base case	141853.3	10837.4	722.1	29.9
20% increase	151011.5	8995.5	772.4	16.8
20% decrease	130714.2	12086.3	661.6	40.6

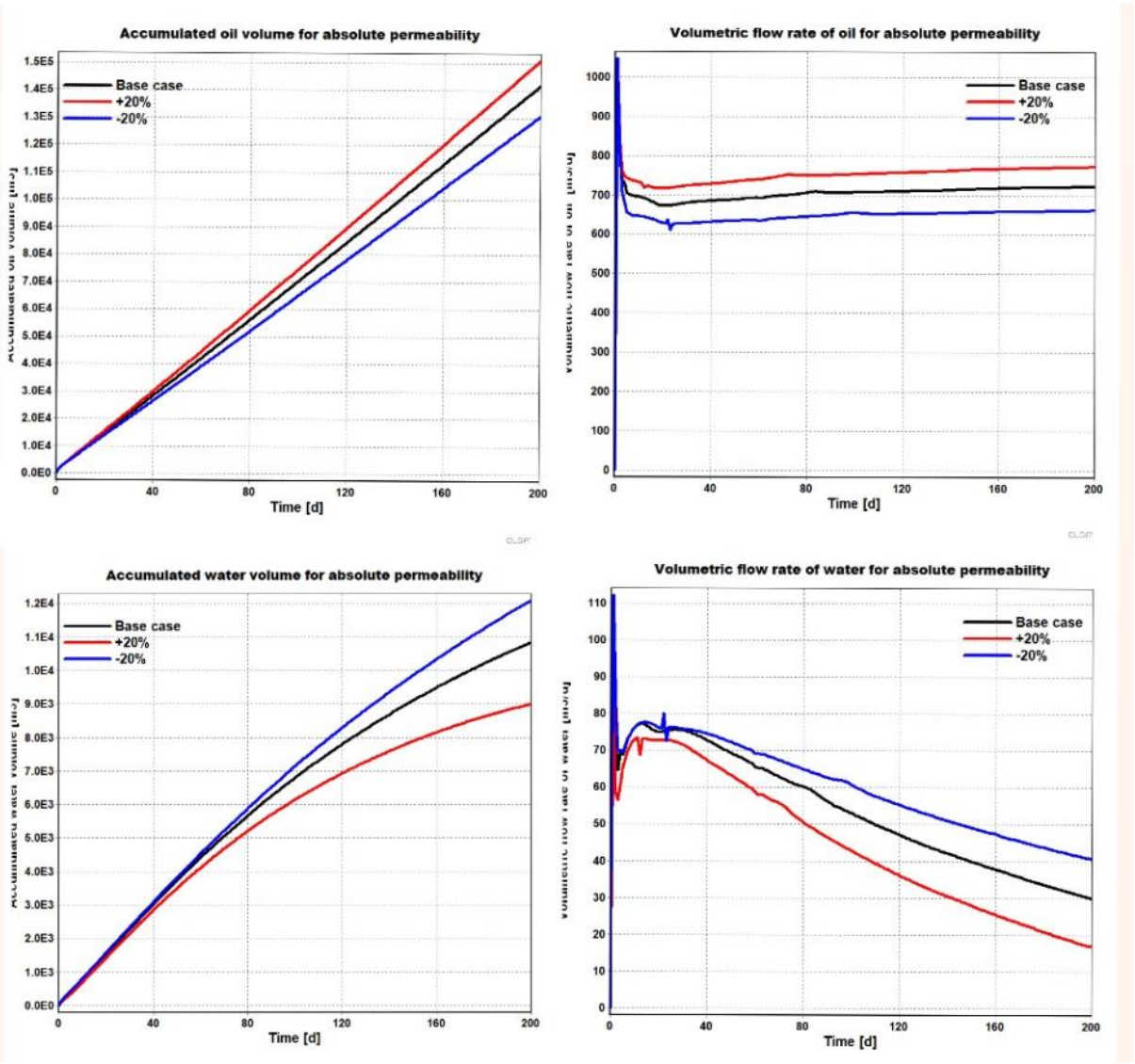

Figure 7.4: Sensitivity analysis of oil and water for absolute permeability

7.2.3 Oil density

Oil density is the only parameter in the sensitivity analysis which is changed by only 10% of its mean value and it has already been discussed in subchapter 6.3 that because of the reason that the density of oil can never be higher that the density of water only 10% value was altered for the sensitivity analysis and the result is shown in Figure 7.5.

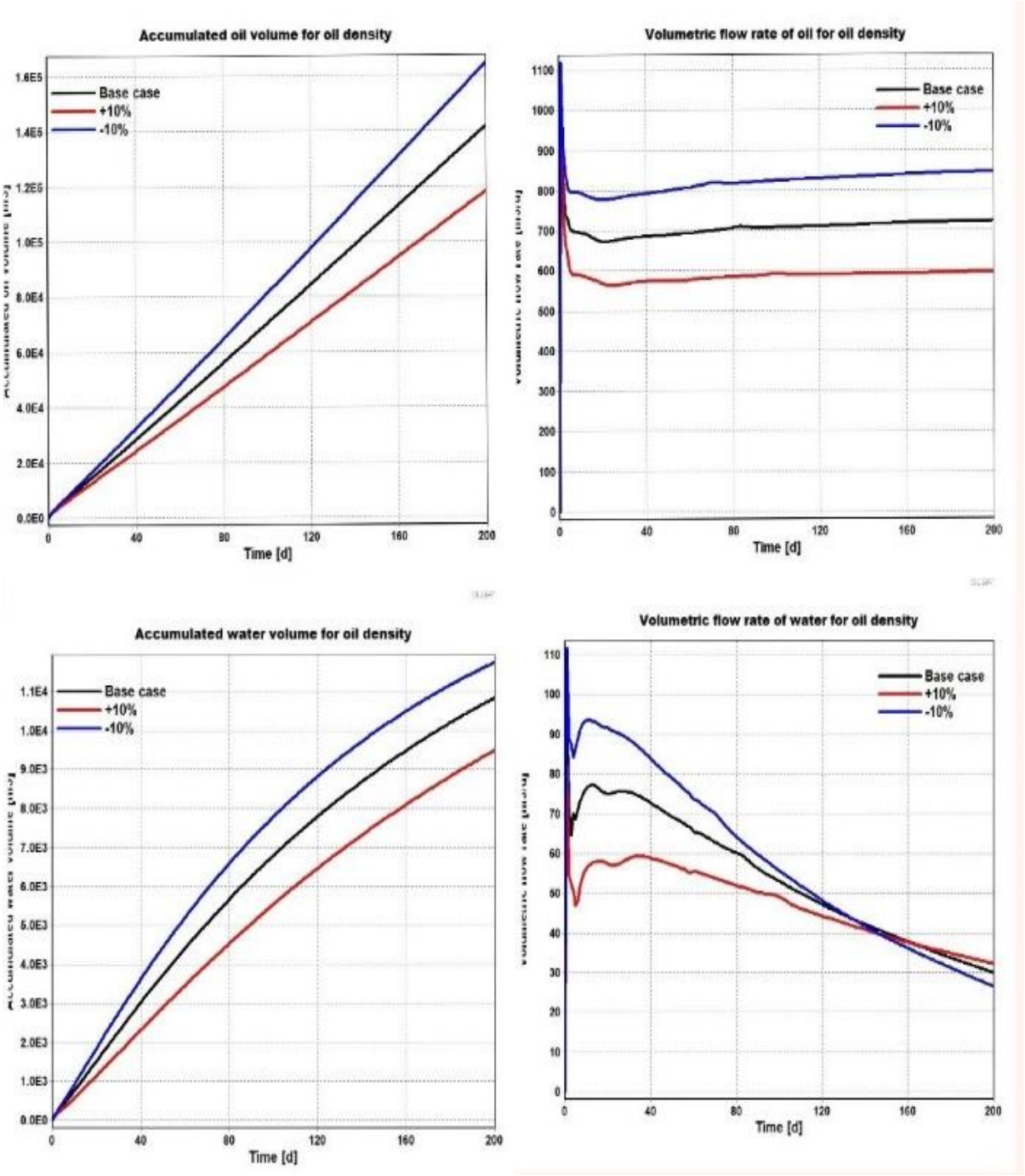

Figure 7.5: Sensitivity analysis of oil and water for oil density

In the graph, it can be seen that when oil density is decreased, the accumulated volume and volumetric flow rate of oil is increased and the case is same for water as well. The value change by sensitivity analysis is presented in the Table 7.3

Table 7.3: Values of accumulated volume and volumetric flow rate of oil and water for oil density

Item	Accumulated oil volume [m^3]	Accumulated water volume [m^3]	Volumetric flow rate of oil [m^3/d]	Volumetric flow rate of water [m^3/d]
Base case	141853.3	10837.4	722.1	29.9
10% increase	118210.7	9495.9	595.2	32.2
10% decrease	164687.4	11747.4	845.1	26.5

Here, observing the table, the volumetric flow rate of water behaves differently than the accumulated volume of water. In accumulated volume of water the value decreases when density is increased and vice versa while for volumetric flow rate of water the value is decreased initially when density is increased but after about 160 days, but at the end of 200 the value is higher compared to the value when oil density is decreased.

7.2.4 Rock compressibility

The effects of rock compressibility when changed from 0.0001 1/bar to 0.00008 and 0.00012 1/bar is shown in Figure 7.6. From the figure all the lines seems to coincide each other for both oil and water. The percentage change is still 20%from its mean value but according the graphs obtained, it appears to have no change in the output of neither oil nor in water production that is being simulated for 200 days.

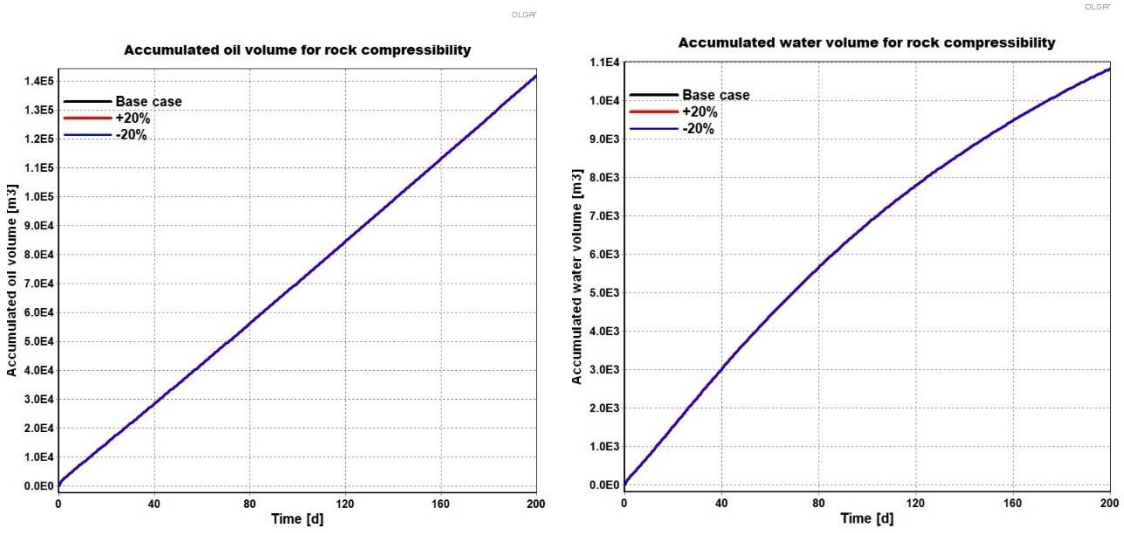

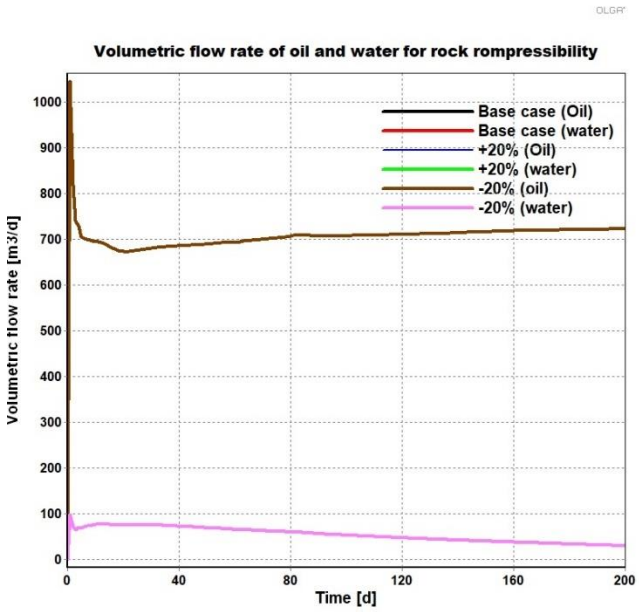

Figure 7.6: Sensitivity analysis of oil and water for rock compressibility

Since the graph clearly shows there is no change in the values of any of the parameter, it can be said that 20% increased and decreased value is exactly as the base value.

7.2.5 Viscosity

The viscosity's sensitivity analysis for the mean value of viscosity which is 0.471107 cP is shown in Figure 7.7.

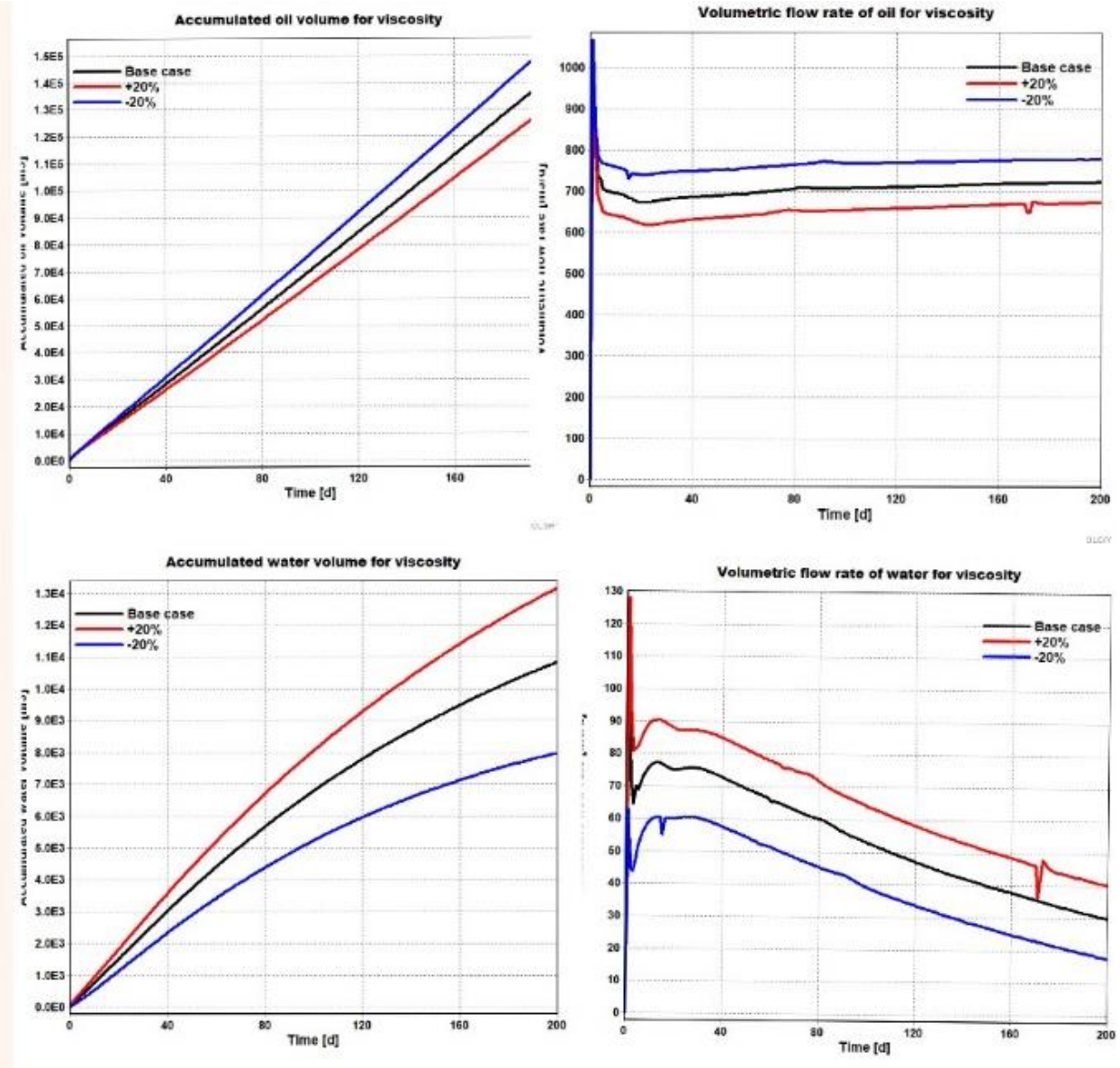

Figure 7.7: Sensitivity analysis of oil and water for viscosity

The percentage change in oil production is smaller than the percentage change in water production as visually seen in the graph. Also in this case, when viscosity is decreased the oil production increases while water production increases and when viscosity is increased, oil production decreases and water production is increased. The change in the values of oil and water accumulated volume and volumetric flow rate is shown in Table 7.4.

Table 7.4: Values of accumulated volume and volumetric flow rate of oil and water for viscosity

Item	Accumulated oil volume [m^3]	Accumulated water volume [m^3]	Volumetric flow rate of oil [m^3/d]	Volumetric flow rate of water [m^3/d]

Base case	141853.3	10837.4	722.1	29.9
20% increase	131392.5	13170.5	672.7	40.2
20% decrease	153776.4	7977.7	777.5	17.5

7.2.6 Initial water saturation

The sensitivity analysis graph of initial water saturation whose mean value is 0.3 is shown in Figure 7.8. The production of oil decreases when the saturation is increased but the case is just opposite in case of water when the initial water saturation value is increased. The change in oil production from its base case is higher as compared to the change in water produced at the end of 200 days. The change in values of oil and water volume and flow rate is given in Table 7.5.

Table 7.5: Values of accumulated volume and volumetric flow rate of oil and water for initial water saturation

Item	Accumulated oil volume [m^3]	Accumulated water volume [m^3]	Volumetric flow rate of oil [m^3/d]	Volumetric flow rate of water [m^3/d]
Base case	141853.3	10837.4	722.1	29.9
20% increase	112202.7	20625.1	600.9	62.2
20% decrease	166086.5	3052.6	821.6	5.49

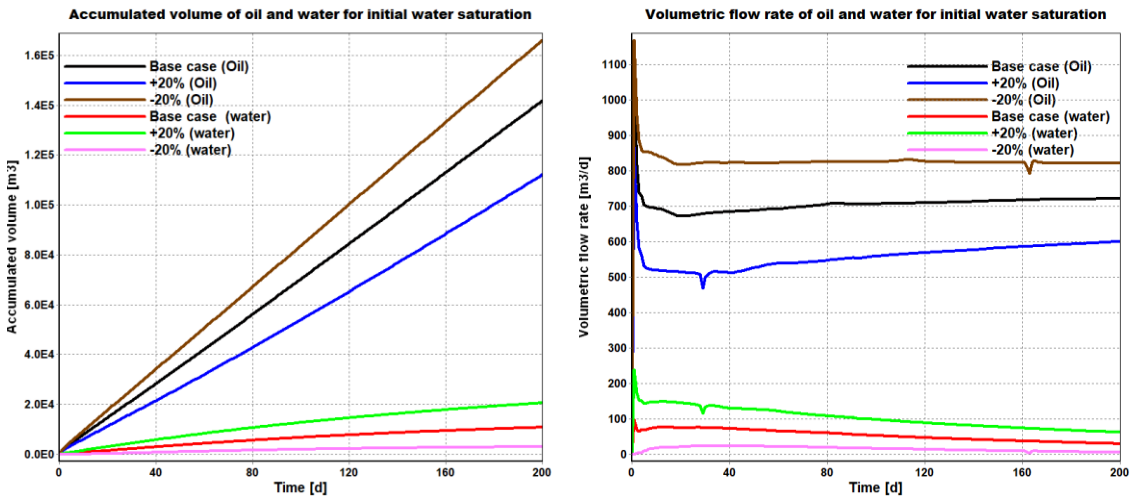

Figure 7.8: Sensitivity analysis of oil and water for initial water saturation

7.2.7 GOR

Gas Oil Ratio (GOR) is the fluid property of the fluid whose value in Norne reservoir is 82 Sm^3/Sm^3 and the sensitivity analysis performed in OLGA/Rocx is shown in Figure 7.9. The graph represents an increase in the value of oil production and very slight increase in water production when the value of GOR was increased. The change in values of the oil production volume and flow rate is presented in Table 7.6.

Table 7.6: Values of accumulated volume and volumetric flow rate of oil and water for GOR

Item	Accumulated oil volume [m^3]	Accumulated water volume [m^3]	Volumetric flow rate of oil [m^3/d]	Volumetric flow rate of water [m^3/d]
Base case	141853.3	10837.4	722.1	29.9
20% increase	148255.7	11186.9	756.1	29.2
20% decrease	135385.2	10443.6	687.9	30.5

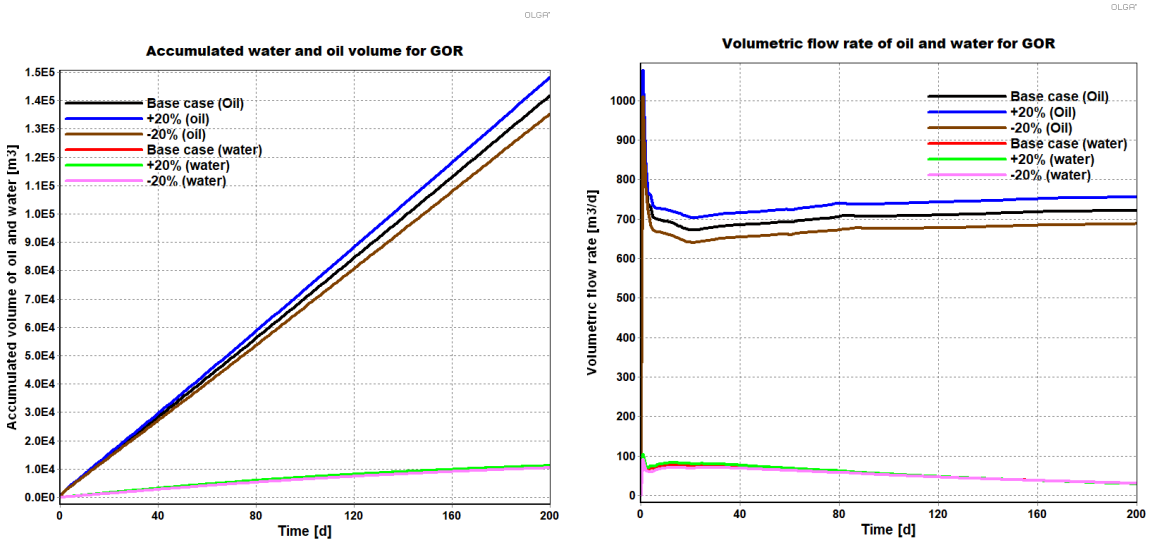

Figure 7.9: Sensitivity analysis of oil and water for GOR

7.2.8 Relative permeability

The sensitivity analysis of relative permeability is shown in Figure 7.10 and the trend in the graph of relative permeability is peculiar because when the value of relative permeability is increased there is only slight increase in the production of oil volume as well as in flow rate however, when the value of relative permeability is decreased, the production change is not symmetrical and can be easily differentiated. The change in water production however remains small for the change in relative permeability and it shows inverse relation for water when it is increased or decreased. Table 7.7 shows the change of values after the analysis.

Table 7.7: Values of accumulated volume and volumetric flow rate of oil and water for relative permeability

Item	Accumulated oil volume [m^3]	Accumulated water volume [m^3]	Volumetric flow rate of oil [m^3/d]	Volumetric flow rate of water [m^3/d]
Base case	141853.3	10837.4	722.1	29.9
20% increase	150548.5	9094.4	769.5	17.4
20% decrease	115409.6	14572.9	585.2	50.9

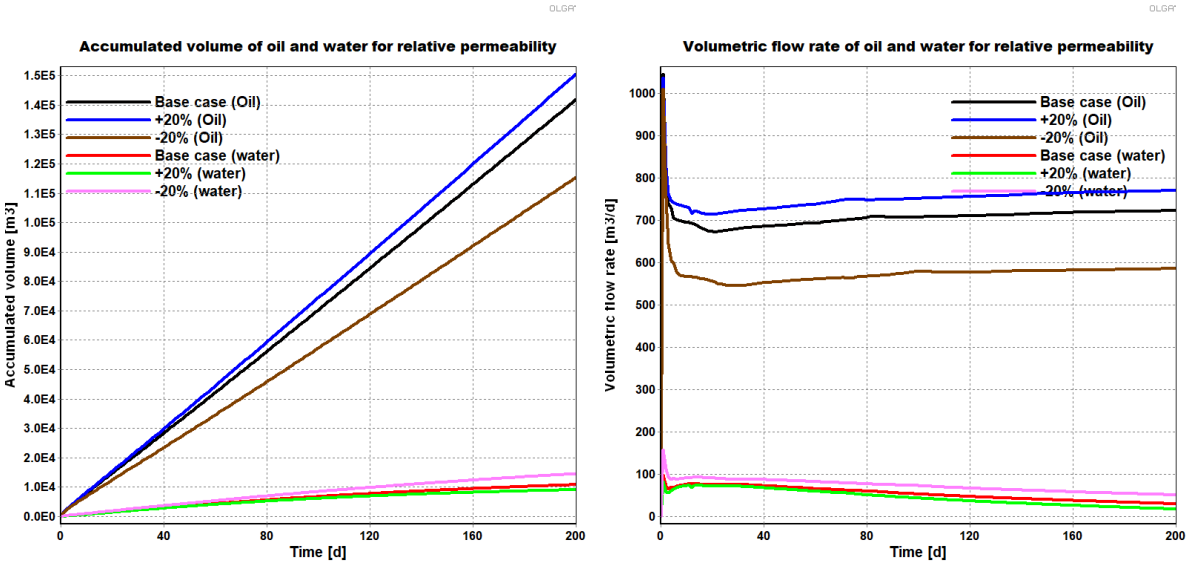

Figure 7.10: Sensitivity analysis of oil and water for relative permeability

7.2.9 Capillary pressure

The capillary pressure sensitivity analysis is shown in Figure 7.11 for the production volume and volumetric flow rate of oil and water. In the graph, it can be seen that the change in the value of capillary pressure have least effects on water and oil production volume and volumetric flow rate as well. From the figure it is difficult to determine whether the value of production of water and oil increases or decreases with the change but from Table 7.8 shows the change of value of data where it can be seen that with the increase in capillary pressure the production of oil increases as well but production of water decreases.

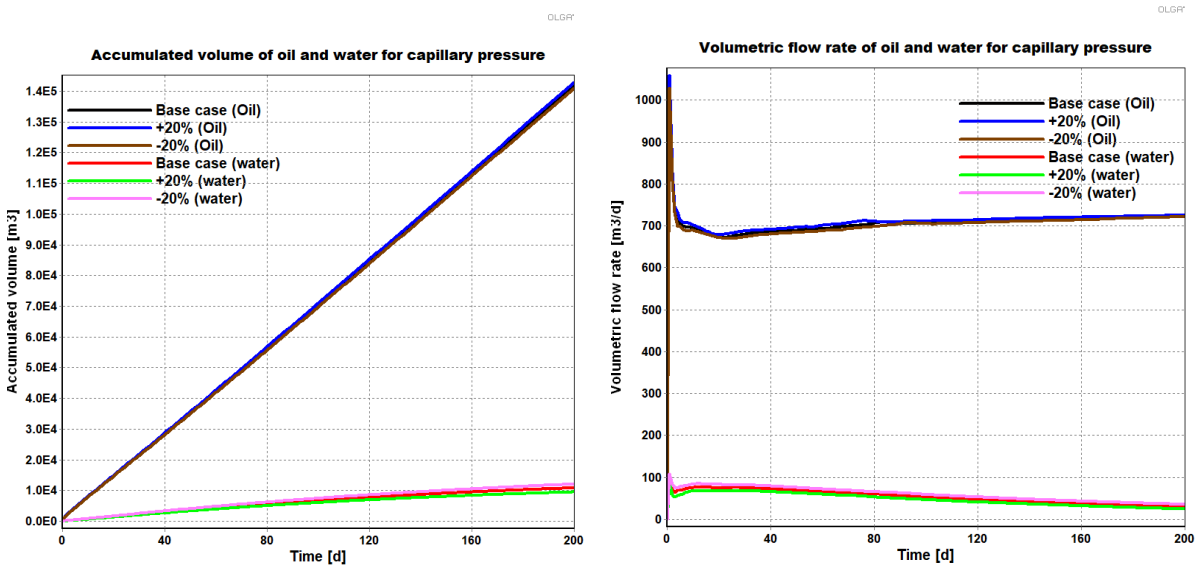

Figure 7.11: Sensitivity analysis of oil and water for capillary pressure

Table 7.8: Values of accumulated volume and volumetric flow rate of oil and water for capillary pressure

Item	Accumulated oil volume [m^3]	Accumulated water volume [m^3]	Volumetric flow rate of oil [m^3/d]	Volumetric flow rate of water [m^3/d]
Base case	141853.3	10837.4	722.1	29.9
20% increase	142882.2	9505.5	725.2	24.3
20% decrease	141083.7	12065.4	721.4	35.3

7.2.10 Permeability anisotropy

The permeability anisotropy is one of the fluid parameters whose sensitivity analysis graph is shown in Figure 7.12. In the figure, the production of oil volume increases, and the production of water volume decreases with the increase of permeability anisotropy. The value changes after sensitivity analysis are shown in Table 7.9.

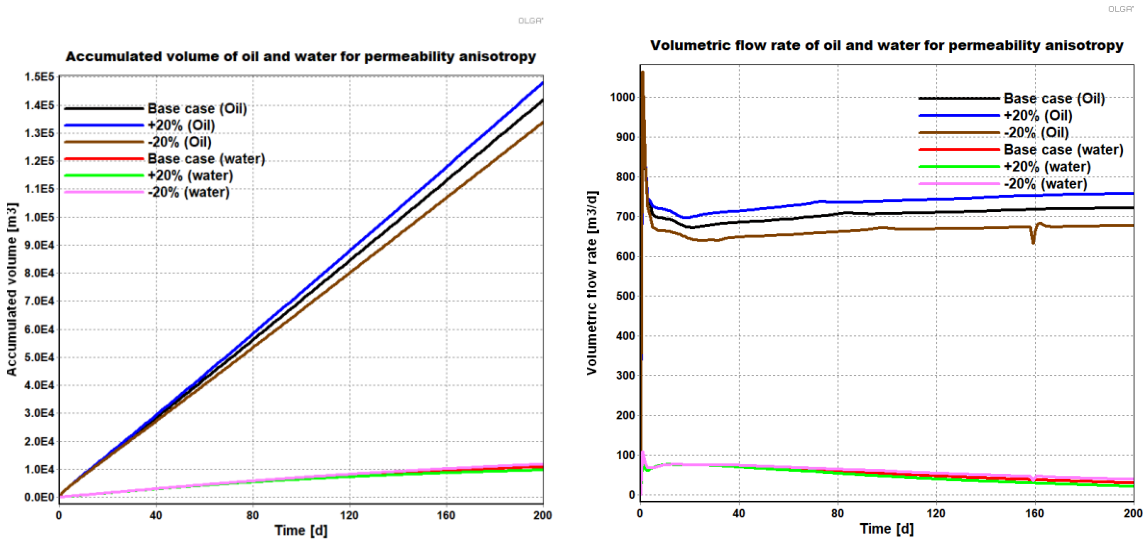

Figure 7.12: Sensitivity analysis of oil and water for permeability anisotropy

Table 7.9: Values of accumulated volume and volumetric flow rate of oil and water for permeability anisotropy

Item	Accumulated oil volume [m^3]	Accumulated water volume [m^3]	Volumetric flow rate of oil [m^3/d]	Volumetric flow rate of water [m^3/d]
Base case	141853.3	10837.4	722.1	29.9
20% increase	148085.5	9675.3	757.7	21.2
20% decrease	133934.9	11822.1	677.3	38.4

7.3 Comparison of results

Based on the sensitive analysis performed on the rock and fluid parameters of well 6608/10-D-2H of Norne field, it is very difficult to compare them using the graphs because of several parameters involved. However, on the basis of the production of oil and water from the reservoir for both accumulated volume and volumetric flow rate, tornado chart is made for clear understanding of which parameters is most sensitive during the analysis. It should be noted that rock compressibility had no effect by doing the analysis so, this parameter is not included in the chart.

7.3.1 Comparison of oil production

Figure 7.13 shows the chart of all the rock and fluid parameters (except rock compressibility). From the graph, the results are clearly represented by the sensitive parameters and arranged from largely affected parameter to least affected parameter.

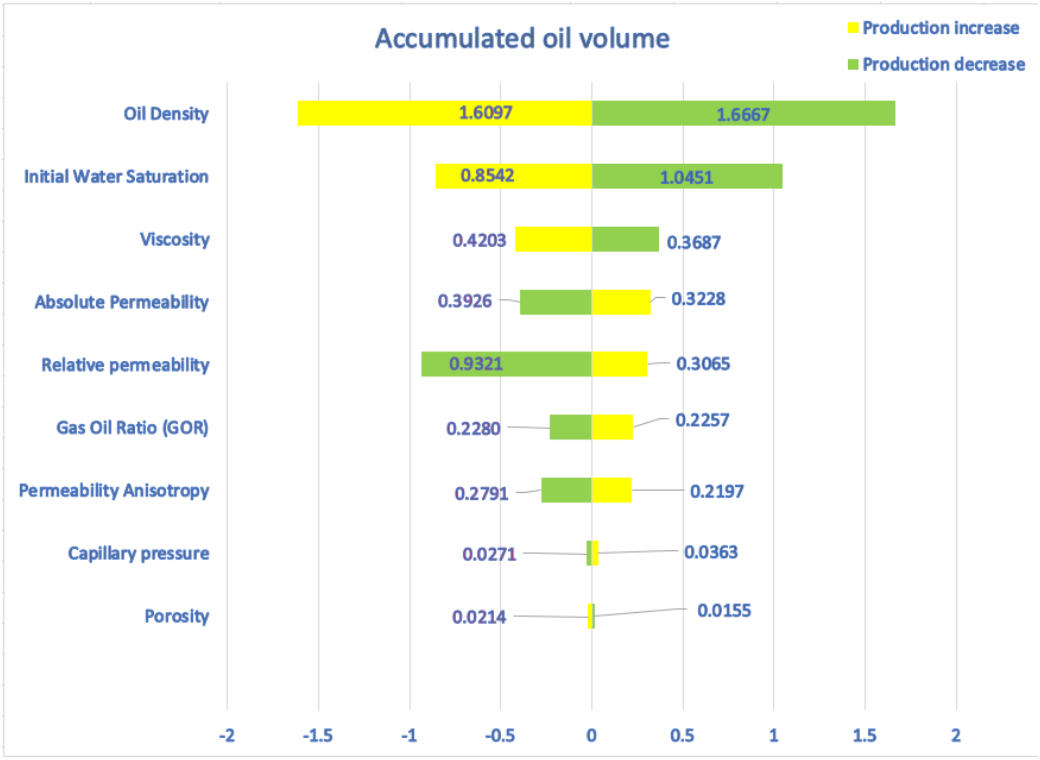

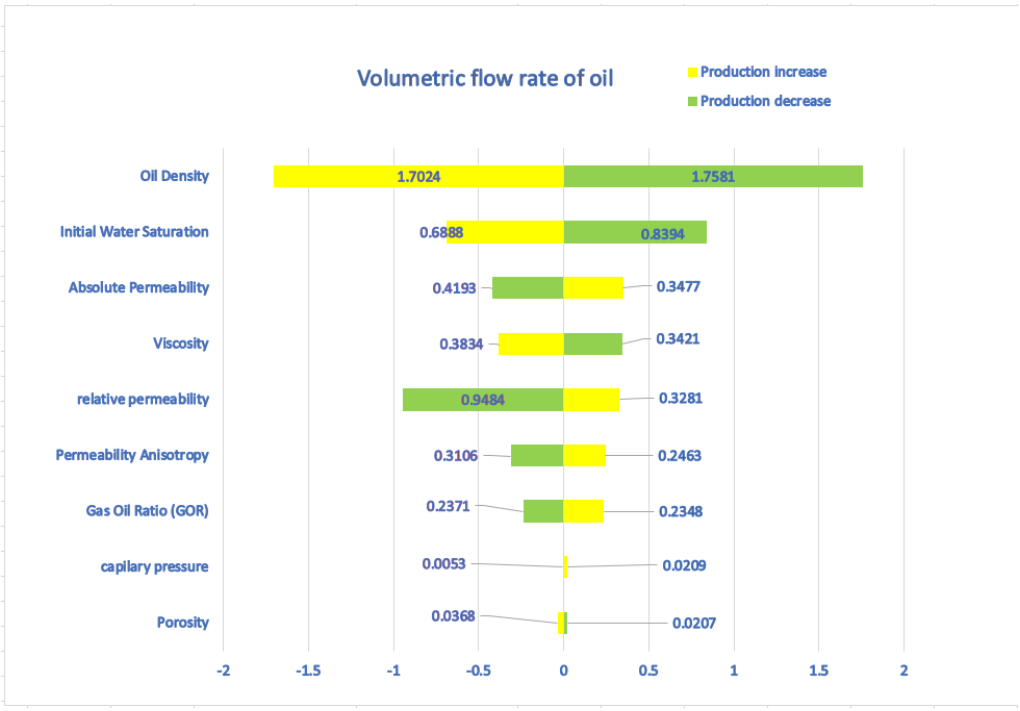

Figure 7.13: Comparison of various rock and fluid parameters for oil production sensitivity analysis

In the figure, the green blocks represent the percentage decrease in oil production while the yellow blocks represent the oil production increase. Understanding the graph is easier because the production of oil is represented so if observed oil density, initial water saturation, viscosity and porosity, the positive axis represents 20% increase of values of parameters while negative axis represents 20% decrease. So, for example in oil density, when the value is increased by 20% (in this case 10% for oil density) the production decreases and is sensitive by factor of 1.6667 and when the value is decreased, the production increases and is sensitive by factor of 1.6097. Similarly, absolute permeability, permeability anisotropy, GOR, relative permeability and capillary pressure, when the value for sensitivity analysis is increased by 20%, the production increases and decreases when the value is decreased.

From the figure, oil density is the most sensitive parameter among all other parameter, followed by initial water saturation, viscosity, absolute and relative permeability, and it should be noted that oil density was changed by only 10% of its mean value but still this parameter is the most sensitive parameter of all. While porosity seems to have the least effect on it and rock compressibility has no effect at all.

7.3.2 Comparison of water production

Figure 7.14 represents the chart obtained by the graphs of sensitivity analysis in previous subchapters for water production in well. In this case as well, the parameters which are affected the most and the least are arranged in order.

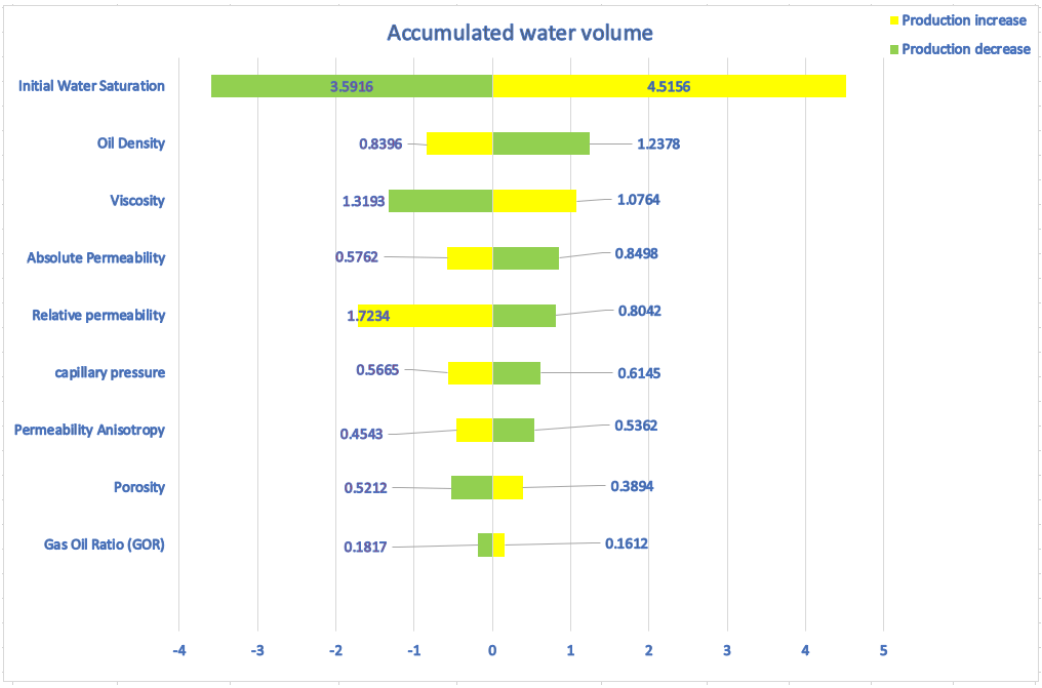

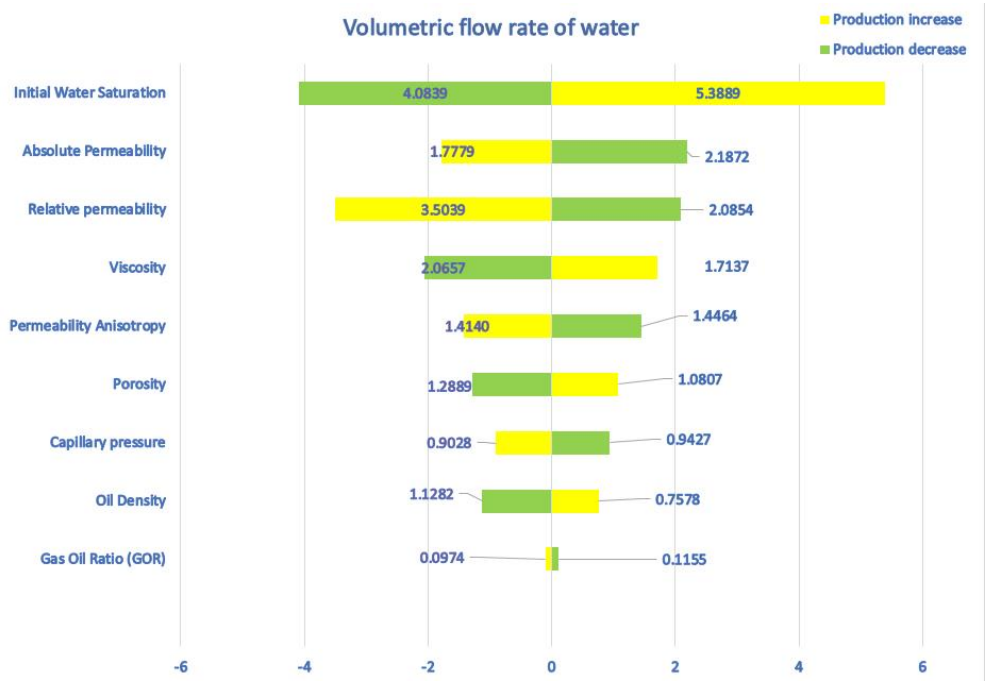

Figure 7.14: Comparison of various rock and fluid parameters for water production sensitivity analysis

The process of analysis in case of water production is similar to that of the oil production but we can see from the results that the parameters which are sensitive in case of water is different to that of the oil. In case of water, the most affected parameter is found to be initial water saturation followed by water density, viscosity, absolute and relative permeability while the least affected parameter is GOR (rock compressibility in this case also has no change).

Parameters such as relative permeability, permeability anisotropy, capillary pressure and absolute permeability has an increased production when the value of parameters are increased while other parameters has increased production of water when the value is increased.

7.4 Discussion

In this chapter, the notable points from the development of model, simulation and results are mentioned.

7.4.1 Model base case behavior

In the model development subchapter 7.1, when the model for well 6608/10-D-2H of Norne oil field was completed, a graphical plot of accumulated oil volume and time was obtained. In the graph the trend shows the oil production increase and water production increase. The reason why this behavior is observed could be due to initial water saturation that comes into the reservoir after some period of time. When water is produced, oil come near the well and the saturation of oil near the well increases for initial water saturation before the water from aquifer comes.

7.4.2 Grid distribution and drainage width

In the early phase of sensitivity analysis, when the mesh sensitivity analysis was done for drainage width and grid distributions, the width for drainage area was being selected. Basically, there is variations in production output when these sizes of widths are varied but in the model case of this thesis there seemed to have very less effect in the production of oil for different width variation. Similarly, grid distribution has helped to determine the nature of the behavior of the model because from the graph in Figure 6.6 it can be seen that improper grid size can also lead to no water inside the reservoir. This is impossible because initial water saturation value says that there is 30% water inside the reservoir. Having no water at all means that there is 100% oil in reservoir and that is never the case in reality. But as the mesh size was increased for z direction from 12 to 24, the nature of water curve in the graph started improving.

7.4.3 Pressure drawdown

Even though for this thesis the pressure drawdown was estimated and not calculated, initially the value was set to 10 bar and in some of the results there was backflow seen in the graph which is not possible for real cases. But when the value was increased to 12 bars, there seemed to have no backflows. Moreover, estimating a proper pressure drawdown value also shows its accuracy which is presented in the graph for good consistency of oil production of the well 6608/10-D-2H for Norne oil field.

7.4.4 Density

When the density initially was increased by 20% of its mean value, it resulted in density higher than that of water so the result had a very high fluctuation in the oil production graph along with some backflow which was logical because the density of oil can never be higher than the density of water. So, the percentage increase had to be reduced in which increasing by 15% was still close to the density of water and therefore 10% increase and decrease of oil density was chosen that resulted to no fluctuation and backflow in reservoir and the oil production was smooth.

8 Conclusion

In this chapter, sensitivity analysis of oil production model to reservoir rock and fluid properties using OLGA/Rocx is concluded where well 6608/10-D-2H of Norne oil field was chosen.

There are basically 3 tasks according to the task description and based on those task descriptions, 10 major objectives of this thesis have been made. All of these tasks have been completed.

The first task and the first objective of the thesis was literature study on sensitivity analysis and rock and fluid properties of reservoir. Out of many sensitivity analysis methods, differential analysis method was chosen. The principle of this method is to change one parameter keeping all other parameters constant and evaluate the change if there are any. Similarly, rock and fluid properties that are relevant to this thesis are all explained in detail. Based on the literature study, it can be argued that all the rock and fluid parameters that are subjected to sensitivity analysis are the building blocks to make a model base case of near-well reservoir but all of them are not as sensitive to production output.

Similarly, study on horizontal wells were also done in the thesis where it was found that because of higher contact surface area between fluid and pipe in horizontal wells, they are more efficient to use rather than using a vertical well. Early water coning and water breakthrough can happen in horizontal wells, but these issues can be reduced by using ICDs. Therefore, horizontal wells with ICDs can increase the well productivity and moreover they can also reduce the sand production due to lower pressure drop and fluid velocity in wellbore.

Based on model development cases, a base case model that describes the well its best is needed and for the model to be made, proper knowledge of the rock and fluid properties of the reservoir is required. It is also extremely important to understand the physical meaning of those parameters and special care must be taken for the units since some of the units in OLGA/Rocx are different than SI units. Therefore, it can be concluded that, for model preparation of a realistic well in OLGA/Rocx, the base model is the most important factor which determines the accuracy of results. The distribution of grids is also of paramount importance because, having a good distribution of block sizes of mesh can give us the idea of closeness of the model made in OLGA/Rocx to the realistic model. This can be visualized in another software called techplot where the mesh setting can be visualized. Grid distributions at the end was selected for $nx = 8$, $ny = 19$ and $nz = 24$ in x y and z directions respectively. However, the results can be made even more better by increasing the number of grids in y and z direction but because of limited time frame the simulation time had to be considered.

Model preparation being the first step of sensitivity analysis needed to be accurate hence it took more time and study on it. And based on the sensitivity analysis performed the value of each parameter was changed by $\pm 20\%$ of its original value and simulated for 200 days. The results are presented in the tornado chart. The chart illustrates the parameters that are most sensitive to the value change to least sensitive ones. The most affected parameter in case of oil production was found to be oil density with sensitivity coefficient 1.6097 but it must be noted that the production does not increase the when the oil density is increased. Rather it decreases but only increases when the value of oil density was decreased. Following oil density were initial water saturation, viscosity, absolute and relative permeability. Observing the results obtained from the sensitivity analysis, it is seen that fluid properties of Norne oil field were more sensitive when compared to rock properties.

On the other hand, in case of water production in the reservoir, with the same parameter input changes, the results were evaluated. From the evaluation, there were some parameters that were very sensitive to the change like initial water saturation has the sensitivity coefficient of 4.5156. Following initial water saturation, were water density, viscosity absolute and relative permeability.

One of the challenges faced during sensitivity analysis was setting a proper and accurate grid size for the model base case and since the simulation time was very long, hit and trial method for the accurate grid size distribution made it more tedious.

Originally, the goal of the thesis was to perform sensitivity analysis of either two different oil fields or two differently located wells of same oil field. The sensitivity analysis performed in only one field can be peculiar to only that field but comparing two or more oil fields can verify the parameter's sensitivity that could general sensitive parameters for all oil fields. But in the given time frame only one oil field sensitivity analysis could be done.

Although for this thesis, the values of those parameters were kept constant but further studies can be done whether the affecting parameters must be changed as well or not. For instance, when doing the sensitivity analysis of porosity, the values effective porosity was changed by $\pm$20%, equation 3.14, which is the equation to find permeability in z direction is also linked with effective porosity in the equation. So, in the theory of differential analysis method no such literature was mentioned for such parameters and future studies can be done for parameter link analysis.

All the simulations that were done for this thesis was done considering the reservoir to be homogenous but in actual practice the reservoir is heterogenous in nature. The parameters involved in sensitivity analysis could behave differently when the reservoir is considered heterogenous. Therefore, future works can be done for the same analysis in heterogenous reservoir. Also, in this thesis ICD valves were used in the model of well 6608/10-D-2H but research can be done for AICV with control valves that can show better results than ICD valves.

9 References

[1] ‘History of the petroleum industry’, *Wikipedia*. Apr. 19, 2021. Accessed: May 03, 2021. [Online]. Available: https://en.wikipedia.org/w/index.php?title=History_of_the_petroleum_industry&oldid=1018716866

[2] R. Lukasz, ‘History of Oil - A Timeline of the Modern Oil Industry’, *EKT Interactive*. https://ektinteractive.com/history-of-oil/ (accessed Apr. 23, 2021).

[3] ‘Herodotus’, *World History Encyclopedia*. https://www.worldhistory.org/herodotus/ (accessed May 03, 2021).

[4] J. Paul Rodrigue, ‘World Crude Oil Production and Consumption, 1965-2016 | The Geography of Transport Systems’. https://transportgeography.org/contents/applications/petroleum-transportation-resource/world-crude-oil-production/ (accessed Apr. 23, 2021).

[5] ‘Exports of Norwegian oil and gas’, *Norwegianpetroleum.no*. https://www.norskpetroleum.no/en/production-and-exports/exports-of-oil-and-gas/ (accessed Apr. 23, 2021).

[6] ‘Norwegian continental shelf’, *Wikipedia*. Jan. 17, 2021. Accessed: May 03, 2021. [Online]. Available: https://en.wikipedia.org/w/index.php?title=Norwegian_continental_shelf&oldid=1000980604

[7] ‘og21--the-national-technology-strategy-for-the-petroleum-industry.pdf’. Accessed: Apr. 23, 2021. [Online]. Available: https://www.npd.no/globalassets/2-force/2019/documents/archive-2010-2018/joining-forces-2016/og21--the-national-technology-strategy-for-the-petroleum-industry.pdf

[8] ‘Historical production on the NCS’, *Norwegianpetroleum.no*. https://www.norskpetroleum.no/en/facts/historical-production/ (accessed Apr. 23, 2021).

[9] A. Moradi, ‘Cost-effective and safe oil production from existing and near-future oil fields’, University of South-Eastern Norway, 2020. Accessed: Apr. 30, 2021. [Online]. Available: http://hdl.handle.net/11250/2688507

[10] R. Timsina, N. C. I. Furuvik, and B. M. E. Moldestad, ‘Modeling and simulation of light oil production using inflow control devices’, *180-187*, 2017, doi: 10.3384/ecp17138180.

[11] L. S. Raastad, ‘Near well simulation of oil production from conventional heterogeneous oil’, Oct. 2015, Accessed: Apr. 23, 2021. [Online]. Available: https://openarchive.usn.no/usn-xmlui/handle/11250/2439040

[12] ‘Field: NORNE - Factpages - NPD’. https://factpages.npd.no/en/field/pageview/all/43778 (accessed Apr. 25, 2021).

[13] D. M. Hamby, ‘A review of techniques for parameter sensitivity analysis of environmental models’, *Environ. Monit. Assess.*, vol. 32, no. 2, pp. 135–154, Sep. 1994, doi: 10.1007/BF00547132.

[14] R. L. Iman and J. C. Helton, ‘An Investigation of Uncertainty and Sensitivity Analysis Techniques for Computer Models’, *Risk Anal.*, vol. 8, no. 1, pp. 71–90, 1988, doi: https://doi.org/10.1111/j.1539-6924.1988.tb01155.x.

9 References

[15] J. C. Helton and R. L. Iman, ‘Sensitivity analysis of a model for the environmental movement of radionuclides’, *Health Phys.*, vol. 42, no. 5, pp. 565–584, May 1982, doi: 10.1097/00004032-198205000-00002.

[16] R. Bellman and K. J. Åström, ‘On structural identifiability’, *Math. Biosci.*, vol. 7, no. 3, pp. 329–339, Apr. 1970, doi: 10.1016/0025-5564(70)90132-X.

[17] T. J. Krieger, C. Durston, and D. C. Albright, ‘Statistical determination of effective variables in sensitivity analysis’, *Trans. Am. Nucl. Soc.*, vol. 28 pp. 515–516, 1978, Accessed: Apr. 27, 2021. [Online]. Available: http://inis.iaea.org/Search/search.aspx?orig_q=RN:9418038

[18] J. C. Helton, R. L. Iman, and J. B. Brown, ‘Sensitivity analysis of the asymptotic behavior of a model for the environmental movement of radionuclides’, *Ecol. Model.*, vol. 28, no. 4, pp. 243–278, Aug. 1985, doi: 10.1016/0304-3800(85)90077-8.

[19] R. W. Atherton, R. B. Schainker, and E. R. Ducot, ‘On the statistical sensitivity analysis of models for chemical kinetics’, *AIChE J.*, vol. 21, no. 3, pp. 441–448, 1975, doi: https://doi.org/10.1002/aic.690210304.

[20] ‘Well types - AAPG Wiki’. https://wiki.aapg.org/Well_types (accessed Apr. 30, 2021).

[21] ‘Figure 3.3. A conventional vertical well (A), and an unconventional...’, *ResearchGate*. https://www.researchgate.net/figure/A-conventional-vertical-well-A-and-an-unconventional-horizontal-well-B-Horizontal_fig13_322641749 (accessed Apr. 30, 2021).

[22] ‘Horizontal Wells and Their Advantages and Benefits’, *Directional Technologies, Inc.*, Oct. 22, 2010. https://www.directionaltech.com/time-tested-advantages-of-horizontal-wells/ (accessed Apr. 30, 2021).

[23] A. G. says, ‘Advantages, limitations, and classification of horizontal wells’, *petroblogweb*, Aug. 14, 2016. https://petroblogweb.wordpress.com/2016/08/14/advantages-limitations-and-classification-of-horizontal-wells/ (accessed Apr. 30, 2021).

[24] ‘Lesson 34 Horizontal Drilling - ppt video online download’. https://slideplayer.com/slide/5770007/ (accessed May 02, 2021).

[25] admin, ‘Directional Drilling Types’, *Drilling Course*. https://www.drillingcourse.com/2016/03/directional-drilling-types.html (accessed May 02, 2021).

[26] D. G. Hatzignatiou and F. Mohamed, ‘Water And Gas Coning In Horizontal And Vertical Wells’, presented at the Annual Technical Meeting, Jun. 1994. doi: 10.2118/94-26.

[27] ‘ProQuest Ebook Central - Reader’. https://ezproxy2.usn.no:2537/lib/ucsn-ebooks/reader.action?docID=648740&ppg=602 (accessed May 02, 2021).

[28] J. Omar, B. Ghosh, and Y. Mohamad, ‘Downhole flow controllers in mitigating challenges of long reach horizontal wells: A practical outlook with case studies’, *J. Pet. Gas Eng.*, vol. 8, pp. 90–103, Nov. 2017, doi: 10.5897/JPGE2017.0272.

[29] Absolute Completion Technologies, *MeshFlux 2014*, (Oct. 02, 2014). Accessed: May 02, 2021. [Online Video]. Available: https://www.youtube.com/watch?v=x3h8T_AI7Mc&ab_channel=AbsoluteCompletionTechnologies

9 References

[30] H. Aakre, ‘The impact of autonomous inflow control valve on increased oil production and recovery’, University College of Southeast Norway, Faculty of Technology, Natural Sciences and Maritime Sciences, Kongsberg, 2017.

[31] ‘Fig. 4. Oil and water production rate with and without ICDs.’, *ResearchGate*. https://www.researchgate.net/figure/Oil-and-water-production-rate-with-and-without-ICDs_fig4_342203804 (accessed May 03, 2021).

[32] A. Malagalage and B. Halvorsen, ‘Near Well Simulation and Modelling of Oil Production from Heavy Oil Reservoirs’, Nov. 2015, pp. 289–298. doi: 10.3384/ecp15119289.

[33] V. M. Birchenko, K. M. Muradov, and D. R. Davies, ‘Reduction of the horizontal well’s heel–toe effect with inflow control devices’, *J. Pet. Sci. Eng.*, vol. 75, no. 1, pp. 244–250, 2010, doi: https://doi.org/10.1016/j.petrol.2010.11.013.

[34] Z. Li, P. Fernandes, and D. . Zhu, ‘Understanding the Roles of Inflow-Control Devices in Optimizing Horizontal-Well Performance’, *SPE Drill. Complet.*, vol. 26, no. 03, pp. 376–385, Sep. 2011, doi: 10.2118/124677-PA.

[35] ‘floreg-inflow-control-device-(icd).pdf’. Accessed: May 04, 2021. [Online]. Available: https://www.weatherford.com/en/documents/brochure/products-and-services/completions/floreg-inflow-control-device-(icd)/

[36] T. Ahmed, *Working Guide to Reservoir Rock Properties and Fluid Flow*. Gulf Professional Publishing, 2009.

[37] A. Y. Dandekar, *Petroleum Reservoir Rock and Fluid Properties, Second Edition*. CRC Press, 2013.

[38] N. Alyafei, *Fundamentals of Reservoir Rock Properties - 2nd edition*. QScience.com, 2021. doi: 10.5339/Fundamentals_of_Reservoir_Rock_Properties_2ndEdition.

[39] UCSI University, ‘Rock Compressibility’, 00:32:07 UTC. Accessed: May 05, 2021. [Online]. Available: https://www.slideshare.net/MTaherHamdani/rock-compressibility-38903459

[40] ‘Chapter 3.pdf’. Accessed: May 09, 2021. [Online]. Available: http://homepages.see.leeds.ac.uk/~earpwjg/PG_EN/CD%20Contents/GGL-66565%20Petrophysics%20English/Chapter%203.PDF

[41] K. Moncada *et al.*, ‘Determination of Vertical and Horizontal Permeabilities for Vertical Oil and Gas Wells with Partial Completion and Partial Penetration Using Pressure and Pressure Derivative Plots Without Type-Curve Matching’, *CTF - Cienc. Tecnol. Futuro*, vol. 3, no. 1, pp. 77–94, Dec. 2005.

[42] T. Yildiz and E. Ozkan, ‘Influence of Areal Anisotropy on Horizontal Well Performance’, presented at the SPE Annual Technical Conference and Exhibition, Oct. 1997. doi: 10.2118/38671-MS.

[43] C. I. Philip, D. Tiab, and O. I. Alpheus, ‘Vertical-Horizontal Permeability Relationships for Sandstone Reservoirs’, presented at the Nigeria Annual International Conference and Exhibition, Aug. 2012. doi: 10.2118/163011-MS.

[44] P. Grover, ‘Formation Evaluation MSc Course Notes Reservoir Fluids Chapter 2: Reservoir Fluids 2.1 Introduction’, Accessed: May 15, 2021. [Online]. Available: https://www.academia.edu/39168259/Formation_Evaluation_MSc_Course_Notes_Reservoir_Fluids_Chapter_2_Reservoir_Fluids_2_1_Introduction

9 References

[45] R. Wheaton, ‘Basic Rock and Fluid Properties’, in *Fundamentals of Applied Reservoir Engineering*, Elsevier, 2016, pp. 5–57. doi: 10.1016/B978-0-08-101019-8.00002-8.

[46] ‘gas/oil ratio (GOR) | Oilfield Glossary’. https://glossary.oilfield.slb.com/en/terms/g/gas-oil-ratio (accessed May 15, 2021).

[47] ‘water cut | Oilfield Glossary’. https://glossary.oilfield.slb.com/en/terms/w/water_cut (accessed May 15, 2021).

[48] H. Dembicki, ‘Density (Mass/Volume) - an overview | ScienceDirect Topics’. https://www.sciencedirect.com/topics/earth-and-planetary-sciences/density-mass-volume (accessed May 15, 2021).

[49] P. I. News, ‘What is API Gravity?’, *Petro Online*. https://www.petro-online.com/news/fuel-for-thought/13/breaking-news/what-is-api-gravity/33309 (accessed May 15, 2021).

[50] G. Haynes, ‘Fall 2012 Lecture 4 Petrophysics. - ppt download’. https://slideplayer.com/slide/10323410/ (accessed May 15, 2021).

[51] ‘Reservoir Fluid Types’. http://fekete.com/SAN/TheoryAndEquations/HarmonyTheoryEquations/Content/HTML_Files/Reference_Material/General_Concepts/Reservoir_Fluid_Types.htm (accessed May 16, 2021).

[52] R. Timsina, ‘Near-well simulations and modelling of oil production from reservoir’, p. 64.

[53] J. Velarde, T. A. Blasingame, and W. D. McCain, ‘Correlation of Black Oil Properties At Pressures Below Bubble Point Pressure - A New Approach’, presented at the Annual Technical Meeting, Jun. 1997. doi: 10.2118/97-93.

[54] M. L. Haider, ‘The Productivity Index’, *Trans. AIME*, vol. 123, no. 01, pp. 112–119, Dec. 1937, doi: 10.2118/937112-G.

[55] D. K. Babu and A. S. Odeh, ‘Productivity of a Horizontal Well (includes associated papers 20306, 20307, 20394, 20403, 20799, 21307, 21610, 21611, 21623, 21624, 25295, 25408, 26262, 26281, 31025, and 31035)’, *SPE Reserv. Eng.*, vol. 4, no. 04, pp. 417–421, Nov. 1989, doi: 10.2118/18298-PA.

[56] S. E. Akpan, ‘Well Placement for maximum production in the Norwegian Sea’, p. 102, 2012.

[57] ‘Wellbore: 6608/10-D-2 H - Factpages - NPD’. https://factpages.npd.no/en/wellbore/pageview/development/all/2913 (accessed May 17, 2021).

[58] ‘NPD FactMaps Desktop’. https://factmaps.npd.no/FactMaps/3_0/?run=WellboreDevByNPDID&NPDID=2913 (accessed May 17, 2021).

[59] ‘Wellbore: 6608/10-3 - Factpages - NPD’. https://factpages.npd.no/en/wellbore/pageview/exploration/all/1732 (accessed May 17, 2021).

[60] Aida, Linn,Lindomar,Spari,Henok, ‘Surfactant Flooding of the Norne Field’, p. 60.

[61] ‘Temperature dependence of viscosity’, *Wikipedia*. Apr. 18, 2021. Accessed: May 18, 2021. [Online]. Available:

9 References

https://en.wikipedia.org/w/index.php?title=Temperature_dependence_of_viscosity&oldid=1018579135

[62] ‘Darcy-Weisbach Formula’, *Pipeflow.co.uk*, p. 3.

[63] V. M. Birchenko, ‘Analytical Modelling of Wells with Inflow Control Devices’, p. 156.

[64] ‘What is Pressure Drawdown? - Definition from Petropedia’, *Petropedia.com*. http://www.petropedia.com/definition/3018/pressure-drawdown (accessed May 19, 2021).

[65] R. A. Novy, ‘Pressure Drops in Horizontal Wells: When Can They Be Ignored?’, *SPE Reserv. Eng.*, vol. 10, no. 01, pp. 29–35, Feb. 1995, doi: 10.2118/24941-PA.

[66] S. D. Joshi, ‘Chapter 10: Pressure Drop through a Horizontal Well | Engineering360’. https://www.globalspec.com/reference/64886/203279/chapter-10-pressure-drop-through-a-horizontal-well (accessed May 19, 2021).

Appendices

Appendix A: Task description

Appendix B: Norne Blend data from Equinor AS

Appendix C: Formation pressure data of well 6608/10-3

Appendix D: Absolute permeability data

Appendix E: Relative permeability data

Appendix F: Calculations procedures

Appendix G: Relative permeability and capillary pressure $\pm$ 20% table

0 Appendices

Appendix A: Task description

University of South-Eastern Norway

Faculty of Technology, Natural Sciences and Maritime Sciences, Campus Porsgrunn

FMH606 Master's Thesis

Title: Sensitivity analysis of oil production models to reservoir rock and fluid properties

USN supervisor: Prof. Britt M. E. Moldestad and Ali Moradi

External partner: -

Task background:
According to DNV GL's Energy Transition Outlook 2019, more than half of today's energy consumption is supplied by oil and gas. Also, the world's energy demand is increasing and it is expected that 46% of the world's energy supply will come from oil and gas in 2050 whereas the share of wind and solar is only 24%. These data indicate that oil and gas will remain the most important source of energy for the foreseeable future and there is an urgent need to increase oil and gas production to meet future energy demands.

Today, the Norwegian Continental Shelf (NCS) is one of the most technologically advanced petroleum regions in the world and Norway is in a very good position to supply petroleum to the global market also in the future. To secure the competitiveness of the NCS in the international market and to ensure that NCS is at the forefront of adopting the latest technological innovations, OG21 (Oil and gas for the 21st century) has developed a national technology strategy for guiding research efforts in the petroleum technology. The main strategic objective of OG21 is to obtain efficient, secure, and environmentally friendly value creation from the Norwegian oil and gas resources for several generations.

In line with the OG21 strategy, there is a promising ongoing research project called DigiWell (digital wells for optimal production and drainage) at USN. Also, Equinor and KDI are the company partners, and SINTEF, UiO, ICL, and MIT are the research partners of USN in this project. One of the main objectives of the project is to increase the efficiency and optimization of oil recovery with a special focus on digitalization. Achieving an optimized and successful automatic production highly depends on the ability to monitor and control the well performances. This requires a suitable dynamic model of oil field and production equipment over the production lifetime. One of the main barriers to developing such dynamic models is that generally, it is very difficult to observe and understand the dynamic of fluid in a porous medium, describe the physical processes, and measure all the parameters that influence the multiphase flow behavior inside a reservoir. Predicting how a reservoir will produce over time and respond to different drive and displacement mechanisms consequently has a large degree of uncertainty attached. Therefore, developing new knowledge and tools for modeling and quantitative prediction of oil and gas field operation with uncertain information is of key importance.

0 Appendices

In order to develop long-term oil production models under uncertainty, it is very important to have a clear understanding of the sensitivity of such models to the input parameters. This helps us to identify the most impactful parameters on the accuracy of the models and allows us to limit the time for focusing on less important data. The sensitivity analysis assesses the contribution of the uncertainty of each model input to the uncertainty of the model outcomes and identifies the most important parameters of the system. The main goal of this thesis is to do sensitivity analysis for investigation of the effect of uncertainty in each reservoir parameters on the outputs of oil production models.

Task description:
The objectives of this research project can be achieved by completing the following tasks:

1. Literature study
   - Uncertainty quantification and sensitivity analysis
   - Reservoir fluid and rock properties
2. Developing a model for simulation of primary oil production from an oil field in NCS
   - OLGA in combination with ROCX is a robust tool for this purpose but Eclipse can also be used
3. Sensitivity analysis of the developed model to the reservoir parameters
   - The sensitivity analysis should be done for porosity, relative permeability, permeability anisotropy, heterogeneity, wettability, capillary pressure, initial water saturation, initial solution gas-oil ratio, viscosity, etc.
4. If time, preparing a paper based on the results for the next SIMS conference is highly appreciated

Student category: PT and EET students

The task is suitable for online students (not present at the campus): Yes

Practical arrangements:
Necessary software will be provided by USN.

Supervision:
As a general rule, the student is entitled to 15-20 hours of supervision. This includes necessary time for the supervisor to prepare for supervision meetings (reading material to be discussed, etc).

Signatures:

Supervisor (date and signature): 28.01.2021 Birkf Moldestad

Student (write clearly in all capitalized letters): BIKASH SHARMA

Student (date and signature): Bikash 01/23/2021

Appendix B: Norne Blend data from Equinor AS

equinor

Crude: **NORNE BLEND 2020 08**
Reference: **NORNEBLEND202008**

Crude Summary Report

General Information		Molecules (% wt on crude)		Whole Crude Properties	
Name:	NORNE BLEND 2020 08	methane + ethane	0.03	Density @ 15°C (g/cc)	0.865
Reference:	NORNEBLEND202008	propane	0.15	API Gravity	32.0
Traded Crude:	Norne	isobutane	0.10	Total Sulphur (% wt)	0.23
Origin:	Norway	n-butane	0.27	Pour Point (°C)	15
Sample Date:	16 august 2020	isopentane	0.27	Viscosity @ 20°C (cSt)	14
Assay Date:	23 november 2020	n-pentane	0.35	Viscosity @ 40°C (cSt)	6
Issue Date:	24 november 2020	cyclopentane	0.05	Nickel (ppm)	1.3
Comments:	-	C_6 paraffins	0.91	Vanadium (ppm)	0.8
		C_6 naphthenes	1.01	Total Nitrogen (ppm)	530
		benzene	0.37	Total Acid Number (mgKOH/g	0.19
		C_7 paraffins	1.13	Mercaptan Sulphur (ppm)	7
		C_7 naphthenes	1.88	Hydrogen Sulphide (ppm)	0.0
		toluene	1.54	Reid Vapour Pressure (psi)	4.1

0 Appendices

Appendix C: Formation pressure data of well 6608/10-3

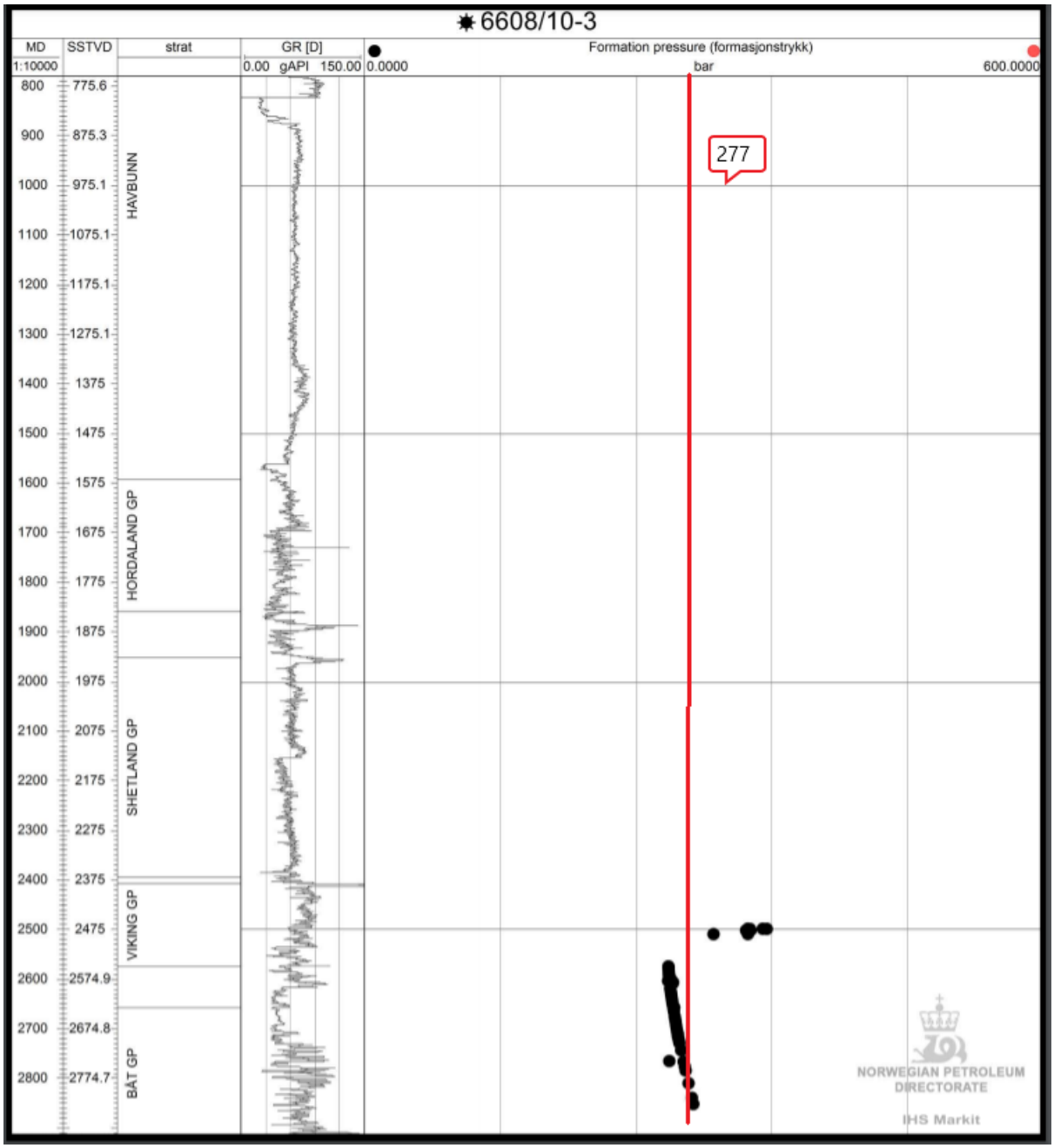

Appendix D: Absolute permeability data

```
'PERMZ' 0.2    1 46 1 112  1  1 /    Garn 3
'PERMZ' 0.04   1 46 1 112  2  2 /    Garn 2
'PERMZ' 0.25   1 46 1 112  3  3 /    Garn 1
'PERMZ' 0.0    1 46 1 112  4  4 /    Not     (inactive anyway)
'PERMZ' 0.13   1 46 1 112  5  5 /    Ile 2.2
'PERMZ' 0.13   1 46 1 112  6  6 /    Ile 2.1.3
'PERMZ' 0.13   1 46 1 112  7  7 /    Ile 2.1.2
'PERMZ' 0.13   1 46 1 112  8  8 /    Ile 2.1.1
'PERMZ' 0.09   1 46 1 112  9  9 /    Ile 1.3
'PERMZ' 0.07   1 46 1 112 10 10 /    Ile 1.2
'PERMZ' 0.19   1 46 1 112 11 11 /    Ile 1.1
'PERMZ' 0.13   1 46 1 112 12 12 /    Tofte 2.2
'PERMZ' 0.64   1 46 1 112 13 13 /    Tofte 2.1.3
'PERMZ' 0.64   1 46 1 112 14 14 /    Tofte 2.1.2
'PERMZ' 0.64   1 46 1 112 15 15 /    Tofte 2.1.1
'PERMZ' 0.64   1 46 1 112 16 16 /    Tofte 1.2.2
'PERMZ' 0.64   1 46 1 112 17 17 /    Tofte 1.2.1
'PERMZ' 0.016  1 46 1 112 18 18 /    Tofte 1.1
'PERMZ' 0.004  1 46 1 112 19 19 /    Tilje 4
'PERMZ' 0.004  1 46 1 112 20 20 /    Tilje 3
'PERMZ' 1.0    1 46 1 112 21 21 /    Tilje 2
'PERMZ' 1.0    1 46 1 112 22 22 /    Tilje 1
```

0 Appendices

Appendix E: Relative permeability data

Data for water-oil relative permeability curves:

--	Sw	Krw	Kro	Pc
	0.000000	0.000000	1.00000	3.75633
	0.0001	0.000000	0.999	3.75632
	0.0500000	0.000860000	0.847820	1.86981
	0.100000	0.00263000	0.697460	1.23731
	0.150000	0.00524000	0.557170	0.91821
	0.200000	0.00877000	0.432860	0.72451
	0.250000	0.0133800	0.327570	0.59341
	0.300000	0.0192700	0.241770	0.49811
	0.350000	0.0267200	0.174150	0.42511
	0.400000	0.0360800	0.122370	0.36691
	0.450000	0.0478100	0.0837400	0.31911
	0.500000	0.0625000	0.0556500	0.27881
	0.550000	0.0809000	0.0357200	0.24401
	0.600000	0.103940	0.0219900	0.21351
	0.650000	0.132770	0.0128400	0.18631
	0.700000	0.168690	0.00699000	0.16161
	0.750000	0.213020	0.00346000	0.13901
	0.800000	0.266670	0.00149000	0.11801
	0.850000	0.329180	0.000510000	0.09831
	0.900000	0.397060	0.000120000	0.07961
	0.950000	0.461030	0.00001	0.06161
	1.00000	0.500000	0.000000	0.04408

Data for gas-oil relative permeability curves:

--	Sg	Krg	Kro	Pc
	0.000000	0.000000	1.00000	0.000000
	0.0500000	0.00165500	0.806888	0.000000
	0.100000	0.00691300	0.633562	0.000000
	0.150000	0.0162130	0.485506	0.000000
	0.200000	0.0299900	0.364043	0.000000
	0.250000	0.0486550	0.267589	0.000000
	0.300000	0.0725730	0.192992	0.000000
	0.350000	0.102046	0.136554	0.000000
	0.400000	0.137287	0.0946710	0.000000
	0.450000	0.178402	0.0641510	0.000000
	0.500000	0.225368	0.0423240	0.000000
	0.550000	0.278030	0.0270350	0.000000
	0.600000	0.336093	0.0165860	0.000000
	0.650000	0.399135	0.00966200	0.000000
	0.700000	0.466631	0.00525400	0.000000
	0.750000	0.538000	0.00259700	0.000000
	0.800000	0.612665	0.00111700	0.000000
	0.850000	0.690169	0.000384000	0.000000
	0.900000	0.770395	0.000088	0.000000
	0.950000	0.854218	0.000007	0.000000
	0.9999	0.9499	0.000000	0.000000
	1.00000	0.950000	0.000000	0.000000

0 Appendices

Appendix F: Calculations procedures

1. **Calculation of horizontal length of well**:

We have from equation 5.5, the length of horizontal well can be calculated from,

$L_{MD} = L_{TVD} + L_{horizontal} + L_{kickoff}$

$\Longrightarrow L_{horizontal} = L_{MD} - L_{TVD} - L_{kickoff}$

Here, the measured depth is 4174 m and total vertical depth is 2647 m. $L_{kickoff}$ can be calculated as

$L_{kickoff} = R_{kickoff} \times \frac{4}{\pi} = 457.2 \times \frac{4}{\pi}$ =582.125 m

In figure 2.4, it is discussed that if the inclination angle is between 2°-6 °/100 ft. then it is long horizontal well which in this case is 5.5°. So, it is assumed that well 6608/10-D-2H of Norne oil field has radius in kickoff section to be 1500 ft. which is 457.2 m.

$L_{horizontal}$ = 944.8 ≈ 945 m.

2. **Calculation of permeability anisotropy**

To calculate the value of permeability anisotropy, equation 5.9 is given, so the value of *k* is 0.3 D obtained from Appendix D, and the value of ϕ_e is 0.27. Now from table 5.1,

$V_{sh,average} = \frac{h_{zone1}.V_{sh,zone1}+h_{zone2}.V_{sh,zone2}+h_{zone3}.V_{sh,zone3}}{h_{zone1}+h_{zone2}+h_{zone3}} = \frac{35\cdot0.31+46\cdot0.15+55\cdot0.14}{35+46+55} = 0.187$

$\phi_e = \frac{0.20+0.24+0.27}{3} = 0.23$

$k_v = k_z = 0.0718 \times \sqrt{\left[\frac{k_H(1-V_{sh})}{\phi_e}\right]^{2.0901}} = 0.0718 \times \sqrt{\left[\frac{k_H(1-0.187)}{0.23}\right]^{2.0901}} = 0.268\ {k_H}^{1.045}$

From equations 3.12 and 3.13,

$k = \sqrt[3]{k_x k_y k_z}$ and $k_H = \sqrt{k_x k_y}$

$\Longrightarrow k = \sqrt[3]{k_H^2 k_z} \Longrightarrow \sqrt[3]{k_H^2 \cdot 0.268 \cdot k_H^{1.045}}$

$\Longrightarrow 0.3^3 = k_H^{3.045} \cdot 0.268$

$\Longrightarrow k_H = \sqrt[3.045]{0.100} = 0.469$ D

$\Longrightarrow k_z = 0.268\ {k_H}^{1.045} = 0.268 \cdot 0.469^{1.045} = 0.121$ D

So,

$k_H = \sqrt{k_x k_y} = \sqrt{k_x^2}$ $(k_x = k_y)$

$\Longrightarrow k_H = k_x = k_y = 0.469$ D

Therefore, permeability anisotropy can be calculated by,

$a = \frac{k_v}{kH} = \frac{0.121}{0.469} = 0.257$

3. Calculation of productivity index

Based on the reservoir rock and fluid properties, and comparing the Odeh's model parameters shown in Figure 3.10 with the geometry of the reservoir considered for developing the model in this thesis shown in Figure 6.1, the Odeh's model is used by considering the following values:

a = 270 m = 885.8 ft ; b = 992 m = 3254.5 ft ; c = 136 m = 446.19 ft

dx = 135 m = 442.9 ft ; dy = 0 ; dz = 10 m = 32.8 ft

r_w = 0.2286 m = 0.744 ft

$B = \frac{V_{res}}{V_{st}} \approx 1.09918$; μ = 1.107 cP

$k_x = k_y$ = 0.469 D = 469 mD ; k_z = 0.121 D = 121mD

First the condition needs to be checked using equation 3.27,

$$\frac{b}{\sqrt{k_y}} > \frac{1.33a}{\sqrt{k_x}} \gg \frac{0.75h}{\sqrt{k_z}}$$

$$\Longrightarrow \frac{b}{\sqrt{k_y}} = \frac{3254.5}{\sqrt{121}} = 295.8 > \frac{1.33a}{\sqrt{k_x}} = \frac{1.33\times885.8}{\sqrt{121}} = 107.1 > \frac{0.75h}{\sqrt{k_z}} = \frac{0.75\times446.1}{\sqrt{469}} = 15.4$$

Since the condition satisfies the equation, equations 3.28 and 3.32 are valid to use. So,

$b = L_w \Longrightarrow P_{xyz} = P_{xy} = 0$

and $dy = 0 \Longrightarrow y_m = \frac{L_w}{2} = 0 = P_x$

$\therefore S_r = P_{xyz} + P_y + P_{xy} = 0$

From equation 3.32,

$$lnC_H = \frac{6.28a}{h}\sqrt{\frac{k_z}{k_x}}\left(\frac{1}{3} - \frac{d_x}{a} + \frac{d_x^2}{a^2}\right) - ln\left[sin\frac{\pi d_z}{h}\right] - 0.5ln\left[\left(\frac{a}{h}\right)\sqrt{\frac{k_z}{k_x}}\right] - 1.088$$

$$\Longrightarrow lnC_H = \frac{6.28\cdot885.8}{446.19}\sqrt{\frac{121}{469}}\left(\frac{1}{3} - \frac{442.9}{885.8} + \frac{196160.41}{784641.64}\right) - ln\left[sin\frac{\pi\times32.8}{446.19}\right] - 0.5ln\left[\left(\frac{885.8}{446.19}\right)\sqrt{\frac{121}{469}}\right] - 1.088$$

$\Longrightarrow lnC_H$ = -2.256260

$\Longrightarrow C_H = e^{-2.256260}$ = 0.104741

From the values of C_H and S_r productivity index of well 6608/10-D-2H can be obtained by equation 3.26 suggested by Babu and Odeh as,

$$J = \frac{7.08\times10^{-3}\times b\sqrt{k_x k_z}}{B\mu\left(ln(C_H\sqrt{ah}/r_w)\right) - 0.75 + S_r} = \frac{7.08\times10^{-3}\times3254.5\sqrt{121\times469}}{1.09918\times1.107\left(ln(0.104741\sqrt{885.8\times3254.5}/0.744)\right) - 0.75 + 0}$$

= 928.16 stb/d/psi = 2140 m^3/d/bar

0 Appendices

Appendix G: Relative permeability and capillary pressure ± 20% table

Sw	Krw	Kro	Value +20%(Krw)	Value -20% (Krw)	kro (+20%)	kro (-20%)
0.000000	0.000000	1.00000	0	0		
0.100000	0.00263000	0.697460	0.003156	0.002104	0.836952	0.557968
0.150000	0.00524000	0.557170	0.006288	0.004192	0.668604	0.445736
0.200000	0.00877000	0.432860	0.010524	0.007016	0.519432	0.346288
0.250000	0.0133800	0.327570	0.016056	0.010704	0.393084	0.262056
0.300000	0.0192700	0.241770	0.023124	0.015416	0.290124	0.193416
0.350000	0.0267200	0.174150	0.032064	0.021376	0.20898	0.13932
0.400000	0.0360800	0.122370	0.043296	0.028864	0.146844	0.097896
0.450000	0.0478100	0.0837400	0.057372	0.038248	0.100488	0.066992
0.500000	0.0625000	0.0556500	0.075	0.05	0.06678	0.04452
0.550000	0.0809000	0.0357200	0.09708	0.06472	0.042864	0.028576
0.600000	0.103940	0.0219900	0.124728	0.083152	0.026388	0.017592
0.650000	0.132770	0.0128400	0.159324	0.106216	0.015408	0.010272
0.700000	0.168690	0.00699000	0.202428	0.134952	0.008388	0.005592
0.750000	0.213020	0.00346000	0.255624	0.170416	0.004152	0.002768
0.800000	0.266670	0.00149000	0.320004	0.213336	0.001788	0.001192
0.850000	0.329180	0.000510000	0.395016	0.263344	0.000612	0.000408
0.900000	0.397060	0.000120000	0.476472	0.317648	0.000144	0.000096
0.950000	0.461030	0.00001	0.553236	0.368824	0.000012	0.000008
1.00000	0.500000	0	0.6	0.4	0	0

Sg	Krg	Kro	Value +20%(Krg)	Value -20% (Krg)	kro (+20%)	kro (-20%)
0.000000	0.000000	1.00000				
0.100000	0.00691300	0.633562	0.0082956	0.0055304	0.7602744	0.5068496
0.150000	0.0162130	0.485506	0.0194556	0.0129704	0.5826072	0.3884048
0.200000	0.0299900	0.364043	0.035988	0.023992	0.4368516	0.2912344
0.250000	0.0486550	0.267589	0.058386	0.038924	0.3211068	0.2140712
0.300000	0.0725730	0.192992	0.0870876	0.0580584	0.2315904	0.1543936
0.350000	0.102046	0.136554	0.1224552	0.0816368	0.1638648	0.1092432
0.400000	0.137287	0.0946710	0.1647444	0.1098296	0.1136052	0.0757368
0.450000	0.178402	0.0641510	0.2140824	0.1427216	0.0769812	0.0513208
0.500000	0.225368	0.0423240	0.2704416	0.1802944	0.0507888	0.0338592
0.550000	0.278030	0.0270350	0.333636	0.222424	0.032442	0.021628
0.600000	0.336093	0.0165860	0.4033116	0.2688744	0.0199032	0.0132688
0.650000	0.399135	0.00966200	0.478962	0.319308	0.0115944	0.0077296
0.700000	0.466631	0.00525400	0.5599572	0.3733048	0.0063048	0.0042032
0.750000	0.538000	0.00259700	0.6456	0.4304	0.0031164	0.0020776
0.800000	0.612665	0.00111700	0.735198	0.490132	0.0013404	0.0008936
0.850000	0.690169	0.000384000	0.8282028	0.5521352	0.0004608	0.0003072
0.900000	0.770395	0.000088	0.924474	0.616316	0.0001056	0.0000704
0.950000	0.854218	0.000007	1.0250616	0.6833744	0.0000084	0.0000056
1.00000	0.950000	0	1.14	0.76	0	0

0 Appendices

Sw	Capillary Pressure	(+20%)	(-20%)
0	3.7563	4.50756	3.00504
0.1	1.233	1.4796	0.9864
0.15	0.91821	1.101852	0.734568
0.2	0.72451	0.869412	0.579608
0.25	0.59341	0.712092	0.474728
0.3	0.49811	0.597732	0.398488
0.35	0.42511	0.510132	0.340088
0.4	0.36691	0.440292	0.293528
0.45	0.31911	0.382932	0.255288
0.5	0.27881	0.334572	0.223048
0.55	0.24401	0.292812	0.195208
0.6	0.21951	0.263412	0.175608
0.65	0.18631	0.223572	0.149048
0.7	0.16161	0.193932	0.129288
0.75	0.13901	0.166812	0.111208
0.8	0.11801	0.141612	0.094408
0.85	0.09831	0.117972	0.078648
0.9	0.07961	0.095532	0.063688
0.95	0.06161	0.073932	0.049288
1	0.04408	0.052896	0.035264